The Pennsylvania State University

The Graduate School

Department of Energy and Mineral Engineering

MAJOR, MINOR AND TRACE ELEMENTS IN DIRECT COAL LIQUEFACTION: EFFECT ON CONVERSION AND PARTITIONING BEHAVIOR

A Thesis in

Energy and Mineral Engineering

by

Sarah Anne Luchner

Submitted in Partial Fulfillment
of the Requirements
for the Degree of

Master of Science

December 2010

The thesis of Sarah Anne Luchner was reviewed and approved* by the following:

Sharon Falcone Miller
Research Associate at EMS Energy Institute
Thesis Adviser

Jonathan P. Mathews
Assistant Professor of Energy and Mineral Engineering

Harold H. Schobert
Professor of Fuel Science

Bruce G. Miller
Senior Research Associate at EMS Energy Institute

R. Larry Grayson
Professor of Energy and Mineral Engineering
Graduate Program Officer of Energy and Mineral Engineering

*Signatures are on file in the Graduate School.

Abstract

With current concerns of depleting oil sources and the environmental impacts of off-shore drilling, the interest in liquid transportation fuels derived from coal is increasing. The direct coal liquefaction process raises the hydrogen content of the hydrocarbon solid to that of a hydrocarbon liquid which can be upgraded to resemble refined petroleum products such as gasoline, diesel fuel, and jet fuel. A difference, however, is that coal contains a wider range and a higher concentration of inorganic material and in direct coal liquefaction processes these inorganic constituents must be accounted for. The objective of this thesis is to determine the partitioning of major, minor and trace inorganic elements during direct coal liquefaction and their effect on conversion. The inorganic constituent partitioning was studied because of potential health effects and operational impacts on equipment. These health effects include contamination to the atmosphere and water by Hg, As, and Se constituents. Important operational impacts include corrosion, fouling, and catalyst poisoning by alkali and alkaline earth metals Ca, K, Mg, and Na. High mineral matter concentrations in the coal liquefaction residues also pose challenges in post-processing.

Two coals, an Illinois No. 6 seam high volatile bituminous coal and a Montana Dietz seam subbituminous coal, were used in direct coal liquefaction experiments while varying temperature (450°C and 375°C), pressure (6.9MPa and 7.9MPa of hydrogen), coal preparation procedures (as-received and float-sink cleaning) and catalyst addition (with and without an FeS catalyst). The reaction conditions were varied to analyze any correlations with inorganic elements. Major, minor, and trace inorganic element concentrations were measured in the

feed coals and their tetrahydrofuran (THF) soluble (liquid) and THF-non-soluble (residue) products. The partitioning of an element was determined by measuring the total mass of the individual inorganic element fed into the system and their mass measured in the solid and liquid products. A total of 16 major, minor and trace elements was studied: Al, Ca, Fe, K, Mg, Mn, Na, S, Ti, As, Hg, Mo, Ni, Pb, Se, V, and Zn. Elemental concentrations were measured by atomic adsorption spectrometry and inductively coupled plasma atomic emission spectrometry.

The highest direct coal liquefaction conversions resulted from tests using the Illinois No. 6 as-received coal. This coal not only had the highest sulfur, iron, and pyrite concentrations, but also contained the smallest particle size distribution of pyrite as determined by computer-controlled scanning electron microscopy. It was found that the majority of the inorganic constituents concentrated in the residue. Commonly the concentrations of inorganic elements were two to six times higher in the residue compared to the feed coal and this could result in operational and environmental concerns. The elements Mg, Na, S, Hg, Mo, V, and Zn often measured more than 5% (averaging about 20%) of their initial weight reporting to the liquids. In the liquid products, the alkali and alkaline earth metal concentrations were higher than those of crude oil. Direct coal liquefaction liquids had Hg, As and Se concentrations similar to that of crude oils. Additionally, the feed coals were chemically fractionated and analyzed to determine if any relationship existed between the element's mode of occurrence and its partitioning to the solid or liquid product. No trends could be concluded in regard to the relation of an element's mode of occurrence and its partitioning in direct coal liquefaction.

Table of Contents

List of Figures: vii
List of Tables: viii
1. Introduction 1
1.1 Motivation 1
1.2 Objective and Approach 2
2. Literature Review 4
2.1 Inorganic Constituents in Crude Oil 4
2.1.1. Occurrence of Inorganic Elements in Crude Oil 4
2.1.2 Behavior of Crude Oil Inorganics During Utilization 6
2.2 Inorganic Elements in Coal 8
2.2.1 Coal Rank and Inorganics 8
2.2.2 Modes of Occurrence of Inorganic Elements 10
2.2.3 Coal and DCL Human Health Risks and Environmental Concerns 13
2.3 Direct Coal Liquefaction and Coal Composition 15
2.3.1 Maceral and Mineral Composition 15
2.3.2 Iron, Sulfur, and Pyrite 17
2.4 DCL Reaction Variables 19
2.4.1. Catalyst 19
2.4.2 Reaction Temperature 20
2.4.3 Reaction Solvent and Hydrogen Gas Pressure 21
2.5 Direct Coal Liquefaction Products 22
2.5.1 Residue Products 23
2.5.2 Liquid Products 25
2.6 Inorganic Element Partitioning in DCL 27
3. Methodology 31
3.1 Experimental 31
3.1.1 Coal Preparation 31
3.1.2 Dense Media Separation 32
3.1.3 Batch Liquefaction Tests 33
3.1.4 Product Extraction 36
3.1.5 Reaction Variables and Test Nomenclature 36
3.2 Analytical 38
3.2.1 Coal Characterization 38
3.2.2 Inorganic Elemental Analysis 38
3.2.3 Chemical Fractionation 39
3.2.4 CCSEM Analysis 41
3.2.5 Residue Ash Yield Analysis 42
3.3 Calculations 42
3.3.1 Liquefaction Conversions 42
3.3.2 Inorganic Element Partitioning 43
4. Results and Discussion 45
4.1 Feed Coal Characterization and Mineral Analysis 45
4.1.1 Coal Compositions 45

4.1.2 Chemical Fractionation 47
4.1.3 Mineral Analysis 49
4.2 DCL Testing and Analysis 52
4.2.1 Confidence in Elemental Analysis in DCL 52
4.2.2 Reproducibility of DCL Tests 54
4.3 Liquefaction Conversions 56
4.3.1 Overall Conversions 56
4.3.2 Relationship between Conversions and Inorganic Elements 59
4.3.3 Residue Ash Yield Analysis 63
4.4 Inorganic Element Partitioning during DCL 65
4.4.1 Overview of Partitioning Results 65
4.4.1.1 Baseline Test Results 65
4.4.1.2 Inorganic Element Partitioning Data for All Tests 69
4.4.2 Coal Composition and Rank 72
4.4.3 Iron, Sulfur and Catalyst 74
4.4.4 Coal Cleaning 80
4.4.5 Reaction Pressure and Temperature 82
4.5 Relationship of Inorganic Occurrence to Partitioning During Liquefaction 85
4.6 Inorganic Elements in DCL Products 88
4.6.1 Alkali and Alkaline Earth Metals and Operational Concerns 88
4.6.2 Mercury, Arsenic, and Selenium and Environmental Concerns 91
4.6.3 Coal Liquids and Other Transportation Fuels 93
5. Conclusions and Recommendations for Future Work 96
5.1 Summary and Conclusions 96
5.2 Future Work 101
REFERENCES 103
APPENDIX A: Coal minerals 111
APPENDIX B: Pringle and Jarvis (1987) product concentrations compared to Luchner thesis results 113
APPENDIX C: Details of computer-controlled scanning electron microscopy 114
APPENDIX D: Experimental detection limits from ICP and AAS elemental analysis 117
APPENDIX E: Chemical fractionation results 118
APPENDIX F: Complete CCSEM results 121
APPENDIX G: Experimental details of all DCL batch tests. 131
APPENDIX H: Raw data of DCL inorganic element partitioning 132
APPENDIX I: Thermogravimetric weight reduction 136
APPENDIX J: Partitioning results of varying temperatures and pressures 137
APPENDIX K: Concentration of major, minor, and trace elements on a per barrel basis 139

List of Figures:

Figure 1: Possible organic association of inorganic elements. Left is an example of an AAEM (sodium cation) associated with a carboxyl group, right is a heterocyclic compound (thiophene) connected to an aromatic moiety 9
Figure 2: Ash to mineral matter associations (Huggins 2002) 10
Figure 3: Free H atom in catalytic dissociation of H_2 redrawn from (Derbyshire 1989) 19
Figure 4: Schematic of coal conversion to DCL products 31
Figure 5: Float-sink separation of Illinois No. 6 coal 33
Figure 6: Photograph of the 100mL microreactor 35
Figure 7: Schematic of the chemical fractionation procedure (Falcone Miller and Miller 2005) 40
Figure 8: Photographs of steps from the chemical fractionation procedure. Liquid leaching wash is on the left and vacuum filtration is shown on the right 41
Figure 9: Liquefaction percent overall conversions with a 0.76% calculated error from repeatability tests (reaction temperature, °C / reaction pressure, MPa) 57
Figure 10: DCL overall conversions compared to the inherent Fe and S weights in each of the six tests 60
Figure 11: Overall conversions of baseline (1), non-catalytic (2), and cleaned coal tests compared to input weights of Fe and S 61
Figure 12: Overall conversions of baseline, non-catalytic, and cleaned coal tests compared to the input weight of molybdenum 61
Figure 13: Overall DCL conversions compared to the total initial mass of inorganic elements charged in each microreactor experiment. Upper: % Overall conversion compared to total weight of inorganic input. Lower: Comparison without including the input weights of Fe and S 63
Figure 14: TGA ash yields with 1.3% absolute error from initial repeatability tests 64
Figure 15: Inorganic partitioning graphs for Baseline tests, y-axis is the percent of the elements initial coal weight that is measured in the solid and liquid products. 68
Figure 16: Number of occurrences of *Hg* by distributions within liquid and solid products 69
Figure 17: Number of occurrences of *K* by distribution within liquid and solid products 70
Figure 18: Occurrences of element in weight % measured in liquid and solid products 71
Figure 19: Mass of the element in the initial coal and liquefaction residue from the baseline tests. Error bars are individual to each element based on reproducibility tests. 73
Figure 20: Relationship of percent conversion to weight percent of the Fe in residue for the baseline runs (left of bar) and the runs without catalyst (right of bar) 75
Figure 21: Normalized S partitioning for baseline (left) and non-catalytic (right) tests 77
Figure 22: Effect of catalyst on element partitioning to the residue product for the IL#6 coal .. 78
Figure 23: Effect of catalyst on element partitioning to the residue product for the PRB coal ... 79
Figure 24: Comparison of element's partitioning for baseline IL#6 test and CL_IL#6 test. Upper: partitioning to solid, Lower: partitioning to liquid 82
Figure 25: Partitioning of elements of environmental interest during reactions of different temperature and pressures for Illinois No. 6 coal experiments 84

Figure 26: Partitioning of elements of operational interest during reactions at different temperatures and pressures for Illinois No. 6 coal experiments 85
Figure 27: Chemical fractionation and normalized DCL results for K and Mg (IE-Ion Exchangeable, AS-Acid Soluble, AIS-Acid Insoluble) 86
Figure 28: Zn, Mo, and Pb partitioning to DCL solid and liquid products and their water solubility (WS) 87

List of Tables:

Table 1: Ranges of element concentrations in selected crude oils. *a)* Elemental minimum and maximum concentrations from 4 crude oils. *b)* Concentration of these elements in a California crude oil and in its distillation fractions, from Filby and Shah, 1977) 6
Table 2: Mineral classifications and possible constituents (Speight 1983; Luttrell et al. 2000) 9
Table 3: Modes of occurrence of elements in coal (Swaine and Goodarzi 1995) 12
Table 4: Total wt% of volatile matter (TVM) and organic volatile matter (OVM) of THF-insoluble residues from DCL with and without a catalyst at 60 min. reaction time, (extracted from (Cui et al. 2002) 24
Table 5: Emissions (lb/10^{12}Btu) from traditional No. 6 fuel oil and coal co-processed fuel oil from (Falcone Miller and Miller 2008) 26
Table 6: Elemental concentrations in pyridine soluble (PS) and pyridine insoluble (PI) fractions from the Wilsonville Plant (Filby et al. 1977a) 28
Table 7: Results from GFAAS analysis of Wilsonville SRC products (Coleman et al. 1978) 29
Table 8: Results from ICP-AES analysis of SRC products in ppmw (Hellgeth et al. 1984) 29
Table 9: Chemical maximum limits for #316 Stainless Steel, % 34
Table 10: Microreactor test list with notations 37
Table 11: Analytical techniques used for various elements 39
Table 12: Potassium raw data for test 1A 43
Table 13: Potassium partitioning for test 1A 44
Table 14: Proximate analysis results for the coals on an as-received basis, wt% 45
Table 15: Ultimate analysis results for the feed coals on a dry basis, wt% 45
Table 16: Inorganic elemental analysis of the coals in ppm (μg/g) and ppb for Hg (ng/g) on an as-received whole coal basis 46
Table 17: Major and minor oxide weight percents for feed coals, ash basis 46
Table 18: Chemical fractionation results of the coals. Elements are listed if portion was over 40%. WS – Water Soluble, IE - Ion Exchangeable, AS - Acid Soluble, and AIS - Acid Insoluble 48
Table 19: CCSEM results of coal mineral concentrations as wt% of total mineral matter and the percent of that total which was found to be extraneous 50
Table 20: CCSEM results of total mineral wt% concentration on a whole coal basis 51
Table 21: Percent of pyritic Fe measured in different size fractions by CCSEM (microns) 52
Table 22: All analyzed inorganic elements with shading are those that will not be discussed in this thesis 53

Table 23: Blank test elements whose weights increased from initial weight in 5.15g samples .. 54
Table 24: Reproducibility test data 55
Table 25: Element's weight measured in the solid and liquid products of the 3RunTests (mg) .. 56
Table 26: Baseline test results showing the initial weight of the element charged in the reactor and the percentages of the initial weight that were measured in the solid and liquid products 66
Table 27: Maceral compositions of PRB and IL#6 coals on a mineral matter-free basis 72
Table 28: Initial and final weights of S (mg) 76
Table 29: Pyrite, S and Fe concentrations in IL#6 and CL_IL#6 coals on a whole coal weight percent basis 80
Table 30: Elemental concentrations for Illinois No. 6 coal and float-sink cleaned Illinois No. 6 coal in parts per million (ppm) 80
Table 31: Temperature and pressure variations 83
Table 32: Concentration of AAEMs in initial coal and solid and liquid products from Illinois No. 6 coal tests 88
Table 33: Concentration of AAEMs in initial coal and solid and liquid products from PRB coal tests 89
Table 34: AAEM concentrations in grams per barrel of THF-soluble liquids 91
Table 35: Concentration of As, Hg, and Se in coals, solid, and liquid products (ppm, Hg-ppb) ... 92
Table 36: Comparison of inorganic elements of interest in liquid products and crude oils and examples of regulations 94

1. Introduction

1.1 Motivation

Direct coal liquefaction (DCL) has been studied for many years. It is well known among the coal community that coal-derived liquids can replace crude oil as a transportation fuel feedstock. In the DCL process, the coal's structure is broken into smaller molecular components and hydrogenated to form lighter hydrocarbons. The process can be generalized by Equation 1 (Probstein and Hicks 1982).

$$\mathbf{C + 0.8\ H_2 \rightarrow CH_{1.6}\quad (slightly\ exothermic)} \qquad \mathbf{[Equation\ 1]}$$

During the process, solvents and hydrogen interact with coal to produce liquid fuels. Commonly the solvents are hydrogen-donating chemicals, and catalysts are added to promote the conversion reactions (Valkovi 1983). Catalytic direct liquefaction usually uses a catalyst, solvent, and gaseous hydrogen to hydrocrack coal and transfer hydrogen. This process is also referred to as hydroliquefaction (Probstein and Hicks 1982).

The main variables in a DCL process are the reaction time, temperature, pressure, solvent and catalyst. These parameters, along with the significant variability of the coal, have led to an abundance of research on this topic. The interest in direct coal liquefaction has been cyclic for decades and currently it is of interest again due to the current concerns of depleting crude oil resources and price variability. Coal liquefaction is especially of interest in China where the 1.46 billion dollar Shenhua DCL plant has been constructed to produce 5 million tons of synfuel per year. Environmental concerns are currently causing setbacks of the Shenhua plant operations (Shui et al. 2010).

If coal derived liquids are to replace crude oil, how will their utilization differ from crude oil? Coal composition is extremely variable; even two samples from the same region can be of two different ranks. Another difference between crude oil and coal is that coal can contain much higher concentrations of inorganic elements not commonly found in crude oil. Throughout the entire context of this thesis, inorganic elements (or inorganics) are here defined as all elements except for carbon, hydrogen, oxygen, and nitrogen; sulfur is considered inorganic for this work. The main inorganic elements found in crude oil are most often sulfur, vanadium, and nickel, which are accompanied by other elements of trace concentrations (Speight 2001). Trace elements are often defined as elements with concentrations less than 0.1%. Coal, on the other hand, is a solid fossil fuel and is comprised of more variety and quantity of inorganic constituents and usually contains higher ash values as a result of its terrestrial origin. If coal is to replace crude oil by means of DCL, the partitioning of the inorganic fraction must be known along with its effects on the DCL process.

1.2 Objective and Approach

This study focused on the major, minor, and trace inorganic constituents in DCL and how their behavior changes with coal rank, temperature, pressure, catalyst, and removal of minerals from the coal. The objective was to study how the elements occur in the initial coals and how that related to their partitioning into either the product liquid or product solid residue during DCL and their effect on overall conversion.

To better understand the behavior of the inorganic constituents during DCL, batch liquefaction tests were performed in 100mL microreactors. The products were separated into liquid and solid fractions based on their solubility in tetrahydrofuran (THF). THF-soluble products include preasphaltene, ashpaltene and oil products. Baseline tests conditions were conducted for 1 hour at 425 °C, ~6.9 MPa (1000 psig) hydrogen pressure with an iron sulfide catalyst and tetralin solvent. Tests were also run without a catalyst, at 375 °C, and at 7.9 MPa (1150 psig) hydrogen pressure to investigate the effects of catalyst, temperature, and pressure. A subbituminous B coal from Montana (PRB) and a high-volatile bituminous C coal from Illinois (IL#6) were compared along with a partially demineralized bituminous coal (CL_IL#6).

Inorganic elements were measured in all initial coals, solid THF-insoluble products, and liquid THF-soluble products with atomic adsorption spectrometry (AAS) and inductively coupled plasma atomic emission spectrometry (ICP-AES). To obtain a better understanding of how the inorganic elements were incorporated into the coals, computer-controlled scanning electron microscopy (CCSEM) was used to identify mineral phases. The coals were chemically fractionated to obtain a better understanding of how the elements were present in the feed coals.

The mode of occurrence of inorganic elements and their partitioning during small-scale batch laboratory direct liquefaction experiments were studied in this work. It is recognized these batch scale procedures do not represent large commercial-scale systems; however, they do provide insight into how the inorganic elements within the initial coals are distributed in the DCL products.

2. Literature Review

2.1 Inorganic Constituents in Crude Oil

2.1.1. Occurrence of Inorganic Elements in Crude Oil

Inorganic elements, here defined as all elements not including carbon, hydrogen, oxygen, and nitrogen, are present in all crude oils and coals. The inorganic elements can be associated with the organic portion of the fossil fuel (e.g. porphyrins) and can affect crude oil and coal utilization with respect to equipment and environmental impacts.

In 2009, 94% of transportation fuels in the United States were derived from crude oil (U.S. Energy Information Administration). The main inorganic constituent in crude oil is sulfur, but other inorganic elements can be present. As stated earlier, the most common inorganic elements in crude oil are sulfur, nickel, and vanadium. In addition, dozens of other elements can be detected, but they are often present in concentrations lower than 1 part per million (ppm) (Filby et al. 1977b) and are primarily in the heavier fractions (Filby et al. 1977b; Duyck et al. 2007). Usually, younger oils are higher in trace metals when compared to older, light paraffinic oils (Speight 2001; Filby et al. 1977b).

Duyck et al. have conducted studies on the inorganic elements in crude oil. In their most recent study, the fractioning of crude oil is discussed and is related to the element's volatility (Duyck et al. 2007). Most of the metals present in the crude oil are of low or negligible volatility and are observed in the heaviest asphaltene fraction, and about 90% of crude oil inorganics separate to the residue fraction after refining (Speight 2001; Duyck et al. 2007; Bergerioux et al. 1979). To accurately measure the inorganic elements in crude oil,

different variations of optical absorption and emission techniques are utilized such as atomic adsorption spectrometry (AAS) and inductively coupled plasma atomic emission spectrometry (ICP-AES); however, the precision of these techniques relies on the sample preparation methods and the consistency of the materials' physical properties (Brown et al. 1982). ICP has been successfully applied to measuring inorganics in Venezuelan crude oils and sulfur contents ranging from 2.8 to 5.7%, nickel from 54 to 107 ppmv, and vanadium from 280 to 1,200 ppmv (Murillo and Chirinos 1994). These results are similar to those from Filby and Shah (Filby et al. 1977b; Shah et al. 1970), who compiled data of four crude oils from Canada, Venezuela, Nigeria, and the United States. The minimum and maximum values from their results are shown in Table 1a. The trace element concentrations in crude oils are highly variable based on the origin of the crude oil. For example, Venezuelan oil has very high vanadium concentrations and California Tertiary oil is extremely high in mercury content. This research also analyzed the composition of a California crude and some of its distillation fractions. These concentrations are shown in Table 1b and it is observed that the heavier fractions, i.e., No. 6 fuel oil, contain higher concentrations of trace elements when compared to lighter fractions such as diesel.

Table 1: Ranges of element concentrations in selected crude oils. *a)* Elemental minimum and maximum concentrations from 4 crude oils. *b)* Concentration of these elements in a California crude oil and in its distillation fractions, from Filby and Shah, 1977)

a)	Range min	Range max
Element	*ppmw*	*ppmw*
S	3,500	12,800
Ni	< 5	117
V	0.02	1,120
Na	0.04	25
Fe	< 0.01	73
Cl	-	8.7
	ppbw	*ppbw*
Co	6.8	13,000
Zn	-	2,600
Cu	-	930
Cr	< 5	634
Se	< 3	360
As	1.5	1,200
Sb	< 0.01	273
Cs	-	0.9
Rb	-	< 10
Sc	-	8.8
Eu	-	0.21
Br	-	91
Hg	< 20	21,000*

b)	Cali. Crude Oil	No. 6 Fuel Oil	Furnace Oil	Diesel
Element	*ppmw*	*ppmw*	*ppmw*	*ppmw*
S	3,200	28,500	2,700	1,200
Ni	2.1	21.7	0.08	0.11
V	2.8	29.2	0.4	0.25
Na	9.1	29.1	0.002	0.002
Fe	0.64	21	< 0.1	< 0.1
Cl	16.2	26.5	3.8	1.25
	ppbw	*ppbw*	*ppbw*	*ppbw*
Co	5.4	59.2	51	63
Zn	76	2,324	17	< 70
Cu	43.4	330	< 5	7.1
Cr	-	147	< 5	< 5
Se	22.5	100	11.8	5.8
As	34.7	160	9.5	4.3
Sb	< 1.0	< 1.0	< 1.0	< 1.0
Cs	-	4.7	0.7	0.9
Rb	-	-	-	-
Sc	0.03	0.35	0.03	0.04
Eu	1.03	1.12	0.13	0.13
Br	218	232	5.6	5.6
Hg	< 4	3.3	< 4	< 4

* California (Tertiary) heavy crude is an outlier for its high Hg concentration

- *Signifies no value obtained*

2.1.2 Behavior of Crude Oil Inorganics During Utilization

During crude oil refining, different catalysts are used to upgrade the oil into more marketable products. Certain inorganic elements present in the initial crude are detrimental to the refining process because they can cause corrosion of equipment and result in catalyst poisoning and degradation of catalyst selectivity. For example, in

reforming applications arsenic and lead poison catalysts and vanadium and sodium cause furnace corrosion (Speight 2001).

Inorganic elements that remain in the transportation fuel fractions derived from crude oil (i.e., diesel and gasoline) can also cause catalyst poisoning if their concentrations are too high. In motor vehicles, catalytic converters can be negatively affected by inorganic contamination. In biodiesel, alkali and alkaline earth metals such as calcium, magnesium, potassium, and sodium are regulated to a maximum of 10ppm total in order to protect post engine emission control catalysts such as those used in catalytic converters (ASTM-D6751-09 2009).

Positive effects of inorganic elements in crude oil utilization have also been found. Clays (e.g., aluminoeilicates such as montmorillonite) can act as catalysts in a refinery catalytic cracking unit and, if this mineral is present naturally in the fuel, it may help in fuel cracking (Schobert 1990, 1992). Minerals such as pyrite and alkali and alkaline earth metals (AAEMs) have also been found to potentially help cracking in fuels by aiding in hydrogenation (Schobert 1992); this will be discussed in more detail later in this thesis.

Environmental concerns in crude oil processing and transportation fuel use have also been raised. Besides concerns of oil spills and refinery processing emissions (Simeonova et al. 1989), emissions from product use can also pose environmental hazards. Most notably, lead additives were regulated in transportation fuels due to their harmful effect on humans. Lead is known to cause neurological damage, specifically in young children and fetal brain development (Goyer 1996).

2.2 Inorganic Elements in Coal

Coal, compared to crude oil, contains a wider range and a higher concentration of inorganic elements. In this overview, the importance of knowing an element's association within coal's structure will be discussed.

2.2.1 Coal Rank and Inorganics

The rank of a coal is defined by ASTM method D 388 (ASTM-D-388 2009) and classifies higher rank coals on their fixed carbon and volatile matter contents, expressed on a dry, mineral matter-free basis, whereas lower-rank coals are classified in terms of their heating value expressed on a moist, mineral matter-free basis. This ranking system does not consider any other attributes of the coal; however, a van Krevelen diagram (Van Krevelen 1961) and Seyler coal band along with other graphs show correlations between rank, carbon, oxygen, and hydrogen contents. High-rank coals, such as anthracites, have very high carbon contents and lower oxygen, hydrogen, and volatile matter. Their structure is heavily composed of large aromatic moieties. Low-rank coals, such as lignites, contain less carbon and more volatile matter, oxygen, and acidic groups. Organically bound inorganic elements within the coal structure are therefore more likely to be present in low-rank coals. For example, Figure 1 shows two inorganic associations within coal. The figure on the left is more likely to be present in low-rank coals where cations can be associated with carboxylic acid groups, such as sodium. The figure on the right shows how sulfur can be integrated into the organic coal structure as a thiophene, which can be common in a wider range of coal ranks including high-rank coals.

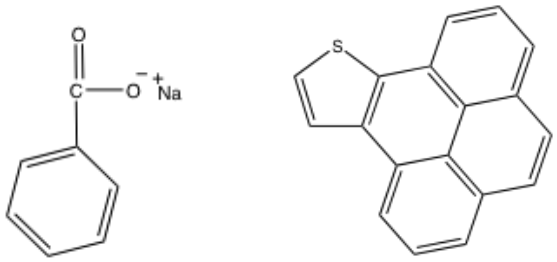

Figure 1: Possible organic association of inorganic elements. Left is an example of an AAEM (sodium cation) associated with a carboxyl group, right is a heterocyclic compound (thiophene) connected to an aromatic moiety

The mineral matter commonly found in coal that is not bound within the coal's organic structure includes silicates, carbonates, sulfates, sulfides, and oxides. A simple guide to some of these associations is found in Table 2.

Table 2: Mineral classifications and possible constituents (Speight 1983; Luttrell et al. 2000)

Classification	Mineral	Possible Formulas
Silicates	Kaolinite	$Al_2Si_2O_5(OH)_4$ or $Al_2O_3{\cdot}4SiO_2{\cdot}nH_2O$
	Illite	$(K,H_3O)(Al,Mg,Fe)_2(Si,Al)_4O_{10}[(OH)_2,(H_2O)]$
	Chlorite	$(Mg,Fe)_3(Si,Al)_4O_{10}(OH)_2{\cdot}(Mg,Fe)_3(OH)_6$
	Montmorillonite	$(Na,Ca)_{0.33}(Al,Mg)_2(Si_4O_{10})(OH)_2{\cdot}nH_2O$
Carbonates	Siderite	$FeCO_3$
	Ankerite	$Ca(Mg,Fe,Mn)(CO_3)_2$
	Dolomite	$Ca,Mg(CO_3)_2$
Oxides	Quartz	SiO_2
	Hematite	Fe_2O_3, α-Fe_2O_3
	Rutile	TiO_2
Sulfates	Gypsum	$CaSO_4{\cdot}2H_2O$
	Thernardite	Na_2SO_4
Iron Sulfates	Szomoluokite	$FeSO_4{\cdot}H_2O$
	Rozenite	$FeSO{\cdot}4H_2O$
	Melanterite	$FeSO_4{\cdot}7H_2O$
	Conquimbite	$Fe(SO_4){\cdot}9H_2O$
	Rosmertite	$Fe_2(SO_4){\cdot}Fe_2(SO_4)_3{\cdot}12H_2O$
	Jarosite	$(Na,K)Fe_3(SO_4)_2(OH)_6$
Sulfides	Pyrite	FeS_2

Eleven major inorganic oxides that are reported in coal ash are shown in Figure 2 along with their potential mineral associations in the coal. This demonstrates how elements in coal can have multiple mineral associations. Additional coal minerals are defined in Appendix A.

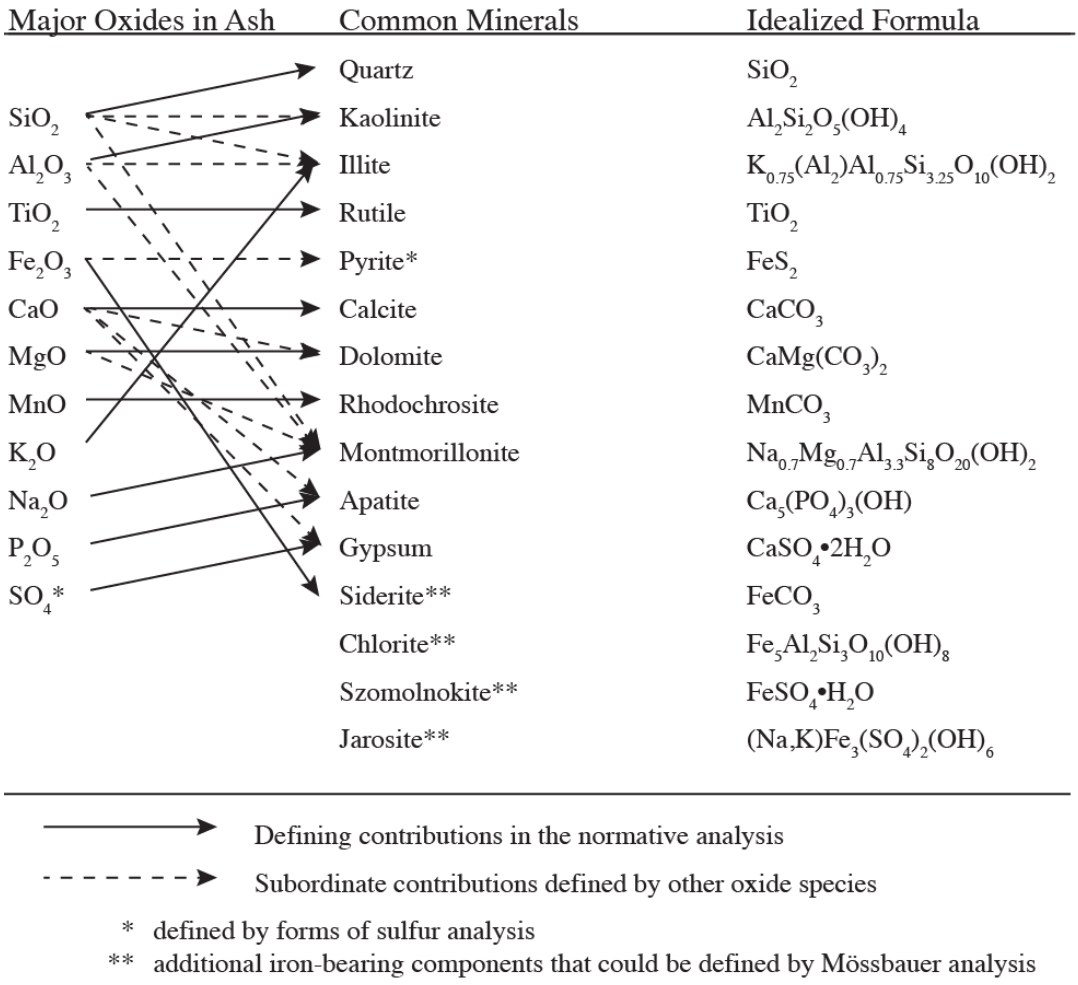

Figure 2: Ash to mineral matter associations (Huggins 2002)

2.2.2 Modes of Occurrence of Inorganic Elements

It has been found that the mode of occurrence of an inorganic element in coal is important when predicting its performance in coal utilization (Klein et al. 1975; Vejahati et al. 2010). The modes of occurrence of the inorganic elements in coal also impact coal

cleaning technologies and coal conversion processes, such as coal liquefaction. The modes of occurrence vary between coal ranks, and heavily rely on pyrite concentrations (Spears et al. 1999). For example, studies by Senior et al. (2000) report that in Wyodak Powder River Basin (PRB) coal, selenium has been found to be entirely organically bound within the coal. By contrast, in an Illinois No. 6 coal, selenium was primarily associated with the mineral matter: 60-80% in pyrite, 20-40% as organic selenium, and 10% as selenate (Senior et al. 2000). Another example is the occurrence of arsenic in the Illinois No. 6 coal compared to the Wyodak PRB. In the Illinois No. 6 coal, arsenic is associated with the mineral matter fraction (pyrite) whereas in the Wyodak coal arsenic is present as organically bound arsenate (Senior et al. 2000).

Similar results with mercury were found with 60% of the mercury associated with pyrite in the Illinois No. 6 coal, while mercury was associated with the organic portion of the PRB coal (Senior et al. 2000). In Illinois No.6 coal, cadmium, chromium, and nickel have all been shown to be associated with the pyrite. Many sources agree that mercury is also predominantly present within the pyrite fraction of most coals (Luttrell et al. 2000; Feng and Hong 1999; Toole-O'Neil et al. 1999). From these findings, it was found that the Illinois No. 6 coal has a significant fraction of inorganics associated with the pyrite. The PRB coal generally has lower concentrations of elements associated with pyrite and contains more inorganic elements associated with the organic portion of the coal. This is due to the previously mentioned rationale that low-rank coals have more sites (e.g., carboxyl groups) for inorganic elements (cations) to bond with, while high-rank coals contain fewer carboxyl and acid groups and more aromatic groups.

Inorganic elements can be organically bound within the coal's structure, present as discrete minerals, or they can be present as finely disseminated minerals within the coal (Clarke 1993). Some of the inorganic elements of focus in this work are listed in Table 3 along with their most common modes of occurrence taken from (Swaine and Goodarzi 1995).

Table 3: Modes of occurrence of elements in coal (Swaine and Goodarzi 1995)

	Element	Most Common Association
Pb	Lead	Sulfides, galena
S	Sulfur	Organic, sulfides, sulfates
As	Arsenic	Pyrite
Hg	Mercury	Pyrite
Mn	Manganese	Carbonates, siderite, and ankerite in high-rank coals, organic in low-rank
Mo	Molybdenum	*Sulfides*
Se	Selenium	Organic, in pyrite, sulfides, and sulfates
V	Vanadium	*In clays and organic associations*
Zn	Zinc	Sphalerite

**If in italics, there was less than 50% confidence from the source.*

One of the ways to understand how elements are bound within the coal's structure is to study what elements are leached out of the coal using different solvents (Finkelman et al. 1990; Falcone Miller 1992; Miller and Given 1986; Karner et al. 1986). This is referred to as chemical fractionation. Chemical fractionation is commonly conducted using three solvents. Each solvent leaches different components from the coal. The first solvent is water, which removes water-soluble salts. The next solvent is ammonium acetate, which removes ion-exchangeable elements such as calcium and sodium. Hydrochloric acid, the final solvent, removes the acid-soluble elements contained within mineral phases from the coal. Elements such as silicon and aluminum contained within the acid-insoluble mineral matter are left in the final residue (Gentzis and Goodarzi 1999). Low-rank coals have a

tendency to contain more carboxyl groups, which provide more bonding sites for elements such as calcium, sodium and potassium. These elements are readily ion-exchangable with the ammonium acetate. The information from chemical fractionation is helpful in understanding how the elements occur in the coal and their reactivity in coal utilization processes.

2.2.3 Coal and DCL Human Health Risks and Environmental Concerns

This section discusses the environmental concerns of coal and the few studied environmental and health issues related to coal-derived liquids. Operational impacts of coal liquefaction liquids are similar to those related to crude oil as discussed in Section 2.1.2 of this thesis. The operational concerns of the residue product from DCL are later discussed in Section 2.5.1.

Coal-derived liquids (CDLs) have been studied for their carcinogenic effects with regard to skin contact. It was found that the heaviest, raw coal liquids were highly tumorigenic (Witschi et al. 1987) and toxic to bone marrow and the liver of laboratory rats (Yagminas et al. 1988). It is known that organic compounds such as primary aromatic amines (PAAs), polynuclear aromatic hydrocarbons (PAHs), and phenols are associated with adverse effects to animals (e.g., cancer and mutations), and it is known that these can exist in CDLs, (especially CDLs without much upgrading) (Gray 1984). Solvent refined coal (SRC) has also been reported to be more toxic to plant-life when compared to heavy fractions of crude oil, and SRC causes more harm to sea plant-life (Gray et al. 1982). Unfortunately there

are no reports that focus on the potential human and environmental risks of inorganic elements in CDLs.

Coal contains elements that pose potential environmental threats; harmful elements released in mining and processing, emissions such as those during combustion, and elements leached from ash in disposal pits or in acid mine drainage. Detailed work has been conducted on the environmental effects of inorganic elements in coal, most of which focus on coal combustion systems (Swaine and Goodarzi 1995; Finkelman et al. 1990; Finkelman 1999; Clarke 1993). In coal power plants, inorganic elements are either found in bottom ash, are captured by emission control devices, or they exit the system in the stack gas where they can mix and react within the atmosphere and eventually redeposit back to the land (Swaine and Goodarzi 1995).

Elements like mercury, selenium and arsenic are volatile and even at low concentrations can contaminate the air and water. According to the U.S. Environmental and Protection Agency (EPA), mercury is a known neurotoxin that can enter a womb and cause brain damage to children and is also considered a possible carcinogen (Environmental Protection Agency). When in the form of methylmercury (CH_3Hg), mercury is concentrated more than a million times in aquatic life-cycling and can be passed to humans through fish consumption (Schroeder and Munthe 1998). Selenium is hazardous to human respiratory and gastrointestinal organs. Selenium sulfide is a carcinogenic compound, and hydrogen selenide and sodium selenite are listed as extremely toxic by the EPA due to animal laboratory tests. Arsenic is a carcinogen and often enters humans through food and drinking water (Environmental Protection Agency).

As mentioned in Section 2.1, about 90% of the inherent inorganic constituents of crude oil can be measured in the residue after refining processes. If inorganic elements in coal are concentrated in a coal-based transportation fuel, it could be necessary for refineries to remove them during processing so they report to the residue. As for DCL solid products, controlling the emissions when utilizing the residue in a combustion or gasification system will be easier than from mobile sources.

2.3 Direct Coal Liquefaction and Coal Composition

2.3.1 Maceral and Mineral Composition

Numerous studies have been conducted on the dependence of coal rank, maceral composition, and mineral matter in regard to direct coal liquefaction yields ad quality. These studies conclude that different trends can be observed with different variables, such as varying coal rank, coal preparation, maceral composition, sulfur and iron concentration, and mineral composition.

Ideal coal selection for direct coal liquefaction is dependent on the reactivity of the coal. DCL is a process that breaks down the structure of the coal to produce lighter liquid hydrocarbons. Coals that contain more available low-energy bonds are more reactive in DCL and can therefore produce higher liquid yeilds. High-rank coals, like anthracite with large aromatic moieties, are more difficult to cleave than low-to medium-rank coals that contain branching and chain structures. On the other hand, low-rank coals like lignite may be more sensitive to process conditions and can yield heavier, less desirable products. Whitehurst et al. concluded that the best coal rank for DCL is medium-rank coal (Whitehurst

et al. 1980). Low-rank, non-swelling coals, such as the Wyodak coal, often require a catalyst to achieve the conversions of medium rank coals, such as an Illinois No. 6 coal (Lee and Cantrell 1991). It has been found that the ideal coal rank for direct coal liquefaction is a high volatile C bituminous coal, but the coal's rank was not as influential as its maceral content, which reflects its geological organic make-up (Speight 1983).

In general, of the three main maceral groups in a coal's composition, vitrinite and liptinite (exinite) are more susceptible to liquefaction (Given et al. 1975) while inertinite is for the most part resistant to liquefaction. Intertinite contains very high carbon content very lower amounts of hydrogen and volatile matter and therefore does not cleave at moderate temperatures such as those used in DCL. The residue from coal liquefaction therefore contains most of the initial inertinite (Bustin, 1985). Even though some coal macerals are more reactive than others, it was found that the macerals alone do not perform as well in DCL when compared to their performance in the original coal matrix (Keogh et al. 1992). In studies conducted by Given et al., lignite was separated by float-sink methods and the sink fractions produced the highest overall liquefaction conversions when compared to four other coals even though the sink fraction contained higher concentrations of interinites. Their study found that the higher iron concentration in the sink fractions may be the dominant attribute in producing higher overall conversions, and not the maceral content (Given et al. 1975).

The inherent inorganic elements in coals also have an influence on DCL reactions. In several studies, increases in a coal's inorganic content has been associated with increases in

DCL conversion (Whitehurst et al. 1980; Valkovi 1983). Sulfur and iron can influence conversion and this is discussed in the following section. Clays, some transition metals, and alkali and alkaline earth elements may also play an important role in DCL conversion. The catalytic effects of these elements are known in gasification process but are not as well documented in DCL reactions (Schobert 1992). Mukherjee and Chowdhury discussed the catalytic effects of kaolinite and titanium (Mukherjee and Chowdhury 1976). Elements such as titanium, manganese, and calcium can deactivate a nickel/molybdenum catalyst in the hydrocracking of coal extract solution (Cloke et al. 1987a).

Along with coal macerals, the mineral matter in DCL has also been studied. DCL has been studied in joint work from The Pennsylvania State University and the Electric Power Research Institute (Walker et al. 1980). In this study, the mineral matter in SRC residue was compared to that in the initial coal. It was found that for multiple coals in a continuous flow reactor (25lbs/hr/ft^3), the mineral concentrations in the initial coal and in the residue did not show any significant differences. Some of these minerals did undergo changes such as pyrite (FeS_2) to pyrrhotite ($Fe_{1-x}S$; $0 \leq x \leq 0.125$). It was also shown that ion-exchangeable calcium cations in the coal were converted to calcium carbonate in the SRC residues (Walker et al. 1980).

2.3.2 Iron, Sulfur, and Pyrite

The conversion of coal liquefaction has been linked to the coal's initial mineral matter content mainly to the catalytic effects of iron, sulfur, and pyrite (Valkovi 1983). Iron has been thought to dissociate hydrogen from the solvent to allow reuse in future coal runs

(Li et al. 2008). Sulfur can be associated with the organic (i.e., carbonaceous) and the inorganic (i.e., mineral) portions of the coal. Sulfur in mineral forms occurs in sulfates and sulfides (i.e., pyrite) (Thiessen 1945). General trends show that the high-rank coals contain lower amounts of organic sulfur (George et al. 1991; Huffman et al. 1991).

A study of 104 United States coals ranked by sulfur content found an advantage to using medium-rank, high sulfur coal from the Interior province of the U.S. for DCL (Yarzab et al. 1980). Organically bound sulfur during DCL can be reduced to FeS and can directly react with the hydrogen to form hydrogen sulfide during DCL. Pyritic sulfur can also lead to the formation of hydrogen sulfide, and is converted to pyrrhotite (Trewhella and Grint 1987).

Overall, pyrite within the coal is consumed during DCL processes through its conversion to pyrrhotite (Whitehurst et al. 1980). Coals with higher initial pyrite content have higher overall conversions (Given et al. 1975). Richardson reported that the DCL residue specifically contained Fe_7S_8 and unreacted FeS_2 from a pilot hydroliquefaction plant (Richardson 1972); however, (Montano and Granoff 1980) found that the pyrite form was more likely to reduce to $Fe_{10}S_{11}$. It is possible that the difference may be caused by differences in process conditions. This study also observed a relationship between higher overall conversions to higher elemental iron content in the THF insoluble residues (Montano and Granoff 1980).

2.4 DCL Reaction Variables

2.4.1. Catalyst

Because inherent iron and sulfur constituents, specifically the mineral pyrite, can enhance bond cleavage, DCL processes can be improved by the addition of iron/sulfur compounds as catalysts. DCL with a catalyst is called catalytic liquefaction and that without the addition of a catalyst is referred to as thermal liquefaction. Catalysts increase the cleavage of the stronger aromatic cluster carbon bonds (Kaneko et al. 1998). The catalyst can therefore enhance the overall conversions of coals in DCL, specifically those with lower pyrite concentrations. A schematic of the catalytic action in DCL is shown in Figure 3.

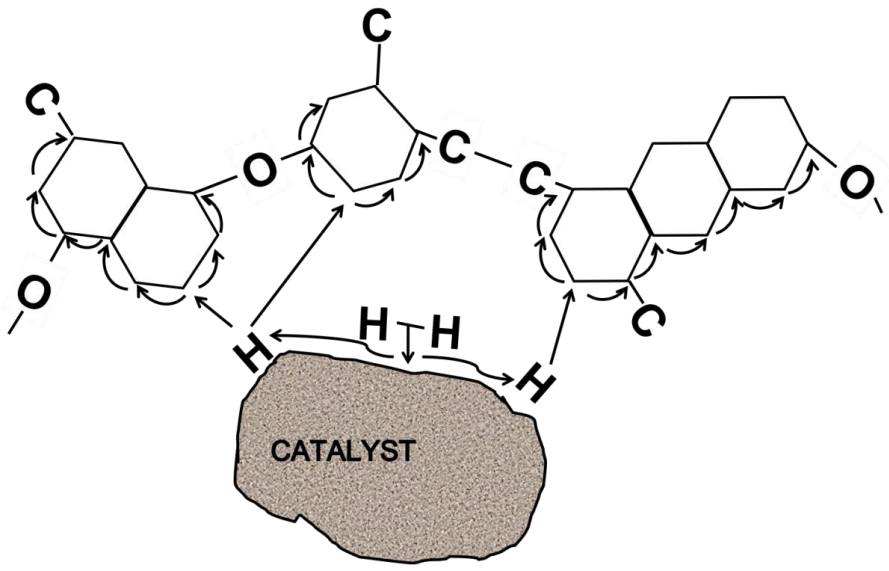

Figure 3: Free H atom in catalytic dissociation of H_2 redrawn from (Derbyshire 1989)

Huffman et al. studied Fe_2O_3 as a catalyst and found that pyrrhotite was the most common post-reactor form of iron after DCL of the Illinois No. 6 and Wyodak coals. Pyrrhotite is most likely formed from the intermediate reaction of hydrogen sulfide and the ferric iron catalyst. The small particle size of the catalyst forms pyrrhotite quickly after its

reaction with hydrogen sulfide even at lower temperatures. This intermediate reaction with hydrogen sulfide is therefore dependent on sulfur concentrations (Huffman et al. 1993). An overabundance of iron or lack of sulfur could lead to the formation of magnetite (Fe_3O_4) (Huffman et al. 1993; Ganguly et al. 1993). Therefore, Fe_3O_4 can be the post-reaction iron state in the residue similar to the pyrrhotite end state for pyrite (Suzuki et al. 1985).

There is disagreement about what the actual catalyst is, i.e., iron-sulfur pyrite or hydrogen sulfide (Guin et al. 1978; Lambert 1982; Guin et al. 1983; Mukherjee and Mitra 1984). The general consensus is that since iron sulfur catalysts are transformed in the DCL reaction, they are not true catalysts.

2.4.2 Reaction Temperature

The process temperature at which coal liquefaction occurs can affect the overall conversion and the product yields for each fraction. For untreated high-sulfur coals, reaction temperatures of 400 °C and below tend to favor the formation of increased preashpaltene and asphaltene yields. DCL above 400 °C favors the formation of oil products (Gozmen et al. 2002). At temperatures above 450 °C, coal liquefaction reactions can lead to coke formation and retrogressive reactions can dominate and have a negative effect on overall conversions (Whitehurst et al. 1980).

In batch coal liquefaction, varying the reactor temperature enhances conversions of low-rank coals. As discussed earlier, the coal is heated to promote bond cleavage. Because coals vary in structure and not all their bonds cleave at the same conditions, some of the bonds, especially those in low-rank coals (e.g. alkanes), are likely to cleave at lower

temperatures. For this reason, it is advantageous to allow the reaction to begin at a lower temperature (< 350 °C) for these bonds to break first. This can allow a period for hydrogenation of the weaker bonds to occur before the temperature increases and the stronger bonds (e.g. aromatics) cleave and undergo their own stabilization. This staged heat-up was found to be beneficial in low-rank coal liquefaction conditions in the absence of good solvents and catalysts (Huang and Schobert 2005).

2.4.3 Reaction Solvent and Hydrogen Gas Pressure

The purpose of the solvent in DCL is to increase hydrogen donation to cleaved bond sites. It has been shown that with the addition of a solvent there may be less need for hydrogen gas and vice versa, as both the solvent and gas promote hydrogen donation (Artok et al. 1994). The hydrogen gas in DCL dissolves into the solvent and reacts with the coal's structure, and the hydrogen gas and solvent can facilitate reactions with the coal's constituents to form water, ammonia, and hydrogen sulfide molecules from the oxygen, nitrogen and sulfur in the coal (Probstein and Hicks 1982).

A solvent is most effective if it can easily diffuse into the coal's pores. Recently research has been conducted on ionic solvents for their abilities to improve contact between coal and catalysts of Illinois No. 6 and PRB coals (Painter et al. 2010). In general, smaller organic solvents, such as methanol, can penetrate into the coal's smaller pores when compared to the tetralin solvent that is used in this thesis (Tye et al. 1985). However, it has been found that for DCL, pure tetralin is a superior solvent over pure methanol (Kuznetsov et al. 1991). It has also been reported that hydroaromatic solvents combined

with a phenolic group allow better interaction between the coal, catalyst and solvent (Orchin and Storch 1948). It has also been found that for the greatest overall conversion a 3:1 solvent-to-coal ratio can be the most effective (Mochida et al. 1989). It has been found that at a 3:1 tetralin solvent-to-coal ratio or higher the effects of hydrogen pressure variations are negligible (de Marco Rodriguez et al. 1998).

In large-scale DCL facilities, the solvents are recycled and are not pure compounds such as tetralin. For the batch DCL tests in this research, it was decided that it was more important to obtain high conversions so that a sufficient quantity of products would be generated for analysis. For this reason, pure tetralin was chosen as the solvent, as it is one of the most commonly used solvents in batch, laboratory-scale DCL research reported in the literature. It is also recognized that the final products generated in this thesis may not be identical to those found in a commercial 2-stage DCL facility, or the Shenhua plant, which can produce products closer to gasoline instead of products which also contain asphaltenes and preasphaltenes, as produced in this thesis (Shui et al. 2010, Robinson 2009).

2.5 Direct Coal Liquefaction Products

The solid and liquid products of direct coal liquefaction are defined by their solubility in specific solvents from lighter hexane soluble fractions to heavier tetrahydrofuran (THF) liquid fractions. The solid, or residue, products can be used in different applications. The DCL liquid product can be used for the production of gasoline and diesel fuel with additional production potentials for jet fuel, utility fuel oil, and other fuel blends. The solid product can be utilized to produce hydrogen via gasification or process heat in a boiler. It has also

been suggested that it may be possible to market DCL residues for metals such as aluminum and vanadium (Pringle and Jervis 1987).

2.5.1 Residue Products

The residue product of direct coal liquefaction varies with the input coal and process condition. It is mostly comprised of non-reactive macerals and inorganic solids (Walker et al. 1980). Inorganic solids in DCL residue have been described as either "unaltered minerals" (i.e., quartz), "altered minerals" (i.e., dehydrated clays) or "neo-minerals" (i.e., carbonate formation) (Mitchell 2008). The overall conversion (THF soluble) has been related to the H/C atomic ratio and organic volatile matter concentration of the residue (Cui et al. 2003). It is important to know the organic composition of the DCL residue to consider its use in a future conversion process. The inorganic content can also affect gasification or combustion efficiency through catalytic effects, and it is important to identify the inorganic composition of the residue due to concerns related to the environment and process equipment.

Direct coal liquefaction residue (DCLR) was studied by Cui et al. (2002) using thermogravemetric analysis. Devolatilization was related to the DCL process conditions and a notable difference between total volatile matter (TVM) and organic volatile matter (OVM) was found (see Table 4). This relationship is due to the presence of volatile inorganic materials in the residue. At 425 °C, volatiles in the residue are lower than that in the 375 °C residues (Cui et al. 2002). It is interesting to note that the difference between TVM and OVM is less for thermal DCL than in catalytic DCL. There is a 5 wt% difference between TVM

and OVM in the thermal processes and more than a 10 wt% difference between TVM and OVM in the catalytic processes for both temperatures. This could imply that there are more volatile inorganics in the catalytic DCL residue, which contains an inorganic iron sulfur catalyst.

Table 4: Total wt% of volatile matter (TVM) and organic volatile matter (OVM) of THF-insoluble residues from DCL with and without a catalyst at 60 min. reaction time, (extracted from (Cui et al. 2002)

DCLR VM Type	375°C	425°C
Thermal TVM	29	20
Thermal OVM	24	15
Catalytic (Fe_2S_3) TVM	32	25
Catalytic (Fe_2S_3) OVM	21	12

Direct coal liquefaction residue can be used to produce hydrogen for the DCL process by gasification with steam. Chu et al. (2006) compared the reactivity of the parent coal, the DCLR and their respective chars. The DCLR contained about twice the ash yield of the parent coal with an increase in concentration of all measured oxides except for alumina, which was reduced from 0.68 to 0.40% and phosphorus pentoxide that remained at 0.01%. Increases in oxide wt% concentrations were observed for SiO_2 (0.94 -> 2.80), Fe_2O_3 (1.08 -> 3.78), CaO (1.74 -> 2.31), NaO_2 (0.09 -> 0.16), MgO (0.23 -> 1.65) and SO_3 (1.48 ->1.65). As for their respective chars, the DCLR char also contained more than twice the ash yield of the parent coal char. The reactivity of DCLR char was found to be lower than that of the parent coal char while the DCLR char surface area also produced higher concentrations of H_2S during gasification due to the formation of pyrrhotite during catalytic liquefaction. The DCLR char's BET surface area was less than 20% of the initial coal char and was less reactive

than the initial coal chars in all the tests. For THF solvent extracted residue, the carbon conversion was even lower in gasification processes (Chu et al. 2006).

2.5.2 Liquid Products

Coal-derived liquids (CDL) are produced from the cleaving and hydrogen capping of the initial coal's structure; therefore, some of the initial coal components are found in the liquid products. Most of the liquids produced in DCL are highly naphthenic and aromatic (Whitehurst et al. 1980). Many of the inorganics in the liquids are likely organically bound (Zhang et al. 2008).

In a study conducted by Herod et al. (2003), a filtered liquefaction extract from a pilot-scale continuous flow reactor was analyzed. They found that the concentration of inorganics in the CDL from different coals did not show any correlation with the oxygen content in the product (Herod et al. 2003). Richaurd et al. stated that the inorganic element distributions in CDL show little relation to their parent coal (Richaud et al. 2000). Herod et al. (2003) fractionated CDL in an attempt to understand the modes of occurrence of individual elements by testing their molecular mass solubility. This was not an easy task and the mass balances of these tests were very poor. Approximately one-fourth of the elements had a recovery of less than 10%. The authors claimed that iron bound as an organometallic species because it did not show up in any solvent (Herod et al. 2003) and this agrees with other studies (Zhang et al. 1996, 2008).

The THF-soluble products of DCL may only have a C/H atomic ratio of 0.7-0.9 (Whitehurst et al. 1980) and contain a higher concentration of nitrogen, oxygen, sulfur, inorganic species, and aromatic compounds when compared to petroleum products. These

liquids would still have to enter refining processes and upgrading to form more marketable transportation liquid fuels (Anderson 1992). After distillation, these liquids contain higher yields of naphtha, kerosene and heavy fuel oils and lower yields of gas oils when compared to natural crude oil yields (Speight 1983). Just as with petroleum refining, certain inorganic metals poison catalysts in nitrogen and oxygen removal processes along with fuel upgrading processes such as catalytic cracking. Additionally, if these inorganic elements are organically-bound in heteroatoms or organometallic compounds they are also more likely to remain in the lighter products of refining, such as the diesel and gasoline fractions (Song et al. 1994; Speight 2001). If this were to occur, then the prior discussed equipment and environmental concerns could be relevant, e.g., poisoning of vehicle exhaust system catalysts and emissions of harmful elements.

Falcone Miller et al. (2008) compared the inorganic emissions of traditional petroleum based No. 6 fuel oil and that of fuel oil comprised of petroleum co-processed with coal when fired in boiler. It was found that the emissions from the combustion of the co-processed No. 6 fuel oil were higher for every measured element on a lb/Btu basis except for V and Ni which are often inherently more concentrated in crude oils (Falcone Miller and Miller 2008). The emissions of some elements of environmental concern are shown in Table 5.

Table 5: Emissions (lb/10^{12}Btu) from traditional No. 6 fuel oil and coal co-processed fuel oil from (Falcone Miller and Miller 2008)

Element	Petroleum Derived Fuel Oil Average	Co-Processed Fuel Oil
As	19.51	224.08
Hg	0.45	2.09
Se	4.33	6.85
Pb	8.95	1580.45

Coal contains more inorganic elements than crude oil and, therefore, increases the emissions when burning co-processed fuel oil. One of the main goals of DCL is to concentrate the coal's mineral matter into the residue for a clean liquid fuel product. Therefore, it is important to understand the partitioning of the inorganic elements during CDL production, which is the focus of this thesis.

2.6 Inorganic Element Partitioning in DCL

Following is a discussion on the distribution of inorganic elements from the feed coal into DCL products. In the late 1970's and early 1980's, solvent refined coal (SRC) pilot plants were constructed to produce low-sulfur utility boiler fuels and later were modified to produce other products such as transportation fuels and combustible gases (Dadyburjor and Liu 2000). Since then, there have not been many detailed studies on the partitioning of inorganic constituents in DCL processes.

The partitioning of inorganic elements was evaluated at a 50 ton/day continuous thermal hydrogenation SRC pilot plant in Fort Lewis, Washington (Filby et al. 1977a). In this study, which was similar to studies on trace elements they performed on crude oil, instrumental neutron activation analysis (NAA) was used. NAA is capable of measuring

trace elements at very low concentrations. In Table 6, the elemental partitionings are shown as calculated percents based on their solubility into the solvent pyridine. Selenium is the element with the highest error with a 189% sum for the solid and liquid streams. This particular research found that the elements As, Sb, Se, Hg, Ni, Co, Cr, and Na are most likely associated with the organic portion of the SRC pyridine soluble liquid just as they are in the initial coal (Filby et al. 1977a).

Table 6: Elemental concentrations in pyridine soluble (PS) and pyridine insoluble (PI) fractions from the Wilsonville Plant (Filby et al. 1977a)

	%PS	%PI	Total
As	6.2	53.5	59.7
Sb	8.9	81.2	90.1
Se	5.8	183	189
Hg	19	48.2	67.2
Br	67.5	30.6	98.1
Ni	8.1	10.9	117
Co	5	86	91
Cr	11.5	122	134
Fe	2.4	97.1	99.5
Na	3.9	81.8	85.7
K	12.6	103	116
Sr	1.7	72.7	74.4
Ba	2.4	78.1	80.5
Tl	2	99.5	102

Research conducted by Coleman et al. (1978) studied trace elements from the Wilsonville continuous flow pilot plant. Here they analyzed the SRC products broken down into THF-soluble and THF-insoluble fractions. They noted that their results differed from those of past work on inorganic distributions specifically with respect to Ca and Fe (Coleman et al. 1978). Their results, obtained by AAS on ashed samples, are shown in Table 7.

.

Table 7: Results from GFAAS analysis of Wilsonville SRC products (Coleman et al. 1978)

Illinois No. 6 Coal	Mg	Al	K	Ca	Cr	Mn	Fe	Co	Ni	Cu	Pb	Cd
THF-Soluble (ppm)	5	81.9	36.8	6207	< 4.4	6.0	133	7.8	15.0	5.6	3.7	0.3
THF-Insoluble (ppm)	69.8	177	-	-	18.2	29.9	1108	5.4	-	9.2	9.33	0.5

Hellgeth et al. (1984) claimed many metals were organically bound in SRC liquids by batch laboratory-scale reactions. Using ICP-AES, 18 inorganic element concentrations were measured in the SRC liquids (separated into pyridine-soluble and pyridine-insoluble) derived from several coal samples from the Wyodak seam. Solvents were also varied, but showed little influence on the partitioning of specific inorganic elements to the SRC liquids. It was also found that toluene solubles (i.e., asphaltenes and oils) contained much lower metal contents when compared to pyridine soluble SRC products. Metal concentrations are shown in Table 8. These products are derived from DCL using the Wyodak coal sample with the most similar characteristics to the PRB coal used in this thesis. The two sets of results are from duplicate runs (Hellgeth et al. 1984).

Table 8: Results from ICP-AES analysis of SRC products in ppmw (Hellgeth et al. 1984)

Wyodak Coal	Ag	Al	B	Ba	Ca	Cr	Cu	Fe	Mg	Mn	Ni	Si	Ti	V	Zn
SRC Run A	1.5	397	31	3.7	1567	1.1	5.6	125.0	391	19	13	113	49	4.2	11
SRC Run B	1.8	285	23	7.8	1230	3.5	2	417	385	15	14	37	24	1.8	13

Pringle and Jervis (1987) conducted multiple studies on the fate of inorganic elements in coal during DCL. They measured 40 inorganic element concentrations by NAA and photon AA in two different feed coals and their coal liquefaction process streams (THF-soluble and THF non-soluble). Bituminous coal that was reacted with hydrogen gas and tetralin resulted in higher percentages of the inorganic elements in the residue and much

less in the oil products. The mass balances of the initial elemental weight to the sum of that found in the residue and oil streams were over 100% for about one third of the elements, most of which are metals such as Ni and Cr with mass balances of 275% and 378%, respectively (Pringle and Jervis 1987). This study is the most similar to that which is conducted in this thesis and a comparison of results is shown in Appendix B and discussed in Section 4.4.1.1.

Cloke et al. (1987) determined that the use of XRD and SEM/EDX to identify mineral matter in direct liquefaction extracts was inappropriate. This equipment, along with possible filtration issues, prevented drawing any conclusions with regard to the mineral matter in the extract solutions (Cloke et al. 1987b). Difficulty in the detection of trace elements in CDL was also an issue in work by Richaud et al. (2000). In their work, 36 elements were analyzed by ICP-MS but only 10 were above the instrument's detection limits (Richaud et al. 2000).

The inorganic content of coal liquefaction products has not been researched in depth within the last 10 years even though DCL facilities are being constructed. The solid residue products have often been studied in detail due to their higher concentrations of inorganic matter, whereas the liquid fractions, which contain lower concentrations of inorganic material, are more difficult to analyze. It is important to determine, and to the extent possible, quantify the redistribution of inorganic elements in DCL, and this thesis, contributes to data and expands on this very significant topic.

3. Methodology

3.1 Experimental

Batch, single-stage direct coal liquefaction tests were conducted at the laboratory scale to assess the behavior of inorganic elements during liquefaction. Ten different tests were conducted. All tests were performed with 5g of coal, and a 3:1 tetralin-to-coal ratio. Depending on the specific conditions to be tested, coal, catalyst, hydrogen pressure and temperature were varied, but the reaction procedure and extraction methods remained constant. Figure 4 is a generalized flowchart of the procedure with the conditions for the baseline tests. The following sections will include details on the experimental aspects of this work.

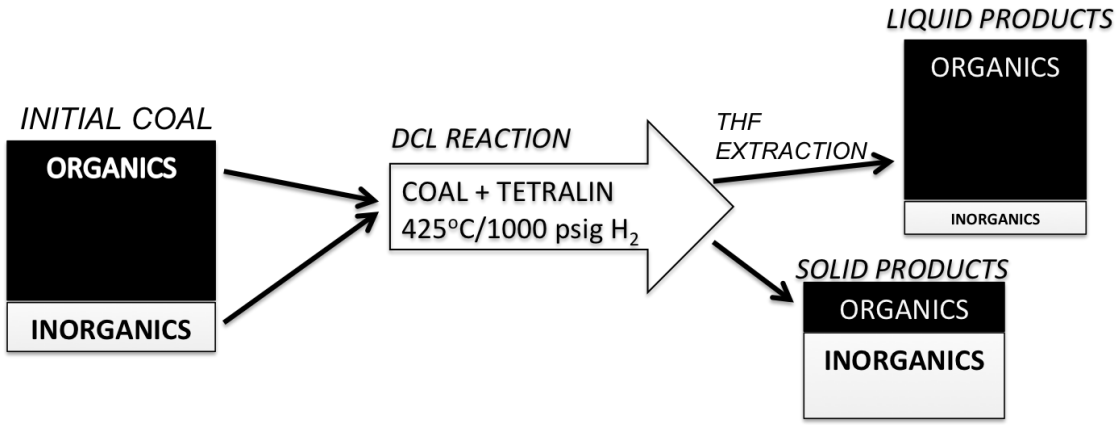

Figure 4: Schematic of coal conversion to DCL products

3.1.1 Coal Preparation

Two coals from the United States were chosen for this study: Dietz seam Powder River Basin (PRB) subbituminous coal from Big Horn County, Montana (DECS-38, PSOC-1578) and Illinois No. 6 seam (IL#6) bituminous coal from Macoupin County, Illinois (DECS-24, PSOC-1564), both from The Pennsylvania State University Coal Sample Bank. For this

thesis, the coals were pulverized to 100% minus 200 mesh (74 microns). It is known that in DCL the coal and catalyst must come into contact. If the coal particle size is larger than the catalyst, then the catalyst can potentially enter the coal's pores, and if the catalyst is larger the coal can enter the catalyst's pores (Speight 1983). For this reason, the FeS catalyst used was minus 100 mesh (150μm) enhancing the surface contact area of the coal and the catalyst. Before and after preparation and in between all tests, the coals were stored in sealed bags in argon gas (Glick et al. 2005).

3.1.2 Dense Media Separation

Cleaned Illinois No. 6 coal (CL_IL#6) used in these experiments was prepared by dense media seperation. Dense media separation relies on the various specific gravities of the materials that comprise coal and can also be referred to as gravity separation or float-sink. If the media's density is properly chosen, a clear distinction can be observed with the "cleaned" coal floating to the top and the mineral matter, along with some coal/mineral matter particles, sinking to the bottom. Many inorganic elements are associated with the pyrite in Illinois No. 6 coal (Huggins et al. 2009), thereby leading to similar reductions as that of pyrite. Luttrell et al. (2000) found that pyritic sulfur reduction from float-sink cleaning of Illinois No. 6 coal correlates with reductions of arsenic, cadmium, mercury, chromium, cobalt, lead, and nickel. Reductions in manganese, lead and cobalt correlated more with the total percent ash yield reduction rather than pyrite reduction (Luttrell et al. 2000).

In this study, mixtures of perchlorethylene and toluene were tested as separation media to determine the required density for a targeted 50% mineral matter reduction in the

cleaned coal product. The appropriate density was found to be 1.478 g/ml for this Illinois No. 6 coal which resulted in a clear separation as shown in Figure 5.

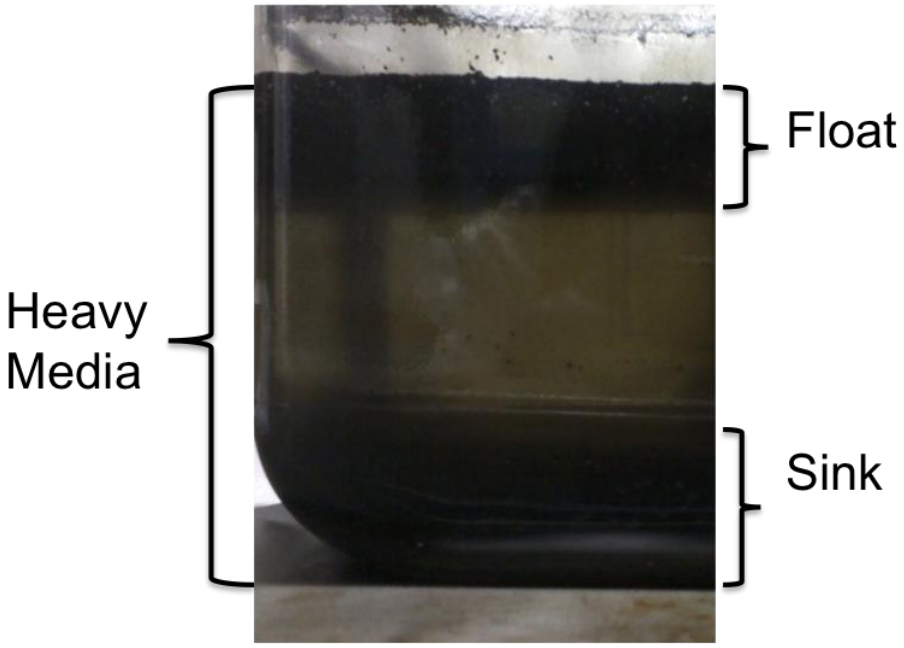

Figure 5: Float-sink separation of Illinois No. 6 coal

Final gravity separation was performed with dried, minus 60 mesh (250 micron) coal. The coal cleaning resulted in a 68.8% coal recovery (collected float) and a 58.5% ash yield reduction (dry basis). After separation, the float (the cleaned coal) was left to dry in an air drying oven. The cleaned coal was then pulverized to 100% minus 200 mesh for the experiments.

3.1.3 Batch Liquefaction Tests

Laboratory-scale batch liquefaction tests were conducted in #316 stainless steel, 1¼-inch (3.175cm) inner diameter, 100-mL volume microreactors. Each reactor was used no more than twice to minimize contamination (which will be explained in more detail later),

and consisted of a built-in pressure gauge and a quick connect gas inlet/outlet. A picture of this microreactor, with approximate length dimensions, is shown in Figure 6. Chemical elemental maximum limits for #316 stainless steel piping are given in Table 9 (Oberg et al. 1992).

Table 9: Chemical maximum limits for #316 Stainless Steel, %

Carbon	Manganese	Phosphorus	Sulfur	Silicon	Nickel	Chromium	Molybdenum
0.08	2.00	0.040	0.030	1.00	14.0	18.0	3.0

All microreactor experiments were conducted with 5g of coal. In selected tests, catalyst was added at 3% by weight. The catalyst used was a minus 100 mesh size iron(II) sulfide, with 99% purity (metals basis). The liquefaction solvent tetralin (1,2,3,4-tetrahydronaphthalene with 98+% purity) was then added at a 3:1 solvent-to-coal weight ratio. The reactors were sealed using a lead-based anti-seize. After being sealed, the reactors were flushed three times with nitrogen gas and then twice with hydrogen gas before the final hydrogen gas was introduced and the system pressurized.

Reactions occurred in a sandbath coupled with a Techne temperature controller. For all experiments, the bath was pre-heated to the desired temperature before immersing the reactors. Inserting the reactors initially lowered the bath temperature, but all tests were run for 60 minutes starting from the time when the bath reheated to the desired temperature. After 1 hour, the reactors were removed from the sand bath, cooled by immersion in water, and the gases were released into a fume hood.

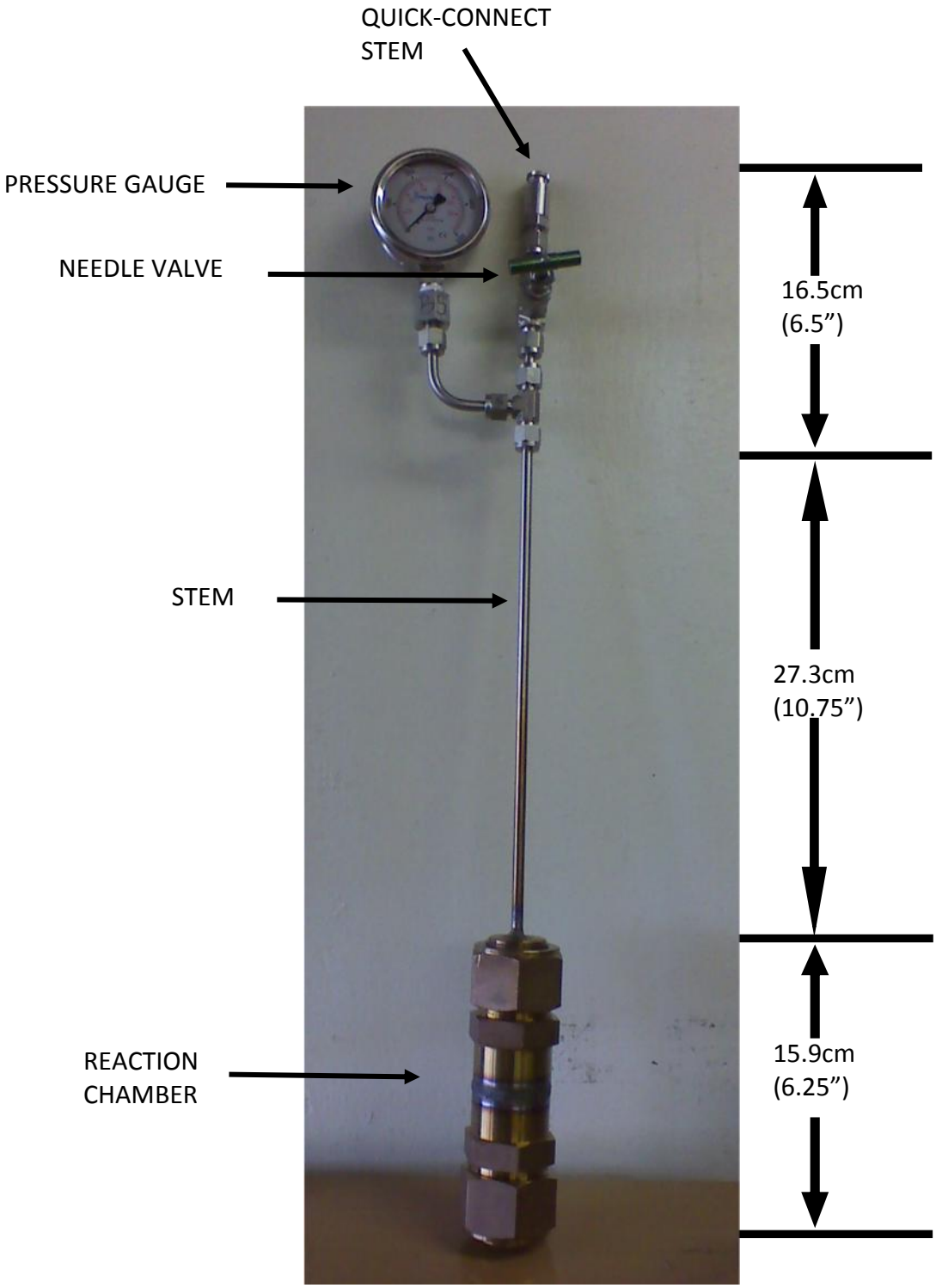

Figure 6: Photograph of the 100mL microreactor

3.1.4 Product Extraction

Products from microreactor liquefaction tests were removed from the reactor at room temperature using 99.9% tetrahydrofuran (THF) solvent (99.9% pure with standards of water-0.05% max; residue after evaporation-0.03% max), and were filtered though a Whatman cellulose extraction thimble with 10.0µm nominal particle retention. Soxhlet extraction was then conducted with 100% aluminum oxide Boileezers, until recycling liquids were clear. After the liquids were clear, the thimble was removed and placed in a vacuum oven until the solids were dry. These solids are referred to as the liquefaction *residue* product. Liquids from the Soxhlet extraction were filtered again using a Whatman No. 4 qualitive cellulose filter paper, with 20-25µm particle retention. After this post-Soxhlet filtering, liquids were then rotary evaporated for the removal of excess THF until the weight change was less than 0.5grams/hour, or a maximum of 3 hours, which was based on equipment limitations. This final liquid product is referred to as the liquefaction *liquid* product. Both final residue and liquid products were stored in certified sterile glassware and kept refrigerated until analysis.

3.1.5 Reaction Variables and Test Nomenclature

After several practice test runs, three microreactor experiments were run simultaneously with similar test conditions (3RunA, B, and C) to determine reproducibility. After these pre-tests were completed, ten experiments were conducted varying coal rank, catalyst, temperature, and pressure; and, in the case of the Illinois No. 6 coal, the quantity and quality of the coal minerals. Table 10 lists these tests along with their nomenclature.

This nomenclature is used throughout the thesis to identify the tests. Each test grouping, separated by horizontal lines, was run concurrently.

Baseline tests 1A and 1B were conducted with the FeS catalyst at 425 °C and 6.9 Mpa (1000 psig) of H_2 pressure with the as-received parent coals. Additionally, two blank tests were run using two different zirconium(IV) oxides in replacement of the coal and catalyst. These tests, with zirconium oxide, were otherwise conducted in exactly the same manner as the baseline test runs and they were performed to investigate possible contamination from the equipment (e.g., reactor, anti-sieze, and glassware).

Table 10: Microreactor test list with notations

Notation	Condition Description	Coal	Catalyst (y/n)	Temperature °C	Pressure MPa
3RunA	Reproducibility A	IL#6	Y	400	6.9
3RunB	Reproducibility B	IL#6	Y	400	6.9
3RunC	Reproducibility C	IL#6	Y	400	6.9
Zr100	100 mesh ZrO_2 blank run	ZrO	N	425	6.9
Zr325	325 mesh ZrO_2 blank run	ZrO	N	425	6.9
1A	PRB Baseline Run	PRB	Y	425	6.9
1B	IL#6 Baseline Run	IL#6	Y	425	6.9
2A	PRB No Catalyst	PRB	N	425	6.9
2B	IL#6 No Catalyst	IL#6	N	425	6.9
3A	PRB Low Temperature	PRB	Y	370	6.9
3B	IL#6 Low Temperature	IL#6	Y	370	6.9
4A	PRB High Pressure	PRB	Y	425	7.9
4B	IL#6 High Pressure	IL#6	Y	425	7.9
5B	Clean IL#6 Baseline Conditions	CL_IL#6	Y	425	6.9
6B	Clean IL#6 No Catalyst	CL_IL#6	N	425	6.9

Batch liquefaction tests were conducted using Dietz seam subbituminous B coal from the Powder River Basin (PRB) in Montana (coal A) and Illinois No. 6 high volatile bituminous coal C from Illinois (Coal B). Baseline tests (1) were run with an iron sulfide catalyst at 425 °C at ~6.9 MPa (1000 psig) pressure for both as-received coals. Additional tests were run without the addition of a catalyst (2), at a lower temperature of 370 °C (3), and at a higher pressure of ~7.9 MPa (1150 psig) H_2 (4). Additionally the Illinois No. 6 coal was cleaned using float-sink gravity separation and run at baseline conditions with a catalyst (5), and without a catalyst (6).

3.2 Analytical

3.2.1 Coal Characterization

The two coals (3 samples), Montana PRB (PRB), Illinois No. 6 (IL#6), and cleaned Illinois No. 6 (CL_IL#6), were characterized by ASTM D-3172 for proximate analysis (ASTM-D-3172 2009) in a Leco Thermogravimetric Determinator with MAC-400 Control Electronics. Proximate analyses were conducted on the coals and the chemical fractionation residues. Ultimate analyses (ASTM-D3176 2009) were conducted on the three samples using a Leco TruSpec CHN for carbon, hydrogen and nitrogen. A Leco SC-144DR was used for sulfur analyses. Oxygen was calculated by difference.

3.2.2 Inorganic Elemental Analysis

To measure the inorganic element concentrations in the coals, liquefaction residue, and liquid products, three analytical devices were used in this thesis: a Perkin-Elmer Model 5100 flame and graphite furnace atomic adsorption spectrometer (FAAS and GFAAS); a Perkin-Elmer Optima 5300 UV inductively coupled plasma atomic emission spectrometer (ICP-AES); and a DMA-80 Direct Mercury Analyzer. Both ICP-AES and GFAAS are common analytical techniques for coal and crude oil analysis and they have been used to determine inorganic element concentrations in coal liquefaction products (Taylor et al. 1981; Hausler et al. 1981; Brown et al. 1982; Hellgeth et al. 1984). A list of the elements studied in this thesis and analytical technique used to measure them is given in Table 11.

.

Table 11: Analytical techniques used for various elements

Analytical Technique	Elements Analyzed per Technique																	
GFAAS	Ag	As	Be	Cd	Co	Cr	Cu	Mn	Mo	Ni	Pb	Sb	Se	Sn	Te	Tl	V	Zn
FAAS	Fe	K	Na															
ICP	Al	Ba	Ca	Mg	S	Si	Sr	Ti	P									
DMA-80	Hg																	

In ICP, along with AAS, the sample must first be diluted in a solution usually of water and strong acid(s). Prior to all AAS and ICP analyses in this thesis, samples underwent microwave digestion. Microwave digestion (EPA Method 3050) is a preparation method used to achieve more accurate measurements of inorganic elements in oil and coal-derived samples as it prevents the loss of volatile inorganics prior to analysis (Nadkarni 1984). This procedure consisted of immersing the sample in water and placing it into a pressured vessel in a microwave where it was heated to 180 °C. After heating, the vessel was cooled, the gasses were released, and the sample was mixed with 8mL of nitric acid and 2mL of hydrochloric acid. The sample was then diluted with water to 100mL for analysis. For reproducibility tests (3Run), 1A, 1B, 2A, and 2B, the amount of sample used for analysis was 0.5g, but this was later increased to 1g to increase the concentration of elements of interest above the detection limits of the analytical equipment.

3.2.3 Chemical Fractionation

Chemical fractionation was performed on the coals to determine which elements in the coals were ion-exchangeable, acid-soluble, or acid-insoluble. The coals were fractionated in duplicate in three solvents: deionized water (H_2O), 1M ammonium acetate

($C_2H_3O_2NH_4$), and 1M hydrochloric acid (HCl). A schematic of the three rinse steps is shown in Figure 7. An initial 50 grams of coal is mixed with 250mL of deionized water and then placed on a heated stir-plate for 24 hours at 60°C. The mixture was then vacuum filtered and rinsed with deionized water three times. Pictures of these steps are shown in Figure 8. Residues were placed in an oven at ~90°C for two days or until dry. When dry, 10g of the remaining coal were removed for analysis along with the filtered solvent and the steps were repeated with the next solvent and the remaining coal.

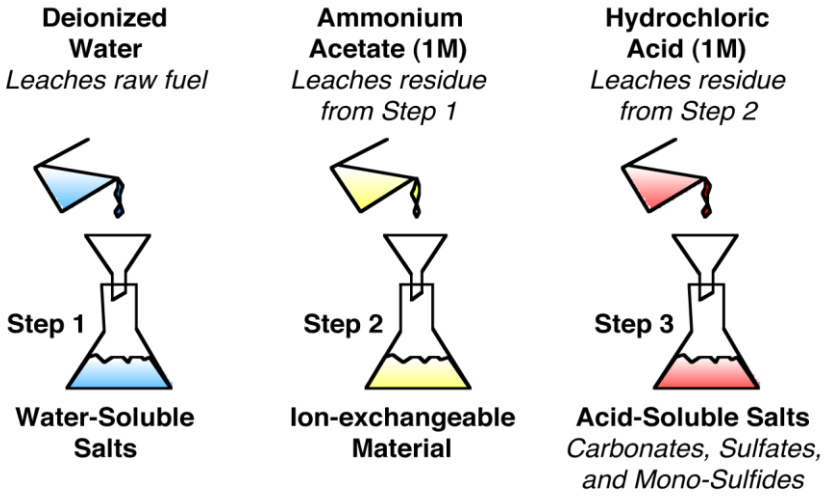

Figure 7: Schematic of the chemical fractionation procedure (Falcone Miller and Miller 2005)

The ICP and AAS analyzes were used to analyze the solid and liquid products from the chemical fractionation procedure. The water and ammonium acetate leachate samples were acidified via nitric acid addition to ensure that no precipitate formed prior to analysis. Proximate analysis was also performed on the solid products.

Figure 8: Photographs of steps from the chemical fractionation procedure. Liquid leaching wash is on the left and vacuum filtration is shown on the right

3.2.4 CCSEM Analysis

The coals were analyzed by computer-controlled scanning electron microscopy (CCSEM) at the University of North Dakota's Energy & Environmental Research Center to determine their mineral composition and particle size distribution. CCSEM analysis is comprised of multiple processes where the sample is first prepared in a cross-sectioned, polished wax plug and scanned via a SEM. Details of the CCSEM methodology are provided in Appendix C and further details of the procedure and calculations can be found in previous work (Falcone Miller 1992).

3.2.5 Residue Ash Yield Analysis

Due to the small product yields, ash concentrations of the liquefaction residues were measured using a Perkin-Elmer TGA-7 Thermogravimetric Analyzer coupled with a Perkin Elmer Thermo Analysis Controller TAC 7/DX. Each test was run according to ASTM ash measurement standard procedure D1374 and initial weights of the residue averaged around 10 to 13 mg (ASTM Standard D1374, 2009). This ash yield was used to determine liquefaction conversions and to evaluate inorganic behavior. By calculating the total oxide weights of the inorganic elemental analysis and comparing it to that of the ash yield, any major analytical discrepancies could be determined. The inorganic elemental sum should be higher since the evaluation does not lose volatiles as the TGA does, but this difference can be considered in such comparisons. For this work, closures in the range of 85 – 125 % were considered acceptable.

3.3 Calculations

3.3.1 Liquefaction Conversions

Direct liquefaction conversions were calculated using the equation from Orchin and Storch (1948). This equation, Equation 2, is the overall liquefaction conversion, which includes the THF-soluble product (Orchin and Storch 1948).

$$\%\ \boldsymbol{Liquefaction} = \mathbf{100}\left[\frac{\boldsymbol{weight\ of\ residue} \times (\mathbf{100} - \%\ \boldsymbol{ash\ in\ residue})}{\boldsymbol{weight\ of\ dry,\ \ ash\text{-}free\ coal}}\right] \quad \textbf{[Equation 2]}$$

3.3.2 Inorganic Element Partitioning

The partitioning of inorganic elements during DCL is the main focus of this research and is defined by the percent of the initial weight of each elements that is found in the product. For an example, the measurements for potassium (K) are shown in Table 12. The total weights of the stream include the total weight of coal in the reactor, the total weight of the residue product, and the total weight of the liquid product for this specific test, 1A. The measured concentration is the concentration of K as measured by AAS.

Table 12: Potassium raw data for test 1A

Stream	Total Wt. of Stream (g)	K Concentration (wt%) per Stream
Coal	5.0053	0.014%
Residue	0.8730	0.078%
Liquid	16.2564	0.0002%

Equation 3 was used to calculate the partitioning of a specific element to the residue. The partitioning to the liquid product was calculated using Equation 4. The liquid is defined as the total THF soluble liquid.

$$residue\ partitioning\ \% = \left[\frac{(wt.\ of\ \ residue \times wt.\%\ of\ \ element\ in\ residue)}{(wt.\ of\ \ coal\ in\ reactor \times wt.\%\ of\ \ element\ in\ initial\ coal)} \right]$$

[Equation 3]

$$liquid\ \ partitioning\ \% = \left[\frac{(wt.\ of\ \ liquid \times wt.\%\ of\ \ element\ in\ liquid)}{(wt.\ of\ \ coal\ in\ reactor \times wt.\%\ of\ \ element\ in\ initial\ coal)} \right]$$

[Equation 4]

By using equations 3 and 4 for both the residue and liquid products for K of test 1A, the following results are obtained:

Table 13: Potassium partitioning for test 1A

Stream	% Partitioning
Residue	97.17
Liquid	4.64
Total	101.81

Table 13 shows the percent partitioning of K to the residue and liquid products measured in test 1A as well as the sum of the residue and liquid percents. This is not "closure" because the gaseous products were not measured in this work; the sum of the residue and liquid partitioning are here referred to as "total." It should also be noted that the number of significant figures in the original data was maintained in all calculations to ensure that the limitations of the equipment were recognized and applied throughout. All the significant figures reflect the analytical detection limits, analytical bias, precision and the equipment's data reproducibility.

4. Results and Discussion

4.1 Feed Coal Characterization and Mineral Analysis

4.1.1 Coal Compositions

Proximate analysis results of the tests coals are given in Table 14. Table 15 lists the ultimate analyses for the three feed coals.

Table 14: Proximate analysis results for the coals on an as-received basis, wt%

	Location	Seam	Rank	Volatile Matter	Fixed Carbon	Ash	Moisture
PRB	Bighorn County, MT	Dietz Seam	subB	34.13	41.19	3.68	20.31
IL#6	Macoupin County, IL	Illinois #6 Seam (Harrin Seam)	hvCb	32.59	42.37	11.58	13.64
CL_IL#6	Macoupin County, IL	Illinois #6 Seam (Harrin Seam)	-	39.65	50.24	5.53	4.58

Table 15: Ultimate analysis results for the feed coals on a dry basis, wt%

	Carbon	Hydrogen	Nitrogen	Sulfur	Ash	Oxygen (by diff)
PRB	75.56	4.71	1.57	0.84	4.66	12.66
IL_#6	66.50	5.32	0.97	6.00	13.38	7.83
CL_IL#6	72.21	4.46	1.03	3.44	5.80	13.06

An initial elemental analysis was conducted on the coals and the results are shown in Table 16 in part per million weight units (ppm), and parts per billion weight units (ppb) for mercury. As stated in the methodology section, these elements were analyzed by AAS and ICP techniques with a maximum analytical error of 3%. The elemental detection limits of the AAS and ICP equipment are listed in Appendix D.

Table 16: Inorganic elemental analysis of the coals in ppm (µg/g) and ppb for Hg (ng/g) on an as-received whole coal basis

ppm	Al	Ca	Fe	K	Mg	Mn	Na	S	Ti
PRB	630	2,500	940	140	390	12	940	3,800	350
IL#6	8,000	4,600	22,500	1,380	240	58	900	51,500	810
CL_IL#6	3,000	20	6,800	1,100	48	14	960	33,000	440

ppm	As	*Hg (ppb)*	Mo	Ni	Pb	Se	V	Zn
PRB	1.2	50	22	3.2	720	0.4	11	60
IL#6	1.6	100	28	50	360	1.8	26	100
CL_IL#6	1.3	38	5	8.5	45	1.0	20	62

The IL#6 coal, with the highest ash yield, also contained much higher concentrations of the inorganic elements. The only elements with higher concentrations in the PRB coal were Pb, Mg and, Na. The CL_IL#6 coal had low concentrations of several elements, specifically Ca, Mg, and Pb

For reference, Table 17 lists the inorganic elements on an oxide, ash basis. High concentrations of Fe_2O_3 and SiO_2 were reported in the Illinois coals, whereas in the PRB coal the concentrations of reported oxides such as Al_2O_3 and CaO were higher.

Table 17: Major and minor oxide weight percents for feed coals, ash basis

Wt% Oxide, ash basis

	Al_2O_3	BaO	CaO	Fe_2O_3	K_2O	MgO	MnO	Na_2O	SiO_2	TiO_2
IL#6 Coal	15.82	0.05	7.37	32.97	1.71	0.77	0.06	1.20	45.26	0.95
PRB Coal	20.02	1.61	21.29	7.31	0.85	7.61	0.05	4.58	33.13	1.68
CL_IL#6 Coal	10.25	0.05	0.05	17.58	2.40	0.14	0.03	2.34	29.78	1.33

4.1.2 Chemical Fractionation

Chemical fractionation was conducted in duplicate on the coals to determine which inorganic constitutes were water soluble (WS), ion exchangeable (IE), acid soluble (AS) or acid insoluble (AIS). Duplicate test results showed good agreement with most differences averaging ±4%. The exceptions were Mg in the IL#6 coal and As in the PRB coal; in these two instances the duplicate tests differed by more than 15%.

Some elements, such as Zn and Pb, were consistently near 100% soluble in the water washes. Elements such as Al, Fe, and V were found AIS for all of the tests, and at least 40% of their initial weight remained in the residue after all of the rinses. Chemical fractionation results are shown graphically in Appendix E. An abridged chart of the results is provided in Table 18. In this table, elements are listed as predominantly WS, IE, AS, or AIS. The "predominant" occurrence was defined as greater than 40%, by weight of the initial element, removal at that stage during chemical fractionation. Elements of mixed occurrence are listed in multiple categories (i.e., >40%, by weight occurring in 2 categories). In the CL_IL#6 fractionation, Mn was split into three categories of ~30% by weight for each fraction.

These percents are fractions of the initial elemental weights present in the parent coal. Most elements leached over 40% of their initial weight within the first two washes using water and ammonium acetate. Water-soluble elements can be present as water soluble salts.

Table 18: Chemical fractionation results of the coals. Elements are listed if portion was over 40%. WS – Water Soluble, IE - Ion Exchangeable, AS - Acid Soluble, and AIS - Acid Insoluble

	PRB COAL				IL#6 COAL				CL_IL#6 COAL			
	WS	**IE**	**AS**	**AIS**	**WS**	**IE**	**AS**	**AIS**	**WS**	**IE**	**AS**	**AIS**
Al	-	-	-	Al	-	-	-	Al	-	-	-	Al
Ca	-	Ca	Ca	-	-	Ca	-	-	Ca	-	-	-
Fe	-	-	Fe	Fe	-	-	-	Fe	-	-	-	Fe
K	K	-	-	-	-	-	-	K	-	-	-	K
Na	-	Na	-	-	Na	Na	-	-	Na	-	-	-
Mg	-	Mg	-	-	**-**	**-**	**Mg**	**Mg**	Mg	-	-	-
Mn	-	-	Mn	-	-	Mn	-	-	*Mn*	-	*Mn*	*Mn*
Pb	Pb	-	-	-	Pb	-	-	-	Pb	-	-	-
Ti	-	-	-	Ti	-	-	-	Ti	Ti	-	-	-
Zn	Zn	-	-	-	Zn	-	-	-	Zn	-	-	-
As	**-**	**As**	**-**	**As**	As	-	As	-	As	-	-	-
Hg	-	Hg	-	Hg	Hg	-	-	Hg	Hg	-	-	-
Mo	Mo	-	-	-	Mo	-	-		Mo	-	-	-
V	-	-	-	V	-	-	-	V	-	-	-	V

-Results in bold red are noted for their inconsistency between duplicate tests

Ammonium acetate removes the cations bound to carboxylic acid groups within coal structure. The main elements that were found to leach in this solvent were Ca, Na, Mg, and Hg for the PRB coal and Ca, Na and Mn for the IL#6 coal. No element was identified as being greater than 40% ion exchangeable in the CL_IL#6 coal. Sodium and Mn were shown to be 25% and 15% ion exchangeable, respectively. Therefore, from these results and from the reductions in mineral matter from coal cleaning, it may be concluded that for these samples the cleaning of the coal removed organically bound inorganic elements from the acid groups, specifically those containing Ca and Mn.

Acid soluble and acid insoluble elements are not organically bound to the coal's structure, but are present within the mineral matter portion of the coal. In all the coals, Al was acid insoluble and is therefore most likely associated with the clay in the coal. Iron was

also not leached out in the first two washes and is therefore present in sulfides and sulfates. In the IL#6 coals, K was acid-insoluble; therefore, the K in these coals is most likely present within the silicates, possible present in the mineral Illite.

4.1.3 Mineral Analysis

Mineral analyses were conducted on the three feed coals by the use of a CCSEM as previously discussed. Results for each sample are composed of three components. The results divide the minerals into size categories, and their sum calculates the total percent of the mineral on a mineral matter basis. Information was also given on the percent of the total that was found to be extraneous in the sample. Extraneous mineral matter is present as individual particles not inherently associated within a coal particle. Table 19 shows the data obtained by CCSEM.

Comparing these CCSEM results to the chemical fractionation results, it was noted that the Ca containing minerals such as calcite and dolominte are more often found to be extraneous in the CL_IL#6 sample compared to the IL#6 sample, possibly due to separation brought forth from the cleaning. It was advised that this particular CCSEM analysis does not do a good job of differentiating from pyrite, pyrrhotite, and oxidized pyrrhotite and that they should all be totaled (D. McCollar, 2010). Both the PRB and CL_IL#6 coals measured about 76% of their pyrite as extraneous, while the IL#6 coal only had 59% of its total pyrites as extraneous. The net pyrite wt% of the IL#6 coal was 38.7% on a mineral basis, and for the cleaned coal the net wt% was 27.3%. This shows a net decrease in extraneous pyrite due to coal cleaning. These data suggest that the pyrite in the IL#6 coal was more finely disseminated within the coal compared to the PRB and CL_IL#6 coals.

Table 19: CCSEM results of coal mineral concentrations as wt% of total mineral matter and the percent of that total which was found to be extraneous

	PRB		IL#6		CL_IL#6	
MINERAL	TOTAL	EXTRANEOUS	TOTAL	EXTRANEOUS	TOTAL	EXTRANEOUS
QUARTZ	20.9	59.2	7.2	7.7	17.2	39.4
IRON OXIDE	0.7	21.5	0.4	46.3	0.0	0.0
PERICLASE	0.0	0.0	0.0	0.0	0.0	0.0
RUTILE	1.0	67.5	0.2	31.2	0.0	0.0
ALUMINA	1.0	93.6	0.0	0.0	0.0	0.0
CALCITE	0.1	0.0	9.9	51.6	0.4	82.1
DOLOMITE	0.0	0.0	0.1	0.0	0.2	89.9
ANKERITE	0.0	0.0	0.0	0.0	0.0	0.0
KAOLINITE	21.7	37.8	3.0	6.9	4.3	34.9
MONTMORILLONITE	4.3	10.6	1.8	9.0	3.2	22.5
K AL-SILICATE	2.9	64.7	3.3	8.0	6.0	28.7
FE AL-SILICATE	1.5	61.9	0.5	8.3	0.2	30.3
CA AL-SILICATE	0.9	0.0	0.0	0.0	0.0	0.0
NA AL-SILICATE	0.0	0.0	0.1	17.2	0.3	39.2
ALUMINOSILICATE	0.6	50.9	0.1	8.9	0.1	10.9
MIXED AL-SILICA	0.7	12.0	0.6	16.7	0.1	23.4
FE SILICATE	0.0	0.0	0.0	0.0	0.0	0.0
CA SILICATE	0.1	86.8	0.1	100.0	0.0	0.0
CA ALUMINATE	0.0	0.0	0.0	0.0	0.0	0.0
PYRITE	0.1	100.0	1.1	59.0	1.2	60.1
PYRRHOTITE	23.2	77.0	60.8	58.7	35.4	76.3
OXIDIZED PYRRHO	2.1	61.4	2.6	62.9	0.6	89.8
GYPSUM	0.8	63.0	0.0	0.0	0.0	0.0
BARITE	1.4	54.1	0.0	0.0	0.0	0.0
APATITE	0.0	100.0	0.5	67.1	0.0	0.0
CA AL-P	1.4	8.4	0.0	0.0	0.0	0.0
GYPSUM/BARITE	0.0	0.0	0.0	0.0	0.0	0.0
GYPSUM/AL-SILIC	0.6	3.9	0.0	100.0	0.0	0.0
SI-RICH	1.5	48.0	1.3	18.6	2.9	25.1
CA-RICH	0.0	0.0	0.1	11.6	0.1	12.4
CA-SI RICH	0.0	0.0	0.0	0.0	0.0	0.0
UNCLASSIFIED	12.4	66.5	6.3	13.8	28.0	14.1
TOTAL PYRITE	25.4	75.8	64.5	58.9	37.2	76.0

To compare these numbers on a whole coal basis rather than a mineral matter basis, Table 20 was prepared. A mineral matter percent was given as it was calculated from the CCSEM analysis. The totals for each coal are, in general, about 2% higher than the ash

percent shown in Table 14. This was is due to the assumptions made with the CCSEM analyses in order to calculate wt% from area% based on assumed densities (see Appendix C). Because there is a specific ASTM analysis procedure that defines coal ash content, the ASTM values are the ones used for all calculations.

Table 20: CCSEM results of total mineral wt% concentration on a whole coal basis

MINERAL	PRB TOTAL	IL#6 TOTAL	CL_IL#6 TOTAL
QUARTZ	0.77	0.83	0.95
IRON OXIDE	0.03	0.05	0.00
RUTILE	0.04	0.02	0.00
ALUMINA	0.04	0.00	0.00
CALCITE	0.00	1.15	0.02
DOLOMITE	0.00	0.01	0.01
KAOLINITE	0.80	0.35	0.24
MONTMORILLONITE	0.16	0.21	0.18
K AL-SILICATE	0.11	0.38	0.33
FE AL-SILICATE	0.06	0.06	0.01
CA AL-SILICATE	0.03	0.00	0.00
NA AL-SILICATE	0.00	0.01	0.02
ALUMINOSILICATE	0.02	0.01	0.01
MIXED AL-SILICA	0.03	0.07	0.01
CA SILICATE	0.00	0.01	0.00
GYPSUM	0.03	0.00	0.00
BARITE	0.05	0.00	0.00
APATITE	0.00	0.06	0.00
CA AL-P	0.05	0.00	0.00
GYPSUM/AL-SILIC	0.02	0.00	0.00
SI-RICH	0.06	0.15	0.16
CA-RICH	0.00	0.01	0.01
UNCLASSIFIED	0.46	0.73	1.55
TOTAL PYRITES	0.93	7.47	2.06

The second set of results from the CCSEM analysis provides information on the sizes of the extraneous portion of the minerals and the average elemental composition of each of

the minerals using twelve inorganic elements: Si, Al, Fe, Ti, P, Ca, Mg, Na, K, S, Ba, and Cl. These results can be found in the Appendix F.

Combining the data from the mineral's elemental composition and size information, comments about elemental modes of occurrences and their size can be made. Iron bound to pyrite was found to be in certain size fractions within the coals as shown in Table 21. The elemental Fe in the mineral pyrite (pyritic Fe) was mostly in the larger size fractions of 22-100µm for the PRB coal. Most of the pyritic Fe in the IL#6 coal was found to be in smaller fractions, i.e., in the particle range of 10-46µm. Most of the pyritic Fe in the CL_IL#6 coal was found in the size fraction range of 4.6-46µm. This is due to the coal cleaning process which removed more of the larger sized pyrite particles. This is desirable because the smaller pyritic iron particles have more surface area and can be active in DCL.

Table 21: Percent of pyritic Fe measured in different size fractions by CCSEM (microns)

%Pyrite Fe	**1.0-2.2**	**2.2-4.6**	**4.6-10**	**10-22**	**22-46**	**46-100**	**TOTAL**	**EXTRANEOUS**
PRB	1.35	1.66	1.57	1.25	3.82	3.78	14.10	72.96
IL#6	1.47	2.12	5.01	8.37	11.33	4.95	33.26	76.71
CL_IL#6	1.38	1.31	4.29	5.59	4.48	1.28	18.33	77.05

4.2 DCL Testing and Analysis

4.2.1 Confidence in Elemental Analysis in DCL

This thesis obtained measurements for 31 inorganic elements; however, only 16 elements were chosen for detailed discussion. All elements are listed in Table 22 where the shaded elements represent elements that were analyzed but not discussed. Some elements are not discussed due to their concentrations being below or near the analytical detection

limits and/or their concentrations being influenced by equipment contamination. The coals had low concentrations of Be, P, Sb, Sn, Te and Tl and, with such small concentrations in the initial coal, it was difficult to have confidence in their partitioning results upon liquefaction. Metals such as Ag, Sr, Cd, Co, Cr, Cu, and Ni are also not discussed because of measurement issues potentially caused by equipment contamination. These elements increased in mass from the initial coal to the mass in the products. Selenium also had low concentrations in the initial coals but it is discussed because of its importance in environmental issues and comments will be made for results whenever there is lower confidence.

Table 22: All analyzed inorganic elements with shading are those that will not be discussed in this thesis

Al	Aluminum
Ba	Barium
Ca	Calcium
Fe	Iron
K	Potassium
Mg	Magnesium
Na	Sodium
Pb	Lead
S	Sulfur
Si	Silicon
Sr	Strontium
Ti	Titanium

Ag	Silver
As	Arsenic
Be	Beryllium
Cd	Cadmium
Co	Cobalt
Cr	Chromium
Cu	Copper
Hg	Mercury
Mn	Manganese
Mo	Molybdenum
Ni	Nickel
P	Phosphorus
Sb	Antimony
Se	Selenium
Sn	Tin
Te	Tellurium
Tl	Thallium
V	Vanadium
Zn	Zinc

To quantify the contamination of metals from test equipment, two microreactor tests were conducted with inert ZrO_2 of minus 100 mesh size (149μm) and minus 200 mesh

size (74μm) to represent the size of the catalyst and coal, respectively. These tests were run using the same procedure as tests performed with coal. Extraction was conducted over 2 days with THF solvent. Results from these tests concluded consistent contamination of Ag, Cr, Ni, and Si in the solid products, and interestingly they also showed increase mass in Si in the liquid products as shown in Table 23.

Table 23: Blank test elements whose weights increased from initial weight in 5.15g samples

Average mass increase of inorganic element in solids		
Ag	0.0016	mg
Cr	0.0081	mg
Ni	0.0186	mg
Si	25.43	mg

Average mass increase of inorganic element in liquids		
Si	58.59	mg

All filters used in this test were silicone-free cellulose filters, and the large increase of Si may have been from the extended use of glassware during the extraction. The metals in the stainless steel reactor (discussed in the Section 3.1) also might be a source of contamination.

4.2.2 Reproducibility of DCL Tests

Reproducibility tests were conducted using three different microreactors. The testing conditions and liquefaction results are shown in Table 24. There were some differences in the initial pressures, specifically with 3RunB. The final hydrogen fill was first performed in 3RunC, then 3RunA, and then 3RunB and the pressure left in the gas cylinder

dropped during this testing. This was not allowed to occur when conducting the final matrix. The final pressure was the pressure read from the pressure gauge on the microreactor at the end of the reaction hour. Even with this difference in pressure, the overall conversions were very similar with the largest difference of 0.76% between tests. The end liquid weights were quite varied, this was most likely due to non-evaporated THF, even though no calculations were dependent on the THF left in the product. Full summary charts and raw results for all the tests are contained in Appendix G and Appendix H, respectively.

Table 24: Reproducibility test data

	3RunA	3RunB	3RunC
Coal (g)	5.0174	5.0248	5.0352
Catalyst (g)	0.1518	0.1479	0.1536
Solvent (ml)	14.9	15	15
Temperature(°C)	400	400	400
Initial P (MPa)	6.8	*6.3**	6.9
Final P (MPa)	17.2	16.2	18.6
Change P (MPa)	10.4	9.9	11.7
End Solids (g)	0.9294	0.993	0.9350
End Liquids (g)	17.96	12.86	24.06
Conversion %	93.52%	92.76%	93.19%

**H_2 cylinder pressure decreased by the end of pressurization step during3RunB*

Table 25 gives the results for each element in the total solid products for the 3Run tests. It can be seen that the reproducibility of the three tests was good with an average error of 3%. There appears to be an influence of pressure as the elemental results of 3RunB test solids were most often the highest with the only exceptions in Hg and Mg. To more accurately calculate the percent error for individual elements, test 3RunB was not included.

Table 25: Element's weight measured in the solid and liquid products of the 3RunTests (mg)

	3runA Solids	3unB Solids	3runC Solids	*%Error Solids*	3runA Liquids	3runC Liquids	*%Diff Liquids*
Al	16.6	18.1	16.8	*1.2%*	0.0180	0.0485	*63.0%*
Ca	7.71	8.04	7.39	*4.2%*	1.185	1.892	*37.4%*
Fe	54.7	58.8	55.6	*1.6%*	0.0359	0.0752	*52.2%*
K	5.48	5.96	5.80	*5.4%*	0.0359	0.0970	*63.0%*
Mg	0.61	0.61	0.64	*3.5%*	0.0359	0.0970	*63.0%*
Mn	0.17	0.18	0.19	*10.5%*	0.00718*	0.02426	--
Na	3.35	3.57	3.27	*2.2%*	0.162	0.218	*26.0%*
S	111	116	110	*0.2%*	75.4	114.0	*33.8%*
Ti	1.35	1.54	1.31	*2.9%*	1.80	2.43	*26.0%*
As	0.00836	0.00894	0.00842	*0.6%*	0.00718*	0.00970*	--
Hg	0.00018	0.00016	0.00017	*4.7%*	0.000180	0.000267	*32.7%*
Mo	0.0902	0.0943	0.0870	*3.5%*	0.0898	0.0970	*7.5%*
Pb	1.86	1.94	1.82	*1.9%*	0.162	0.194	*16.7%*
Se	0.00651	0.00695	0.00655	*0.6%*	0.00718*	0.00970*	--
V	0.177	0.199	0.178	*0.6%*	0.0359	0.0485	*26.0%*
Zn	0.195	0.218	0.182	*6.6%*	0.52	1.19	*56.2%*

**Below the equipment's detection limits and therefore only represents a maximum; no % difference could be obtained for these values*

Table 25 shows that the errors of the solid residues are very low with Mn having the highest error of more than 10%. As for the THF soluble liquids, the differences were much higher because many of these elements were present in concentrations close to the analyzer's detection limits. After it was found that the digested sample concentration was too low for detecting some elements, the liquid sample size digested for analysis was increased from 0.5g to 1.0g to increase the concentrations of the elements.

4.3 Liquefaction Conversions

4.3.1 Overall Conversions

Coal conversions for all ten tests were calculated using Equation 1 and are shown in Figure 9. These conversions represent overall conversions, which for this thesis were based

on calculations of THF non-soluble product and the initial weight of the coal on a dry, ash-free basis. All IL#6 liquefaction tests conducted in this work produced higher overall conversions than their PRB counterparts.

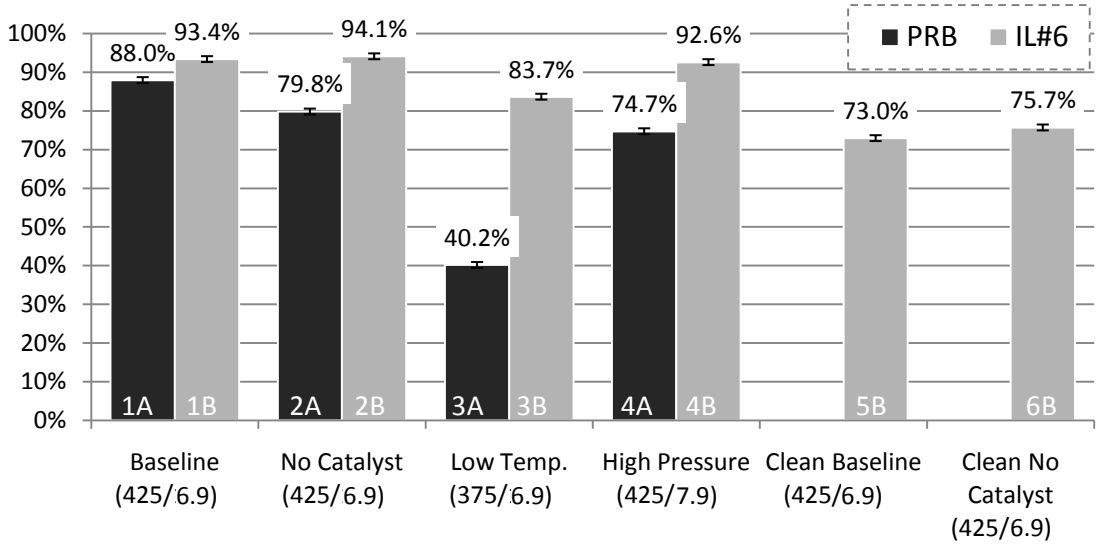

Figure 9: Liquefaction percent overall conversions with a 0.76% calculated error from repeatability tests (reaction temperature, °C / reaction pressure, MPa)

The conversions shown in Figure 9 clearly show that the overall conversions were higher for IL#6 feedstock than the PRB coal. This could be attributed to the lower hydrogen content (Burgess and Schobert 1996) and pyrite content (Garg and Givens 1982) of the PRB coal. Another attribute of the IL#6 coal that could enhance conversion was that the majority of the pyritic iron in the PRB coal had a particle size distribution of 22-100µm whereas for the IL#6 coal, pyritic iron was mostly in the finer 10-46µm range. Finely dispersed inherent Fe results in more reactive surface area that can help catalyze the DCL reactions. When the catalyst was not added to the baseline test conditions, the IL#6 conversion was not affected; however, the PRB coal resulted in a roughly 8% decrease in

conversion when the catalyst was not used. The PRB conversion was more sensitive to the addition of Fe and S as a catalyst.

The low-temperature tests, 3A and 3B, were run at 370 °C, and the results were comparable to other studies in literature (Whitehurst et al. 1980; Song et al. 1994). At this temperature, the coals produced lower conversions than tests at 425 °C presumably due to the higher temperature facilitating additional bond cleavage and increased kinetics. Cleaned coal runs produced even lower conversions compared to the low temperature runs as seen by (Guin et al. 1978).

Conversions of the cleaned IL#6 were lower than those of the as-received IL#6, and the addition of a catalyst to the cleaned IL#6 coal did not greatly enhance the overall conversion. The reduced conversion is possibly a function of the overall reduced Fe and S as there was not a significant shift in the particle size distribution of the pyritic Fe. Coal mineral content has been related to DCL conversions, and coal demineralization has been shown to increase or decrease overall conversions (Guin et al. 1978; Whitehurst et al. 1980; Mochida et al. 1989; Lee and Cantrell 1991). There are possible explanations for this such as the mineral matter's ability to catalyze hydrogenation reactions (Given et al. 1975). Demineralization has been shown to increase conversion, but more so in low-rank coals. This increase in conversion is attributed to the removal of the cations allowing more active sites for hydrogen donation (Mochida et al. 1989). This could explain why demineralization is more beneficial for low-rank coals, since there are fewer inorganic cation associations in high-rank coals.

4.3.2 Relationship between Conversions and Inorganic Elements

Inorganic elements are known to aid in the reaction of the coal during direct coal liquefaction. Elements that are naturally occurring in the coal are good catalysts because of their often high dispersion and proximity over added catalysts, which are separate poorly dispersed entities. Inorganic elements such as iron and titanium (Mukherjee and Chowdhury 1976), and oxides such as MoO_3, FeO_3 and SnO_2 (Tanabe et al. 1986; Hattori et al. 1984) have been shown to enhance DCL conversions. On the other hand, alkali and alkaline earth metal cations (e.g., Na^+, K^+ and Ca^{2+}) have been shown to cause retrogressive reactions in low-rank coal liquefaction (Joseph and Forrai 1992).

This section contains a series of graphs that illustrate the effect of the inherent inorganic elements and the addition of a catalyst on the overall liquefaction conversions for the six reactions run at 425°C and 6.9MPa. No definite trends were found; however, some interesting observations were made. Figure 10 depicts the inherent weights of Fe and S in the ~5g of coal charge in the reactor. In this figure, the IL#6 feed coal with the highest inherent Fe and S resulted in the highest conversion. However, comparison of the CL_IL#6 feed coal and the PRB feed coal shows that conversion is not solely a function of Fe and S.

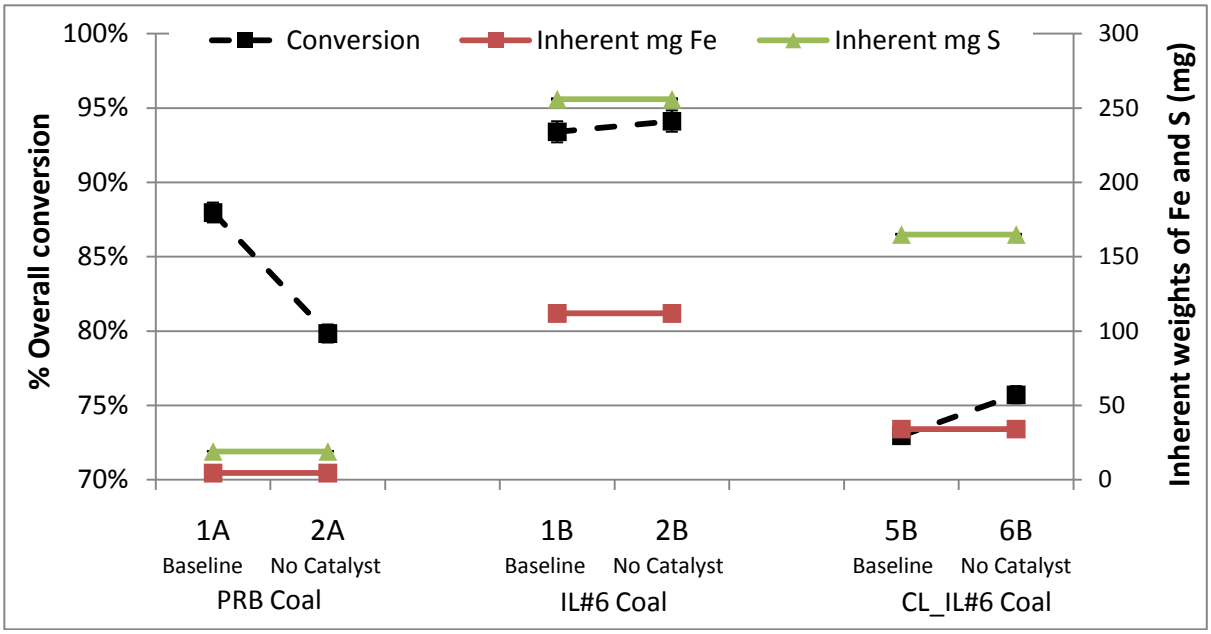

Figure 10: DCL overall conversions compared to the inherent Fe and S weights in each of the six tests

Elements such as Fe, S, and Mo are often added in coal liquefaction processes because of their catalytic properties. Figure 11 shows the conversions of the baseline tests and the non-catalytic tests compared to the total Fe and S input into the reactor for the PRB, IL#6 and CL_IL#6 coals. This figure includes the additional Fe and S weights in the catalyst. Relationships can be determined based on the parallel responses of the trends. Parallel lines between changes in composition and conversion suggest a direct relationship. Figure 11 shows a trend with the PRB coal with a decrease in conversion as Fe and S concentrations decrease suggesting that there is a direct relationship between Fe and S concentration and conversion. This is not evident in the IL#6 coal where there is essentially no effect of initial Fe and S on conversion.

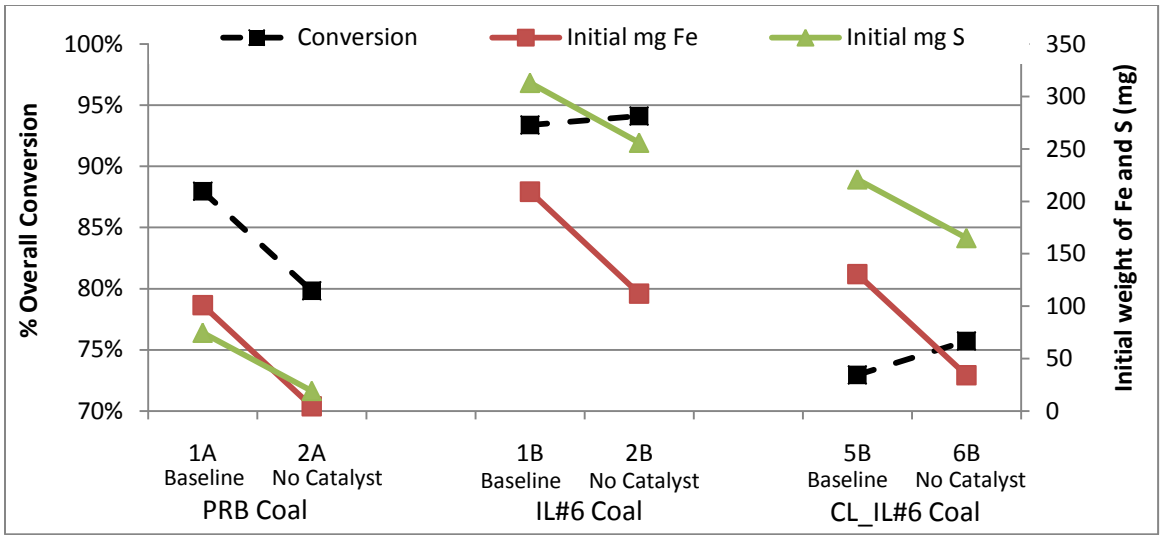

Figure 11: Overall conversions of baseline (1), non-catalytic (2), and cleaned coal tests compared to input weights of Fe and S

Figure 12 shows the effect of Mo on the overall conversions. Molybdenum compounds have been found to be successful coal liquefaction catalysts (Burgess and Schobert 1996). In this comparison, no trends are observed with or without a catalyst for a specific coal. However, comparing different coals, a trend is observed that the higher concentrations of Mo resulted in higher DCL conversions.

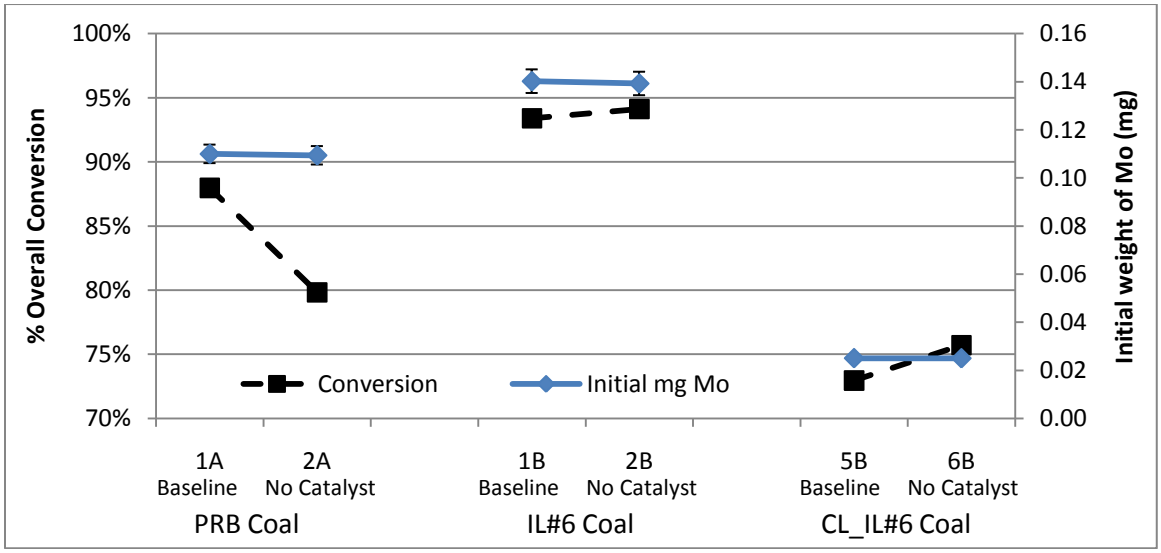

Figure 12: Overall conversions of baseline, non-catalytic, and cleaned coal tests compared to the input weight of molybdenum

The influence of the total amount of the inorganic elements input weights on the overall coal liquefaction conversions from these tests is shown in Figure 13. Figure 13 upper and lower portions compare the overall conversions to the mass of the inorganic elements put into the reactor. Figure 13 upper includes Fe and S in the total weight (these weights were largely due to the addition of the FeS catalyst), and Figure 13 lower is the inorganic element weight total not including the weights of Fe and S. These total weights include the 16 elements that are discussed. Figure 13 shows how the PRB and IL#6 coals in these liquefaction tests may be influenced differently by the inorganic contents of the coal and catalyst in terms of the calculated overall conversions. The IL#6 coal and CL_IL#6 coal DCL conversions, when compared to one another, show that increased inherent inorganic elements relate to an increase of the overall conversions. The PRB coal conversion in these figures was more directly affected by the Fe and S weights of the added catalyst. This may be due to the larger amounts of inherent Fe and S in the Illinois coals, therefore, creating a larger impact on conversion by catalyst addition in the PRB coal.

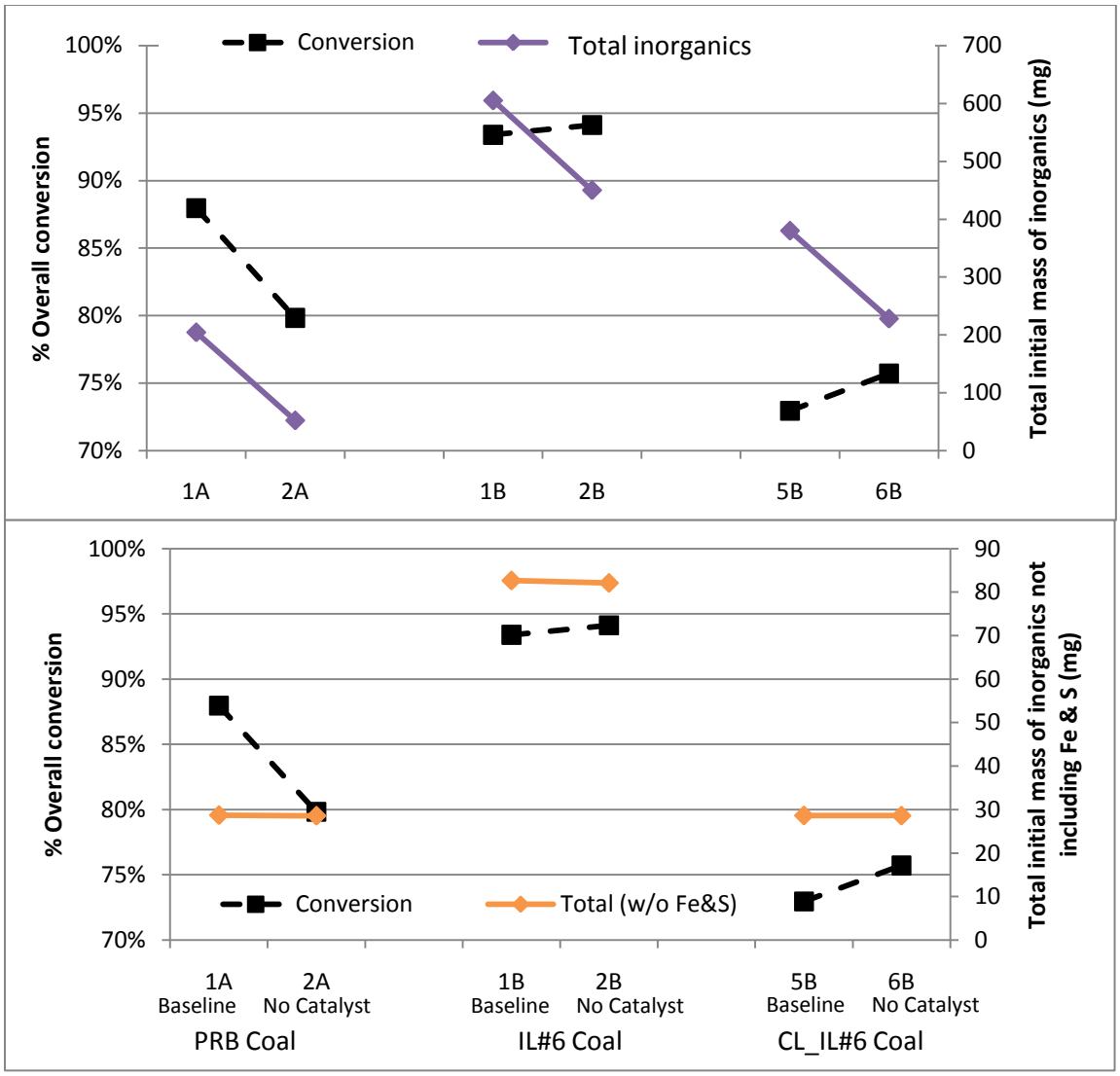

Figure 13: Overall DCL conversions compared to the total initial mass of inorganic elements charged in each microreactor experiment. Upper: % Overall conversion compared to total weight of inorganic input. Lower: Comparison without including the input weights of Fe and S

4.3.3 Residue Ash Yield Analysis

A thermogravimetric analyzer (TGA) was used to measure the ash contents in the liquefaction residues, and the results are shown in Figure 14. Weight reduction graphs are included in Appendix I. The ash yield present in the liquefaction solid residue products represented the portion of the residue left after all moisture, carbon and volatiles were

driven off. Therefore, the residue with the lowest ash yield contained the highest concentration of unreacted material. Characterizing the residue product from direct coal liquefaction is important because on a large scale this residue is often further utilized as discussed earlier. The highest ash yields were found in the as-received Illinois No. 6 coal residues, as expected.

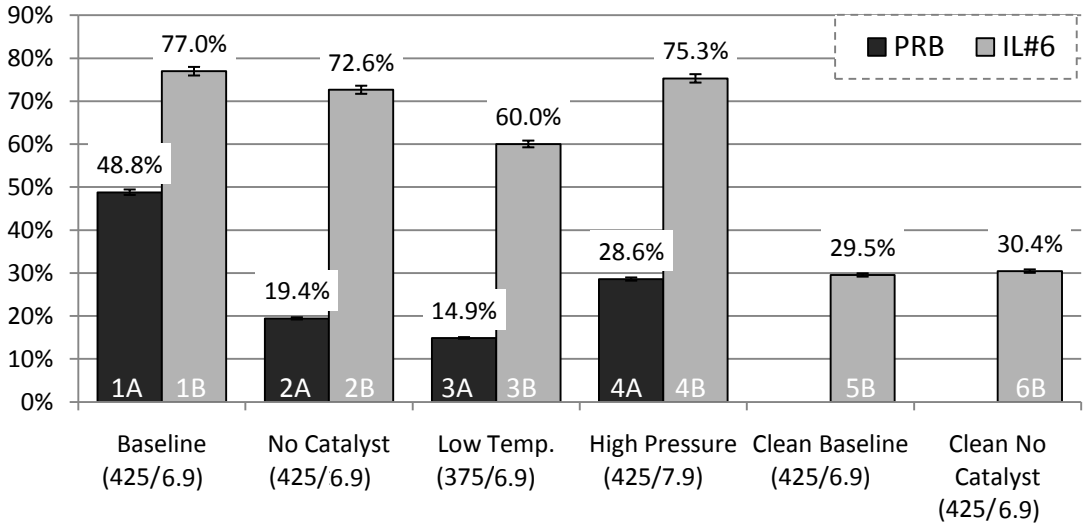

Figure 14: TGA ash yields with 1.3% absolute error from initial repeatability tests (reaction temperature °C / reaction pressure in MPa)

Tests performed with the FeS catalyst contained higher ash yields than those without, possibly due to the addition of the inorganic catalyst weight in the ash. These residues did not undergo a full proximate analysis including a volatile matter analysis, but the catalytic liquefaction residues most likely have a slightly lower amount of organic volatiles compared to the thermal liquefaction residues that contain a higher amount of organic volatile matter (Cui et al. 2003).

If a coal liquefaction plant uses Illinois No. 6 coal as a feedstock and gasifies the product residue for the production of heat and/or hydrogen, the fuel utilization could create a large quantity of ash or slag, which would require disposal. The fuel would also contain a low energy content, as can be assumed from the ~75% ash content, and a co-gasification or co-combustion scheme would most likely be required if the residue was considered for use.

4.4 Inorganic Element Partitioning during DCL

4.4.1 Overview of Partitioning Results

4.4.1.1 Baseline Test Results

The baseline DCL test conditions are discussed in detail in the Methodology section, but as a review these tests were conducted with a 3:1 (by weight) tetralin-to-coal ratio at 425°C under 6.9MPa (1000psig) of hydrogen pressure, with the addition of a FeS catalyst using a reaction time of 1 hour. Two baseline tests were run: one with the PRB coal and one with the IL#6 coal, with two tests being conducted simultaneously.

Table 26 shows the results of these baseline tests. The initial weight of the element was obtained by multiplying the inorganic elemental concentration in the coal and the total weight of coal that was charged to the reactor. In the baseline tests, FeS catalyst was added and, therefore, the initial Fe and S weights include the elemental Fe and S present in the coal plus the amount in the catalyst. The percent recovered was the sum of the solid and liquid percents. This total did not include any gaseous emissions from the reaction, as the gas was not collected and analyzed in this work.

Table 26: Baseline test results showing the initial weight of the element charged in the reactor and the percentages of the initial weight that were measured in the solid and liquid products

*** Maximum values as these data were below the measuring device's detection limits**

PRB COAL	1A Initial (mg)	1A Solids (%of initial)	1A Liquids (%of initial)	% Recovered	**IL#6 COAL**	1B Initial (mg)	1B Solids (%of initial)	1B Liquids (%of initial)	% Recovered
Fe	101	70	0	71	Fe	209	31	0	31
S	75	64	9	73	S	313	44	19	63
Al	3.0	430	2	432	Al	40.1	50	0	50
Ca	13	115	7	123	Ca	23	43	4	47
K	0.7	97	5	102	K	6.9	97	2	98
Na	4.7	66	10	76	Na	4.5	87	9	95
Mg	1.95	297	7	305	Mg	1.20	67	6	72
Mn	0.06	183	27	210	Mn	0.29	83	3*	86*
Pb	3.60	108	1	109	Pb	1.80	139	2	141
Ti	1.75	80	20*	100*	Ti	4.06	49	42*	91*
Zn	0.30	37	163	200	Zn	0.50	136	114	250
As	0.006	100	0*	100*	As	0.008	125	0*	125*
Hg	0.00025	12	8	20	Hg	0.00050	46	24	70
Mo	0.11	11	74	85	Mo	0.14	71	49	121
Se	0.002	50	0*	50*	Se	0.009	89	11*	100*
V	0.055	60	29	89	V	0.130	207	13	220

In some cases, more often with the PRB results, the total recorded was above 125 % (Al, Mg, Mn and Zn for the PRB baseline test and Zn and V for the IL#6). Possible reasons for these high totals were discussed in Section 4.2.1. Raw partitioning data for all the elements from all the tests are included in Appendix H. Similar to past work (Pringle and Jervis 1987), elemental balances of Al, Ca, and Fe did not add to 100% and Mn and Zn totals exceeded 100%. A large difference in results is seen in the low recovery of elemental S in the work here in comparison to Pringle and Jervis (1987) who measured a recovery of over 100% (88% in solids and 23% in liquids).

In Figure 15, the partitioning of the inorganic elements from the baseline tests is shown. The elements are divided into three groups based on the inorganic elements initial weight in the reactor: Group 1 is comprised of elements with an initial weight of 5.00mg and higher, Group 2 is comprised of elements with weights 0.50mg and higher, and Group 3 includes all the elements with weights less than 0.15mg. The groups and associated elements are:

Group 1: Al, Ca, Fe, K, Na, S
Group 2: Mg, Mn, Pb, Ti, Zn
Group 3: As, Hg, Mo, Se, V

These graphs show the percentage of the elements' initial weight that was measured in the solid and residue. In Figure 15, it is observed that most of the inorganic elements' mass was measured in the solid residue products when compared to the liquid products. This is in agreement with past studies (Pringle and Jervis 1987; Filby et al. 1977a; Filby et al. 1977b). The only exceptions were with the PRB coal for Mo and Zn. However, amounts of certain elements were contained in the liquid products.

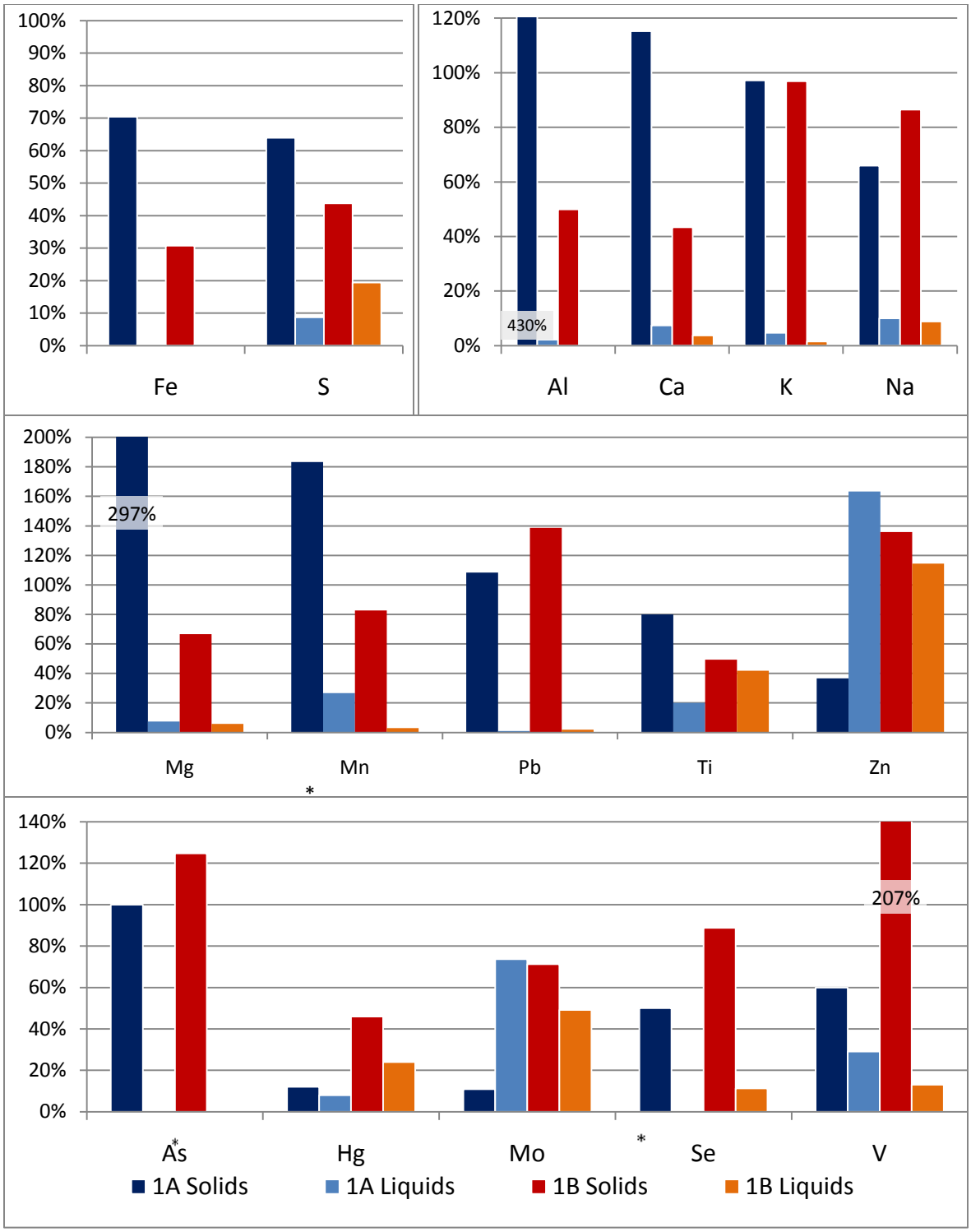

Figure 15: Inorganic partitioning graphs for Baseline tests, y-axis is the percent of the elements initial coal weight that is measured in the solid and liquid products. 1A – PRB coal, 1B – IL#6 coal

***maximum values as these data were below analytical detection limits for liquids*

4.4.1.2 Inorganic Element Partitioning Data for All Tests

To determine overall trends in inorganic element partitioning, the products from all 10 tests were reduced to groupings that represented the percent of the initial element measured that was in either the solid or liquid products The graphs are independent of the process variables. These results were used to determine if any overall trends existed for the individual elements.

Figure 16 and Figure 17 show grouped results for, respectively, Hg and K solid and liquid products from all 10 tests. The pie charts show that the Hg results were more variable depending on the test conditions, while the distributions of K in the DCL products were more consistent with lower concentrations in the liquids (0-5%) and higher concentrations in the solid products (>78%). This suggests that the partitioning of K was not significantly affected by the test conditions.

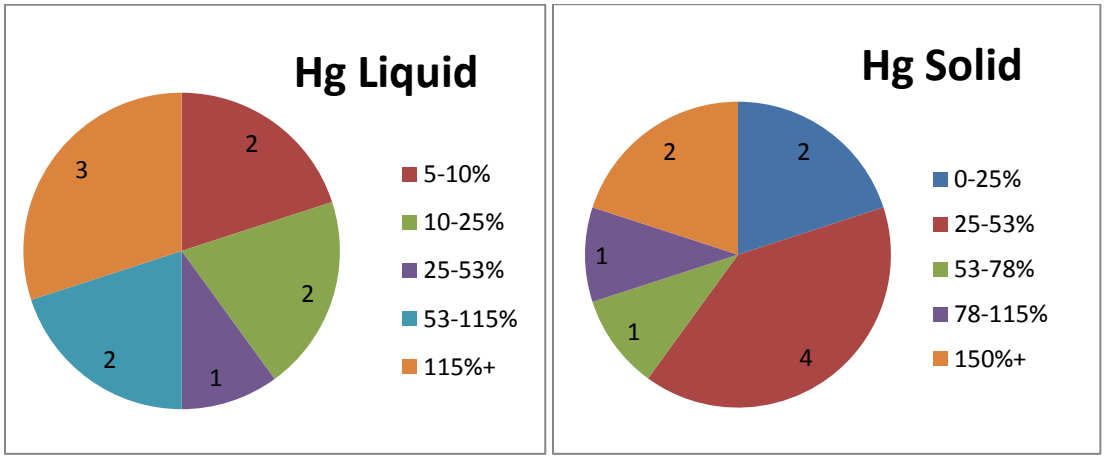

Figure 16: Number of occurrences of *Hg* by distributions within liquid and solid products

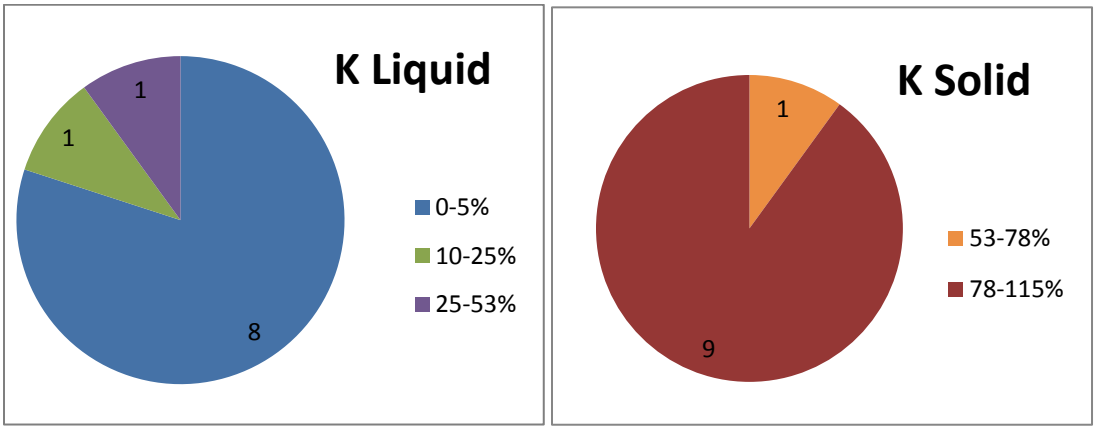

Figure 17: Number of occurrences of *K* by distribution within liquid and solid products

The results for all the elements using this analysis technique are provided in Figure 18. Figure 18 shows that for some elements, such as Al and Na, no more than 25% of the initial elemental weights were measured in any liquid products regardless of the test conditions. Sodium, Mn, K, and As were consistently concentrated in the solid residue (>53%) for all 10 tests. By contrast, Zn was consistently concentrated in the liquid products (>53%) regardless of test conditions. Some elements in Figure 18 concentrated in both the solid and liquid products for multiple tests (i.e., Zn, Hg, As, and Mn). This is due to these elements recovering over 100% of their initial weight within the solid and liquid products. It should be noted that even though elements show a lower partitioning to the liquid products, their concentrations can still be large enough to distinguish them from crude oil concentrations and may cause operational and environmental concerns, as will be discussed in upcoming sections of this thesis.

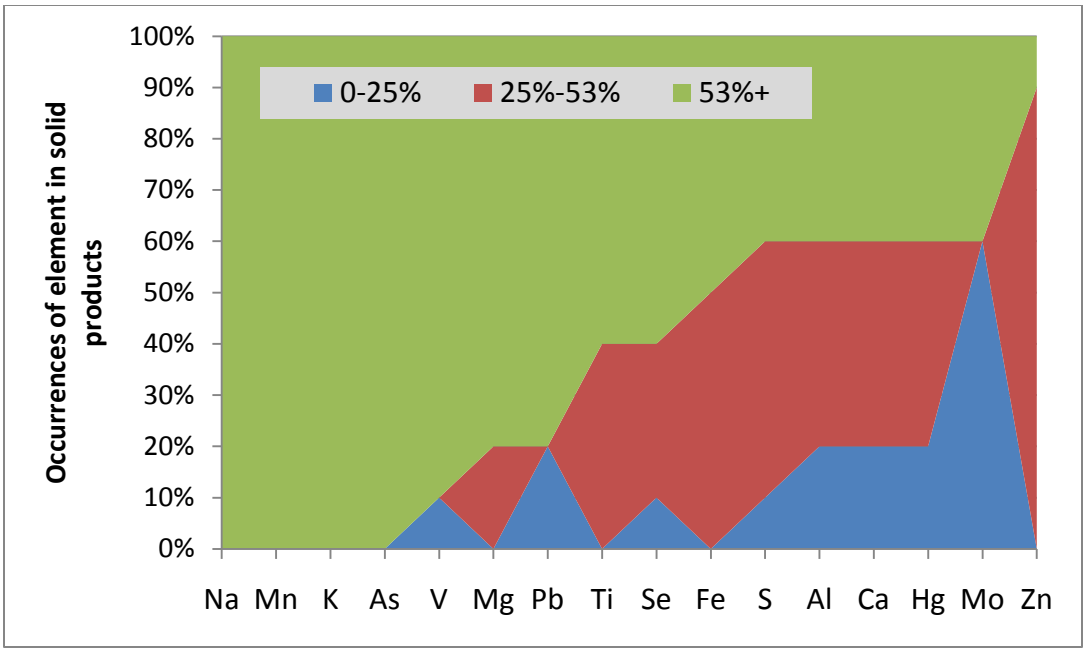

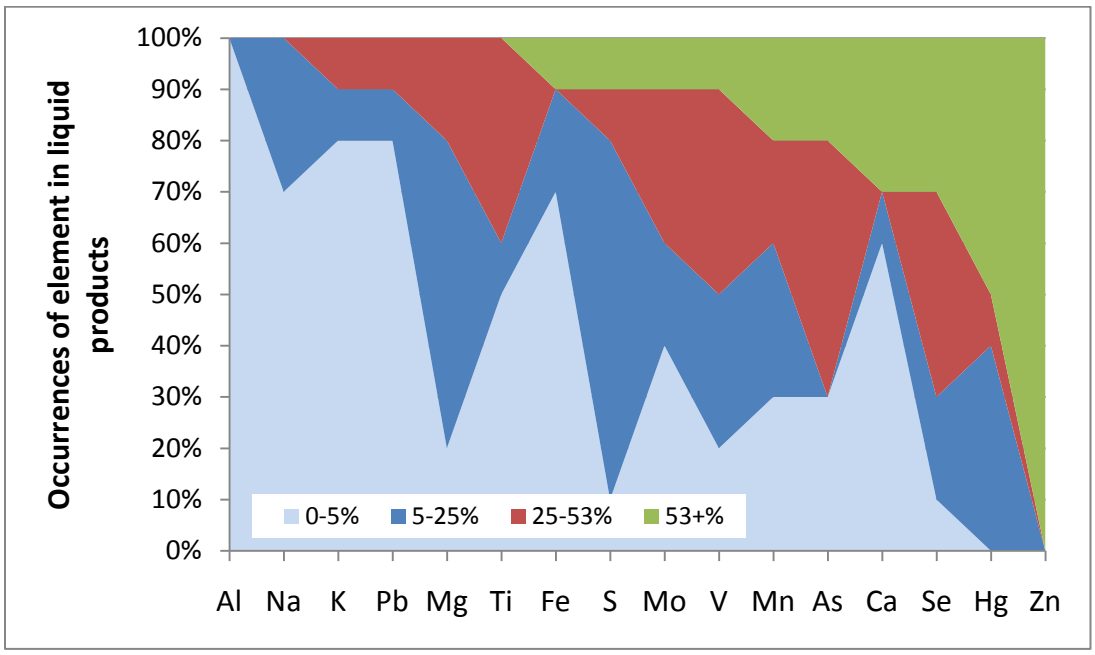

Figure 18: Occurrences of element in weight % measured in liquid and solid products (i.e. 100% = range occurred in all 10 tests, 60% = 6 out of 10 tests, and so on)

4.4.2 Coal Composition and Rank

The proximate and ultimate analyses of the feed coals were provided in Table 14 and Table 15, respectively. In Table 27, the maceral contents of the two coals are given. The higher inertinite content of the PRB coal could also be an influence on its overall lower conversions, since most macerals in the intertinite group are non-reactive (Bustin and Geological Association of Canada. 1985).

Table 27: Maceral compositions of PRB and IL#6 coals on a mineral matter-free basis

Mineral-matter free basis	PRB	IL#6
Total vitrinite/humanite	85.5	90.2
Total liptinite	2.8	3.0
Total inertinite	11.7	6.8

The influence of composition and rank attributes on the inorganic elements during direct coal liquefaction were studied. Figure 19 compares an element's initial weight to its weight measured in the residue on the baseline tests. Elements are separated into graphs based on their initial weight charged into the reactor using the same grouping scheme as described in the previous section: Figure 19 Upper contains the elements in Group 1; Figure 19 Middle consists of the elements in Group 2; and elements in Group 3 are shown in Figure 19 Lower. Some elements such as Zn, Mg, and V showed an increase in weight in one of the coals, but not the other. This could be the result of sampling errors or contamination.

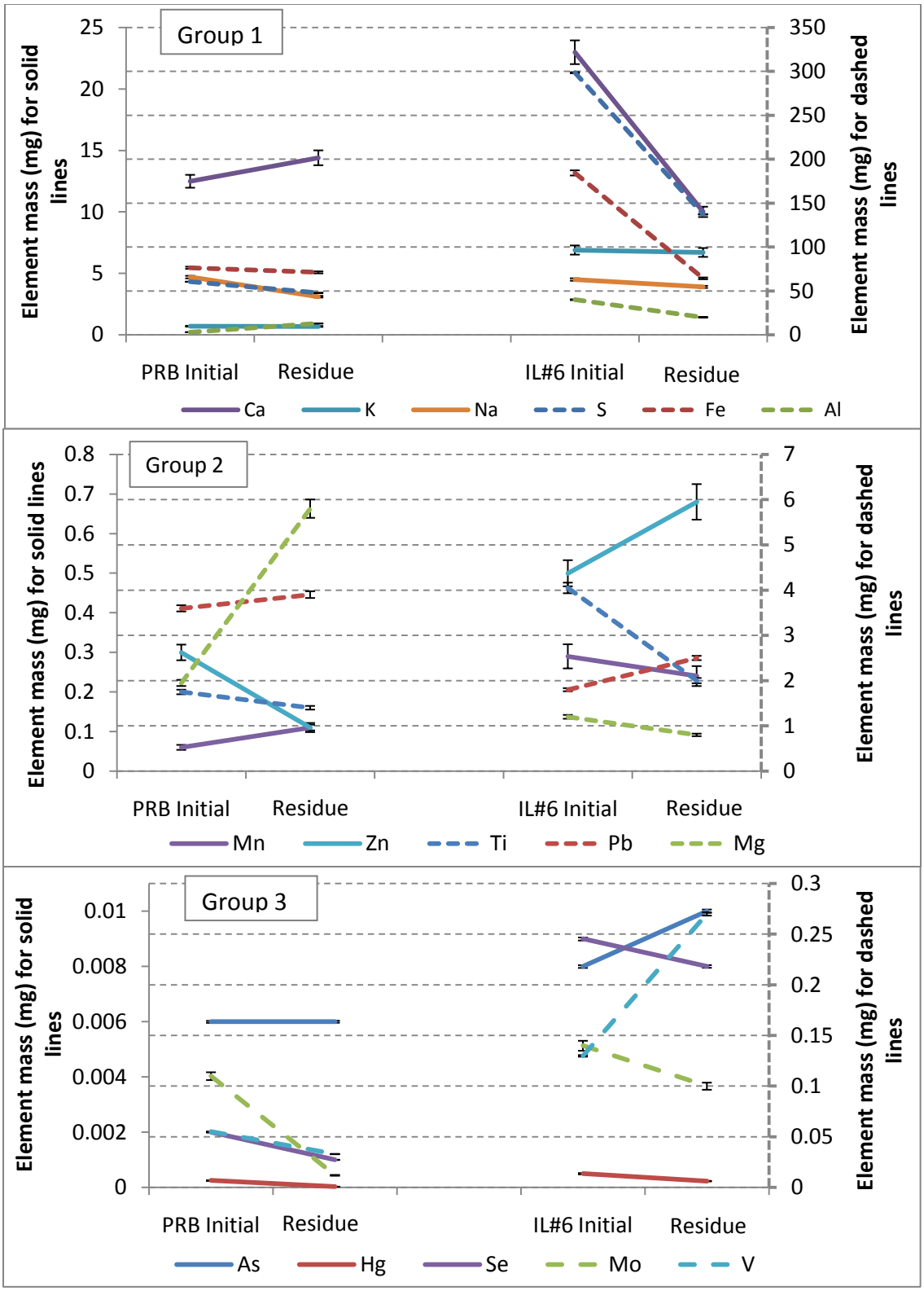

Figure 19: Mass of the element in the initial coal and liquefaction residue from the baseline tests. Error bars are individual to each element based on reproducibility tests.

In the Group 1 elements, it can be observed that there is little difference exhibited between the mass in the coal and the residue for the PRB coal. However, for the IL#6 coal, elements such as Ca, S, and Fe showed significant decreases in mass in the residue products. Calcium was interesting because it is known for its ability to form $CaCO_3$ during low-rank coal liquefaction (Walker et al. 1980). This could be a possible reason why its initial weight remained in the residue for the PRB coal. In the Group 2 elements, Mg also showed an increase in the residue product for only the PRB coal and a slight decrease in weight in the IL#6 residue. It is possible that, similar to the formation of $CaCO_3$, the Mg in the residue could be present as $CaMgCO_3$ or $MgCO_3$; unfortunately, $MgCO_3$ has not been studied. In the Group 3 elements (i.e., the inorganics with the lowest mass in the coal charge), the two coals did not show any significant differences except for V in the IL#6 residue.

4.4.3 Iron, Sulfur and Catalyst

While the importance of Fe and S on the overall conversion during batch-scale liquefaction has been discussed, there may also be an impact of these catalytic elements influencing the partitioning of other inorganic elements. The partitioning of Fe and S and the effect of catalyst on the partitioning of the other inorganic elements are discussed.

Fe partitioning is rarely significant in the liquid products; therefore Fe partitioning to the residue was a more valid basis for comparison. The presence of Fe in the residue was heavily dependent on process conditions, especially on whether or not an Fe catalyst was used. Montano and Granoff noted that the weight percent of elemental Fe present in the

residue was related to overall conversion, but they did not consider the use or absence of an Fe-containing catalyst (Montano and Granoff 1980). Figure 20 shows the weight percent of Fe in the residues of the baseline test run with and without a catalyst for the PRB, IL#6 and cleaned IL#6 coals. The test nomenclature is again defined in Table 28.

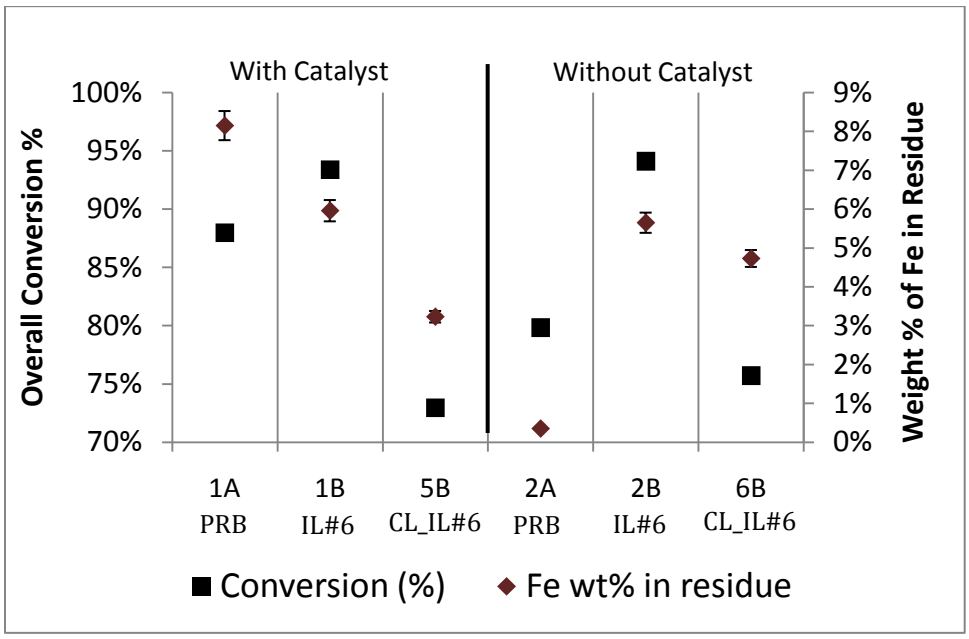

Figure 20: Relationship of percent conversion to weight percent of the Fe in residue for the baseline runs (left of bar) and the runs without catalyst (right of bar)

Figure 20 does not show a clear relationship between the weight % of elemental Fe in the residue and the conversion when comparing all the coals. There does, however, appear to be a trend when comparing the Illinois No. 6 coals (IL#6 and CL_IL#6). Conversion decreases as the Fe concentration decreases. Also, it is noted that, for the PRB coal, conversion is higher for the test with catalyst, i.e., higher Fe concentration.

Sulfur is very active in direct coal liquefaction. The pyritic S can convert to pyrrohtite and release H_2S; the organic sulfur can also form H_2S (Trewhella and Grint 1987). The mass of elemental S in the initial coal, catalyst, solid residue and THF soluble liquids are shown in

Table 28. The recovered amounts of S from the solids and liquids did not equal the total S that was present in the coal and the catalyst. This was most likely due to gas phase S compounds (e.g., H_2S) that were not measured. The PRB coal runs resulted in higher recoveries. This may have been because the PRB coal was less reactive and a smaller percent of S was converted to H_2S. This table shows that the concentration of S in the coal directly relates to the concentration in the products, which is in agreement with past studies (Whitehurst et al. 1980).

Table 28: Initial and final weights of S (mg)

Test ID	Description	Initial S	Catalyst S	Residue S	Liquid S	Total Product S	Product / Total Initial
1A	PRB Baseline	19.2	55.4	47.7	6.5	54.2	0.726
1B	IL#6 Baseline	257.7	55.4	137.2	60.8	198.0	0.632
5B	CL_IL#6 Baseline	165.4	55.4	94.4	44.9	139.3	0.631
2A	PRB No Catalyst	19.1	0.0	6.6	6.9	13.5	0.708
2B	IL#6 No Catalyst	256.0	0.0	72.1	63.5	135.6	0.530
6B	CL_IL#6 No Catalyst	165.1	0.0	56.0	39.7	95.7	0.580

Not accounting for the potential loss of S to the gas phase and solely focusing on partitioning to the solid and liquid products, Figure 21 shows the normalized percents of the initial S mass that were measured in the residue and liquid products. Here it is observed that the tests run without a catalyst had a smaller difference between the weight of S in the residue product and the liquid product. This is most likely because in the catalytic tests solid FeS catalyst is added and the S present in the catalyst could concentrate in the solid products. This addition could produce a larger gap between the S in the solid and liquid products.

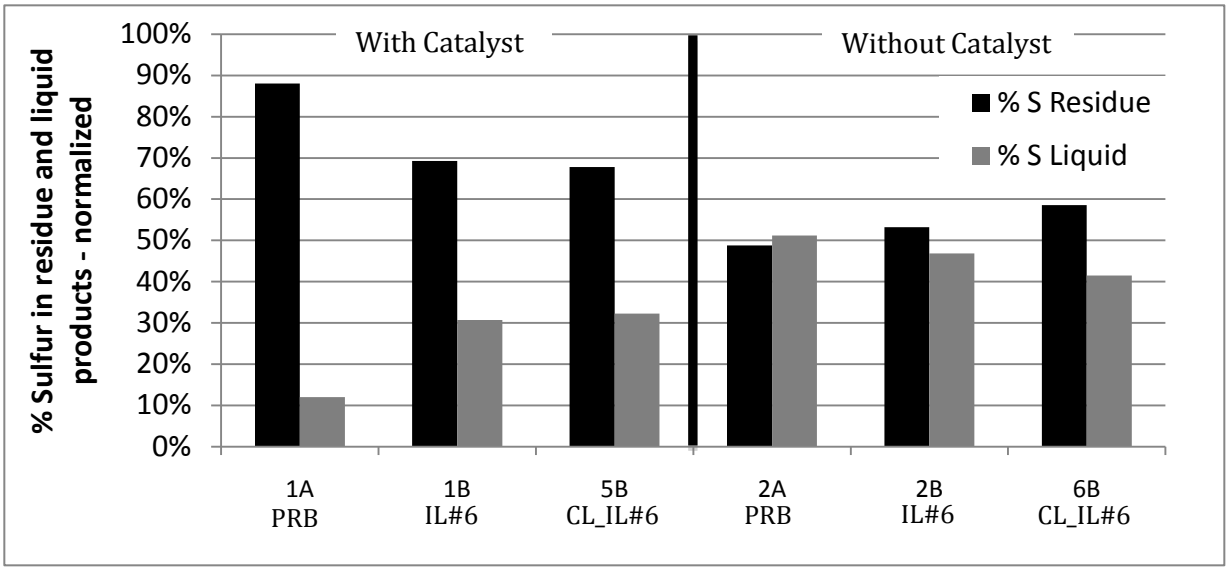

Figure 21: Normalized S partitioning for baseline (left) and non-catalytic (right) tests

The effect of a catalyst on all the elements studied is shown in Figure 22 and Figure 23 for the IL#6 and PRB coals, respectively. These figures show the mass percent of the initial element that was measured in the residue product for the Illinois No. 6 and Montana PRB coals in the baseline test and the non-catalytic tests. For most of the elements, the catalytic liquefaction residue contained a higher percent of the initial element than the thermal liquefaction residue. The only exceptions seen here were with elemental Al and Fe in the IL#6 coal (Figure 22). This may have occurred because the catalyst promotes conversion and may have concentrated more inorganic elements in the solid. The ash yield of the catalytic residue was about 4 % higher than that of the thermal, non-catalytic residue for the IL#6 coal, and these results show that this is not only due to the addition of S from the catalyst, even though it was shown earlier that this was a very large factor. In general, catalytic liquefaction resulted in higher partitioning of inorganic elements to the solid product than did thermal liquefaction.

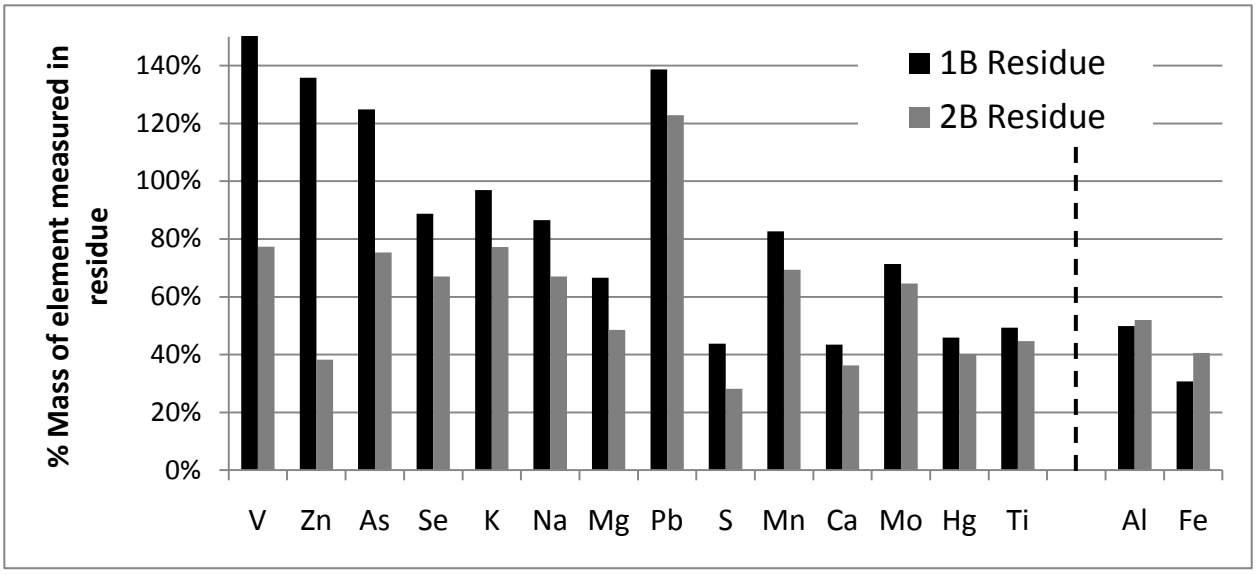

Figure 22: Effect of catalyst on element partitioning to the residue product for the IL#6 coal, 1B - with catalyst; 2B – without catalyst

The difference in ash yield between the catalytic and thermal liquefaction residue was much larger in the PRB coal residues compared to the IL#6 residues. The ash yield in the PRB baseline residue (with catalyst) was 28.6% higher than the ash percent of the thermal liquefaction residue. A similar partitioning pattern is still seen in Figure 23 with higher percents of the initial elemental masses going to the residue in the catalytic liquefaction tests. Iron and Se showed almost no difference in partitioning to solid products in thermal DCL compared to catalytic DCL. As mentioned earlier, Fe_3O_4 can be a post-reaction Fe state in the residue, specifically when less S was available (Suzuki et al. 1985), such as in the two tests with no catalysts. This could have been a reason why the Fe and S were not following the same partitioning patterns in catalytic and thermal DCL tests. It would be interesting to see what oxidation state the Fe in the residue is present as.

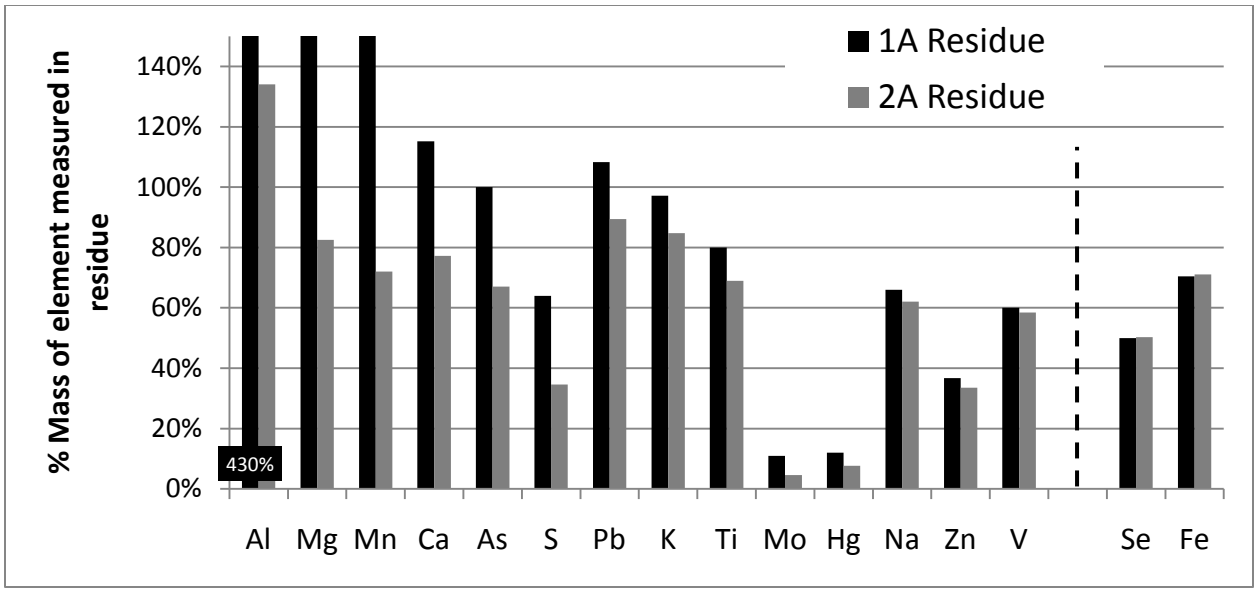

Figure 23: Effect of catalyst on element partitioning to the residue product for the PRB coal, 1A - with catalyst; 2A – without catalyst

Total pyrite, S and Fe reductions in the cleaned coal were determined by CCSEM data, proximate analysis data, and elemental analysis determined by AAS, and ICP. For the Illinois No. 6 coal (IL_#6) and the float-sink cleaned Illinois No. 6 (CL_IL#6) coal, these reductions are shown in Table 29. The cleaned coal retained a higher concentration of the initial S (64% of the initial concentration) compared to pyrite (27% of the initial concentration). This might be because the sulfur in the parent coal is split evenly between pyritic S and organic S: 2.64% S in each pyritic and organic form on a dry basis, as determined by the Penn State Coal Sample Bank (Scaroni et al. 1999). Organic sulfur may have remained in the float fraction while the pyritic S separated to the sink. The effect of the cleaned coal on element partitioning is briefly discussed in the following section.

Table 29: Pyrite, S and Fe concentrations in IL#6 and CL_IL#6 coals on a whole coal weight percent basis

	IL#6	CL_IL#6	% Of initial value
As received Ash	11.58%	5.53%	47.75%
Whole coal basis pyrite	7.47%	2.06%	27.58%
Whole coal basis sulfur	5.15%	3.30%	64.13%
Whole coal basis iron	2.25%	0.68%	30.22%

4.4.4 Coal Cleaning

Float-sink coal cleaning was conducted on the Illinois No. 6 coal and the product coal ash yield was reduced by roughly 50%. The majority of inorganic element concentrations in the coal were also reduced and the reductions are shown in Table 30 in ppmw.

Table 30: Elemental concentrations for Illinois No. 6 coal and float-sink cleaned Illinois No. 6 coal in parts per million (ppm)

Element	IL#6	CL_IL#6	Element	IL#6	CL_IL#6
S	51,461	33,000	Mg	240	48
Fe	22,500	6,800	Zn	100	62
Al	8,000	3,000	Mn	58	14*
Ca	4,600	20	Mo	28	5
K	1,380	1,100	V	26	20
Na	900	960	Se	1.8	1.0
Ti	810	440	As	1.6	1.3
Pb	360	45	Hg	0.100	0.038

**Mn partitioning was extraordinary high, with 10x as much initial mass found in all solid and liquid samples, possibly due to a low initial sample concentration measurement*

Float-sink cleaning reduced the concentrations of nearly all the elements. The relationship between element partitioning and coal cleaning for baseline test conditions is shown in Figure 24. These graphs are organized such that: 1) the elements with similar partitioning are in the center; 2) partitioning of elements that favor the product when as-received coal was used are on the left; 3) elements whose partitioning was higher in the cleaned coal product are on the right. Elements such as Pb and Ca are concentrated in the residue in the as-received IL#6 coal baseline test (1B), but concentrated in the liquid in the CL_IL#6 test (5B). This is observed in Figure 24 as these elements are present to the left of the dashed line in the residue chart, but they are located to the right of the dashed line in the liquid chart. In theory, the two bars would be even if the partitioning was independent of cleaning. Sulfur, Al and K did not show a significant difference in their partitioning. Vanadium resulted in higher partitioning to the liquid and solid in the as-received coal, and Hg consistently measured more partitioning to both products in the cleaned coal test run.

In summary, coal cleaning resulted in less partitioning of V and S to both of the products, and Pb, Zn, and Ca were reduced in the residue. On the other hand, the partitioning of Pd and Ca to the liquid product increased in the cleaned coal tests.

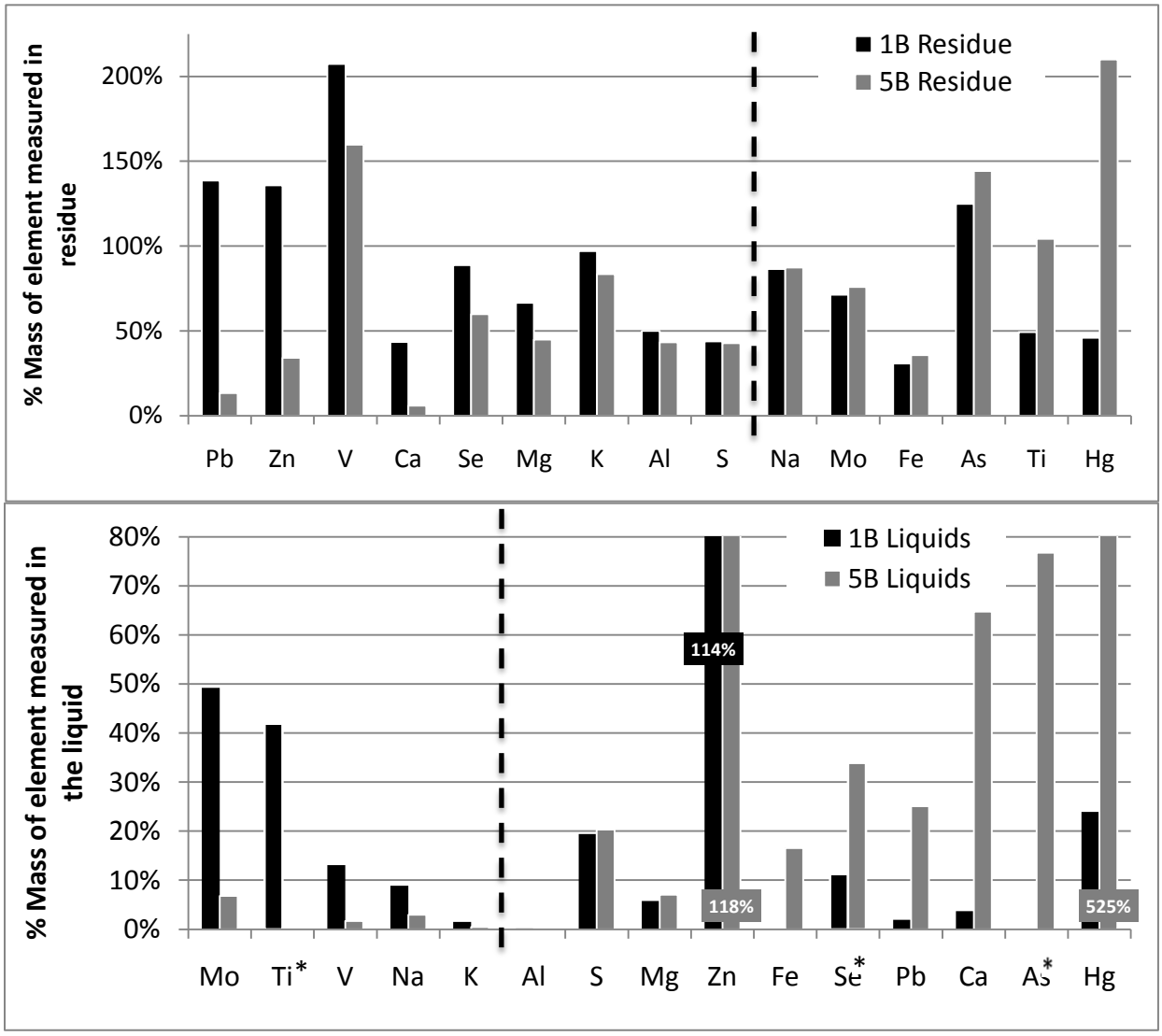

Figure 24: Comparison of element's partitioning for baseline IL#6 test and CL_IL#6 test. Upper: partitioning to solid, Lower: partitioning to liquid. 1B – As-received IL#6 coal, 5B – Float-sink CL_IL#6 coal.

**Maximum values as these data were below analytical detection limits*

4.4.5 Reaction Pressure and Temperature

The reaction pressures and temperatures were varied as shown in Table 31 for both coals: PRB (A coal runs) and IL#6 (B coal runs). Selected elements from the IL#6 coal testing are discussed in this section; more results can be found in Appendix J. Seven elements were

selected for discussion in this section: As, Hg and Se because these pose environmental health risks; and Ca, K, Na and Mg because these pose operational concerns.

Table 31: Temperature and pressure variations

Test #	Conditions	Temperature	Pressure
3 (A&B)	T low, P low	370 ^{0}C	6.9 MPa (1000 psig)
1 (A&B)	T high, P low	425 ^{0}C	6.9 MPa (1000 psig)
4 (A&B)	T high, P high	425 ^{0}C	7.9 MPa (1150 psig)

The overall conversions to THF-soluble products are affected more by the change in temperature than with a change in pressure. The elemental partitioning of most elements did not produce a clear dependence on reaction temperature and pressure. It was clear, however, that the partitioning of some elements varied with changing pressure and temperature. Figure 25 shows results for As, Hg, and Se in the solid and liquid products for three test runs. Arsenic and Se liquid concentrations fell below the equipment detection limit for the 1B test only; this was most likely due to the 0.5g sample size used for this test analysis compared to the 1.0g sample size used for tests 3 and 4. Mercury and As, which are commonly bound (but not exclusively) in the same pyrite fraction of coal (Spears et al. 1999), showed somewhat similar results in that their lowest concentrations in the residue and liquid were in the 1B tests which were performed with a higher temperature and lower pressure (T_HP_L). Mercury and As partitioning was higher in both the solid and liquid products during the lower pressure and higher temperature tests (3B and 4B) compared to the baseline test (1B).

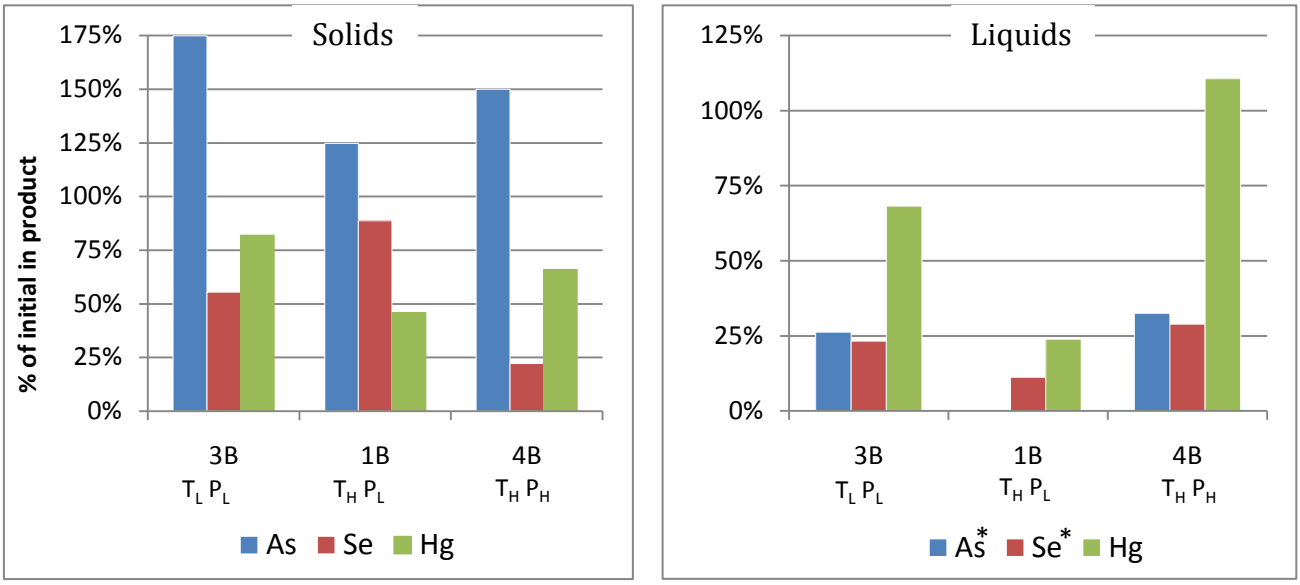

Figure 25: Partitioning of elements of environmental interest during reactions of different temperature and pressures for Illinois No. 6 coal experiments, **maximum values were used because these were below the detection limits*

Figure 26 shows variations in the partitioning of elements of potential operational or equipment concern (i.e., Ca, Na, K and Mg). As discussed earlier, these elements are known to poison catalysts in refineries, and other catalytic systems, as well as foul and corrode combustion and gasification equipment.

For the most part, these alkali and alkaline earth metals did not show any trends with operating conditions, specifically with the Ca and K partitioning where there was no clear influence of pressure or temperature changes. The Mg partitioning to the liquids was much higher for the low-temperature and low-pressure conditions (3B test) compared to the others, while its partitioning to the solids remained comparatively stable. Sodium was slightly more mobile to the liquids in the baseline tests (T_HP_L) in comparison to the other tests.

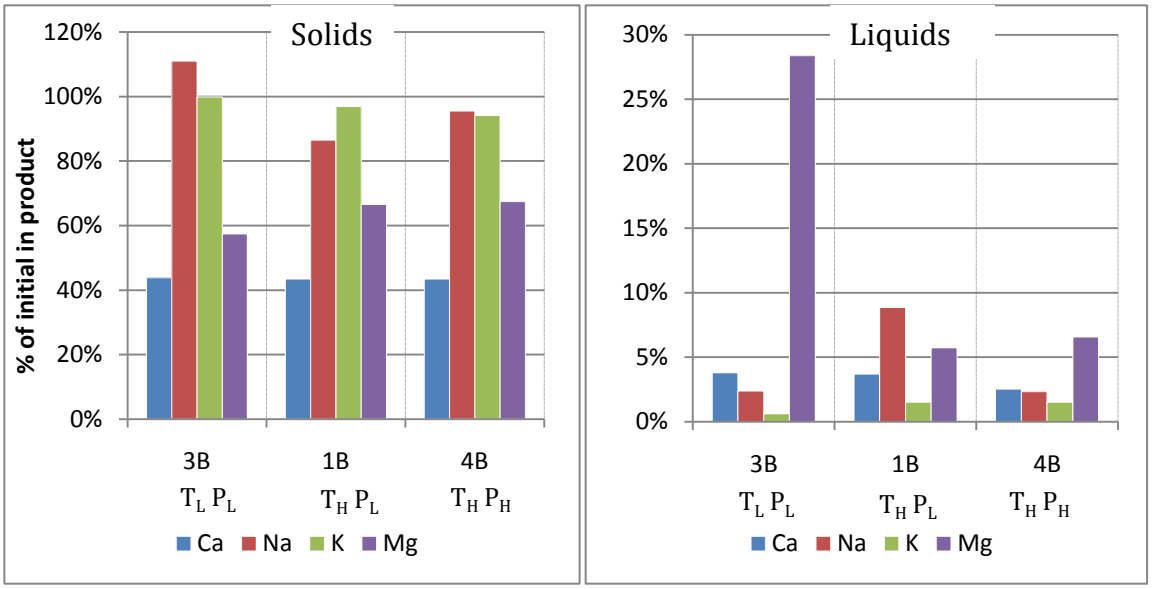

Figure 26: Partitioning of elements of operational interest during reactions at different temperatures and pressures for Illinois No. 6 coal experiments

4.5 Relationship of Inorganic Occurrence to Partitioning During Liquefaction

The results from the chemical fractionation work consistently showed Al, Fe, and V as acid insoluble elements. Of these three, Al and Fe followed a similar pattern in the baseline tests where their partitioning favored the residue over the liquid product. When the catalyst was removed from the reaction, the Al and Fe were also the only two elements to increase their partitioning to the residue in the IL#6 coal while V had the largest decrease in its partitioning to the residue. In the PRB coal, Al decreased in its partitioning to the residue in thermal liquefaction test runs, although in both runs Al was over 100% while the behavior of Fe and V did not change significantly.

Chemical fractionation of the different coals showed that a few elements differed in their acid insolubility. Titanium, which was only found to be acid insoluble in the PRB coal,

had higher partitioning to the solid products and less to the liquid products in the PRB coal for the baseline test runs as compared to the baseline test for the IL#6. The IL#6 coal had more insoluble elements (i.e., K, Mg, Ti, and Hg) and Figure 27 is a plot of the occurrence of K and Mg in the parent coals and their occurrence in the DCL residue and liquid. Figure 27 shows that even though there was a difference between the modes of occurrence of K and Mg in the two coals, they both produced similar normalized distributions in the baseline liquefaction test run. These elements are examples of no association between the mode of occurrence of an element and its distribution in the DCL products.

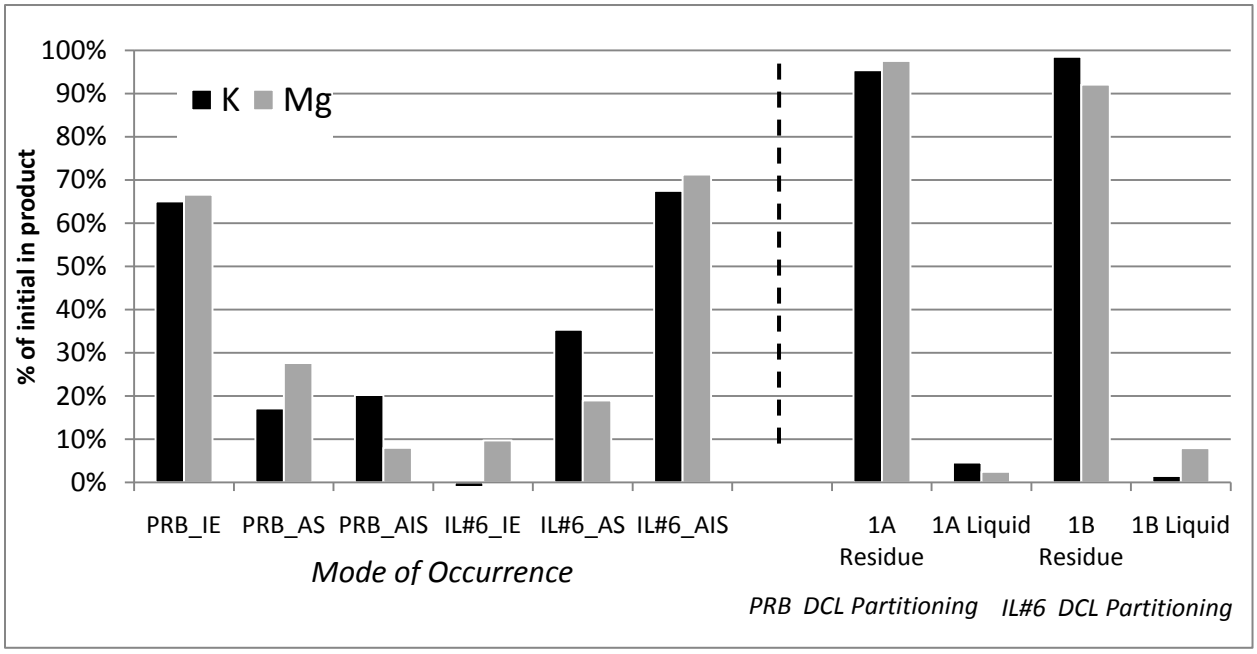

Figure 27: Chemical fractionation and normalized DCL results for K and Mg (IE-Ion Exchangeable, AS-Acid Soluble, AIS-Acid Insoluble)

Molybdenum and Zn displayed a noticeable greater partitioning to the liquid DCL THF-soluble product (>40%). In chemical fractionation, Zn and Mo were also consistently leached in the water washes. Figure 28 shows that Mo and Zn (water soluble elements) had

significant partitioning to the liquid products. However, Pb, which was the most water soluble element, was concentrated in the solids and not the liquids during the DCL reactions. This is shown graphically in Figure 28. Therefore, a trend cannot be concluded between water solubility and partitioning to the DCL liquid products using these data.

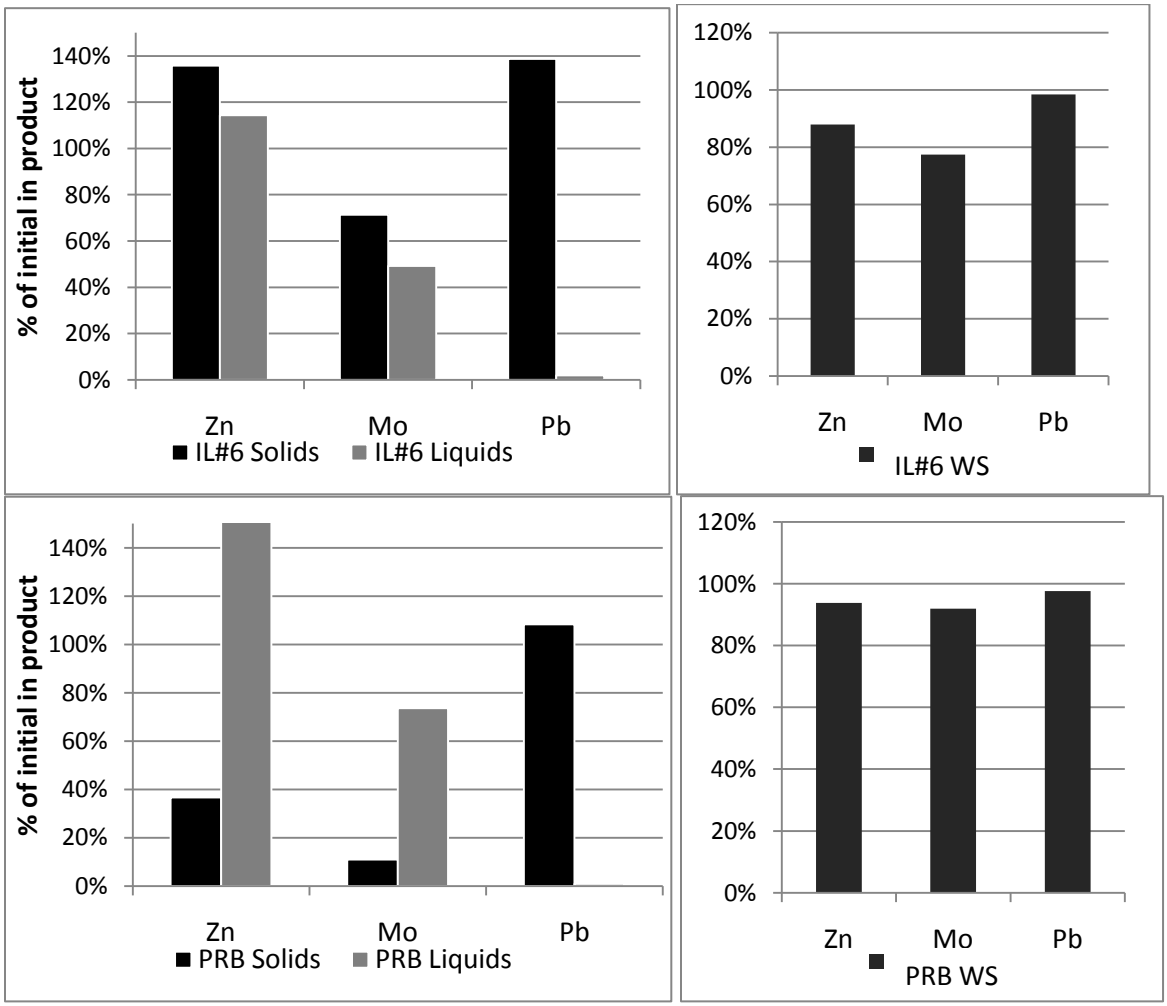

Figure 28: Zn, Mo, and Pb partitioning to DCL solid and liquid products and their water solubility (WS)

4.6 Inorganic Elements in DCL Products

4.6.1 Alkali and Alkaline Earth Metals and Operational Concerns

In this thesis, Ca, K, Mg, and Na have been studied to observe any potential concerns they may cause by being present in DCL products. Table 32 lists the concentrations of these alkali and alkaline earth metals (AAEMs) from the IL#6 coal tests.

Table 32: Concentration of AAEMs in initial coal and solid and liquid products from Illinois No. 6 coal tests

SOLIDS PPM	IL#6 Feed coal	1B Baseline	2B No catalyst	3B Low T & P	4B High T & P	CL_IL#6 Feed coal	5B Baseline	6B No catalyst
Ca	4600	10000	10300	6600	9000	20	4	2
K	1380	6200	6600	4500	5800	1100	3200	3800
Mg	240	700	720	450	720	48	75	120
Na	900	3600	4000	3000	3800	960	2900	3000

LIQUIDS PPM	IL#6 Feed coal	1B Baseline	2B No catalyst	3B Low T & P	4B High T & P	CL_IL#6 Feed coal	5B Baseline	6B No catalyst
Ca	4600	49	63	41	22	20	3.9	54
K	1380	6	6	2	4	1100	1.5	4.3
Mg	240	4	6	16	3	48	1	1.4
Na	900	23	9	5	4	960	8.6	7.4

Cleaning the Illinois No. 6 coal resulted in significant reductions in concentration in all of the AAEM elements in the solid products, except for Na which did not experience a reduction from the float-sink cleaning process. In the liquid products, the coal cleaning only showed a reduction in Mg concentration and did not have a significant influence on the other three elements.

The same results from tests conducted with the PRB coal are shown in Table 33. In low-rank coals, Sondreal et al. (1977) have studied ash fouling with an emphasis on the Na content of the coal because Na concentrations are often higher in low-rank coals and their associated deposits are more difficult to remove. It has been found that it was best to have less than 2% Na_2O in the ash and less than a 10% ash yield in the coal for the coal to have an acceptable fouling factor (Sondreal et al. 1977). Inherent calcium and magnesium can be helpful in reducing fouling because they can increase the ash fusion temperature (Sondreal et al. 1977).

Table 33: Concentration of AAEMs in initial coal and solid and liquid products from PRB coal tests

SOLIDS	PRB	1A	2A	3A	4A
PPM	Feed coal	Baseline	No catalyst	Low T & P	High T & P
Ca	2500	16500	10400	10100	16500
K	140	780	640	280	550
Mg	390	6600	1700	1400	4100
Na	940	3600	3100	1500	3600

LIQUIDS	PRB	1A	2A	3A	4A
PPM	Feed coal	Baseline	No catalyst	Low T & P	High T & P
Ca	2500	57	380	29	18
K	140	2	16	2	7
Mg	390	9	50	3	4
Na	940	29	42	5	7

Crude oil refinery residues are often used as gasification feedstocks and this residue usually contains about 20ppm of Ca and 0.15-5% ash (Speight 2001). These values are significantly lower than the residues of this work. Similarly, the solid residue product of DCL is often discussed as a feedstock to a gasification facility. Since the DCL residue has concentrated ash, the concern for equipment fouling is an important one since ash contents are much higher in coals compared to crudes. In Table 32 and Table 33, it can be seen that

the concentrations of these AAEMs were much higher in all the solid residue products when compared to the initial coal concentrations, with Ca as one exception (using the CL_IL#6 coal). On average, Ca and Mg concentrations doubled and K and Na concentration quadrupled in the IL#6 coal residue. In the PRB residue, the Ca concentration was more than 5 times greater than the initial coal concentration; K was 4 times greater, Mg was almost 9 times greater, and Na residue was 3 times greater. These are significant increases. Borio et al. published a nomograph to obtain a relationship of bituminous coal ash constituents to high temperature corrosion rates (Borio et al. 1977), but the oxide contents of the residues from these tests were too high to fit on the nomograph, suggesting that corrosion rates of the residues could be extremely high. This is especially true if Cl concentrations are included as well. The presence of inorganic elements in the residue can cause problems with fouling in equipment and can lead to decreased efficiencies by creating pressure drops in the equipment, and require more costly maintenance (Fernandez-Turiel et al. 2004; Babcock & Wilcox 2005).

Coal derived liquids, similar to heavy crude oil fractions, can be considered for use in an oil-fired boiler. If so, the AAEMs in the liquids can contribute to boiler deposition. These elements can form deposits of sulfates such as Na_2SO_4 and $MgSO_4$, and the acidity of these sulfates can be corrosive to boiler equipment (Jackson 1977).

In liquid upgrading processes, CDL's high concentrations of AAEMs have been found to directly inhibit catalyst activity (Thakur and Thomas 1985; Yoshimura et al. 1991; Speight 2001). It was found that K was the most detrimental, followed by Na, Ca and finally Mg.

The concentrations of major, minor and trace elements in a barrel of coal derived liquid produced using the different reaction variables in this thesis were calculated. Detailed results are shown in Appendix K, and the AAEM element concentrations from the reaction conditions of the baseline tests are shown in Table 34. Sodium and K have the highest total mass per barrel in the PRB coal baseline CDLs. Coal cleaning significantly reduced the masses of all four of the metals which would be beneficial for most catalytic upgrading processes.

Table 34: AAEM concentrations in grams per barrel of THF-soluble liquids

g/barrel	PRB Baseline	IL#6 Baseline	CL_IL#6 Baseline
Na	4.61	3.65	1.37
K	0.32	0.95	0.24
Ca	9.07	7.79	0.62
Mg	1.43	0.63	0.16

4.6.2 Mercury, Arsenic, and Selenium and Environmental Concerns

Mercury, As and Se are highly volatile elements and in DCL products they are of concern because of their potential use in coal utilization processes such as gasification (Bunt and Waanders 2008). Concentrations measurements of the feed coals, direct coal liquefaction residues (DCLR), and coal derived liquids (CDL) are shown in Table 35.

Arsenic and Se concentrated in the solid products. In the liquid products, the differences between concentrations in the first two tests and the later tests was due to increasing the liquid sample from 0.5g to 1g for analyses. Mercury liquid results were analyzed with a separate analyzer and showed fairly low concentrations in all the liquid products except for the interesting case of the CL_IL#6 coal.

Table 35: Concentration of As, Hg, and Se in coals, solid, and liquid products (ppm, Hg-ppb)

SOLIDS PPM	**PRB** Feed coal	1A Baseline	2A No catalyst	3A Low T & P	4A High T & P
As	1.2	7	4	9	6
Hg ppb	38	32	21	270	100
Se	0.4	1	1.0	3	1

SOLIDS PPM	**IL#6** Feed coal	1B Base-line	2B No catalyst	3B Low T & P	4B High T & P	**CL_IL#6** Feed coal	5B Base-line	6B No catalyst
As	1.6	10	8	9	11	1.3	6.5	5.9
Hg ppb	120	210	250	270	290	38	280	260
Se	1.8	7	8	3	2	1	2.0	2.4

LIQUIDS PPM	**PRB** Feed coal	1A Baseline	2A No catalyst	3A Low T & P	4A High T & P
As	1.2	0.5*	0.5*	0.1	0.1
Hg ppb	38	1	1	16	14
Se	0.4	0.5	0.5	0.1	0.1

LIQUIDS PPM	**IL#6** Feed coal	1B Base-line	2B No catalyst	3B Low T & P	4B High T & P	**CL_IL#6** Feed coal	5B Base-line	6B No catalyst
As	1.6	0.5*	0.5*	0.1	0.1	1.3	0.3	0.3
Hg ppb	120	7	7	16	21	38	60	40
Se	1.8	0.5*	0.5*	0.1	0.1	1	0.1*	0.1*

** Values are maximums based on detection limits of analytical equipment*

Even though the As content in the liquids was below the detection limits, it was still present in the feed coal and concentrated in the residue. Arsenic is of concern if it deposits on the DCL catalyst. The EPA classifies spent catalyst with more than 5 ppm of As as a hazardous waste, which therefore requires special disposal (Sikonia 1985). Arsenic and Se are not as volatile as Hg and are often present in fly ash. Arsenic and Se have been found to concentrate up to 10 and 3 times, respectively, of their initial concentration in the coal

(Nadkarni 1980). If the IL#6 coal is used for gasification, a similar trace element concentration scheme occurs, the fly ash could contain 100ppm of As and over 20 ppm of Se. This is higher than the current median values of 4.6 ppm for As and 7.7 ppm for Se (EPA 2010).

In gasification, the chalcophilic As and Se can potentially bond to sulfides and remain in particulate form for easier recovery, but because of their volatility they still may need to be condensed and cleaned via emissions controls. Mercury, which was heavily concentrated in the IL#6 residue products (Table 35), is the most volatile. If the residue is gasified without any further cleaning, then its high concentration will most likely result in it being emitted with the raw gas during the gasification process, which will require removal (Bunt and Waanders 2008; Clarke 1993).

4.6.3 Coal Liquids and Other Transportation Fuels

In the United States there are regulations imposed on some inorganic elements in crude oils and transportation fuels. Some of these are due to operational concerns such as poisoning of catalysts and corrosion of materials, and others are government regulations due to health and environmental risks. Even though the liquids in this report were defined as THF-soluble and are not transportation fuels, they are compared to current liquid hydrocarbons and their current guidelines and limits as seen in Table 36. Table 36 lists several elements and shows that the AAEM concentrations in the THF-soluble product range measured in this thesis were higher than the listed common crude oil range.

Table 36: Comparison of inorganic elements of interest in liquid products and crude oils and examples of regulations

Element	Crude Oil Range (ppm)	Current Research Range (ppm)	Element Guidelines and/or Regulations	References
Calcium	0.7-25.6	4 – 380	5 ppm wt. combined max for B100	(Jones 1975; Shah et al. 1970)
Magnesium	0.1-3.2	1 – 50		
Sodium	0.04 -28.1	4-42	5 ppm wt. combined max for B100	(Shah et al. 1970; Filby et al. 1977b)
Potassium	2.0-5.6	2-16		
Arsenic	0.0015-1.2	<0.1 - <0.5, 0.3	5 ppm on spent catalyst 10 ppb in water	(Filby et al. 1977b)
Selenium	0.026-1.4	<0.1 - <0.5, 0.1	50 ppb in water	(Jones 1975; Filby et al. 1977b)
Mercury	<0.004-2.078	0.001 - 0.060	State regs. ~require 90% reductions, (crude preference <5 ppb)	(Jones 1975; Filby et al. 1977b)

Potentially hazardous elements are listed with their environmental regulations. For one crude oil company, there is a mercury equipment-preferred limit of less than 5ppb of Hg in crude oil due to equipment issues such as corrosion, fouling, and equipment plugging (Gangstad and Berg 2006). Regarding Hg environmental regulations, new utilization facilities are may be regulated by individual states and are often set at a required 90% reduction, and stricter regulations are under development (i.e., Pennsylvania Mercury Rule, 2009). There are concerns about As and Se in drinking water, and there is a maximum contaminant level (MCL) of 10ppb for As and 50ppb for Se according to the National Primary Drinking Water Regulations from the EPA (EPA 2010). Those elements that pose health risks had THF-soluble concentrations in the ranges of crude oil and may not pose any new concerns upon refining processing.

The AAEM elements may be of concern as their range contains much higher concentrations in the THF-soluble product. Alternative transportation fuels such as biodiesel are defined by ASTM standard D6751-09. For the alternative fuel to be certified 100% biodiesel (B100), it must contain less than 5ppm wt. of Ca and Mg combined and less than 5ppm wt. of total Na and K (ASTM-D6751-09 2009). If high concentrations of these inorganic elements are in the fuel, they can poison post-engine catalysts that are present in emission control devices such as catalytic converters (Kotrba 2010). This is an issue only if the AAEMs remain in the final product, but, as discussed earlier, these high concentrations can cause problems during upgrading while the impure liquids are being processed into the transportation fuel.

5. Conclusions and Recommendations for Future Work

5.1 Summary and Conclusions

This study focused on major, minor, and trace inorganic constituents in DCL and how their behavior changes with coal rank, temperature, pressure, catalyst, and removal of minerals from the coal. The objective was to study how the elements occur in the initial coals and how that related to their partitioning into either the product liquid or product solid residue during DCL and their effect on overall conversion.

Ten batch-scale direct coal liquefaction tests were conducted and the liquid products and solid residues were analyzed to assess the behavior of the inorganic constituents. The partitioning of major, minor, and trace elements were analyzed, along with their effect on the liquefaction process.

Overall conversions of baseline conditions were the highest with the Illinois No. 6 seam coal (93.4%), and were lower with the Dietz seam coal (88.0%). The lowest baseline conversions were obtained with the cleaned Illinois No. 6 coal (73.0%). The Illinois No. 6 coal contained the largest concentrations of sulfur, volatile matter, mineral matter, as well as pyrite (7.5%) with the smallest size distribution as determined by CCSEM (31.4% <22µm). These factors promoted the highest overall conversions in DCL experiments. The addition of an iron sulfide catalyst increased the overall conversion of the Dietz seam coal by ~10% but did not enhance the overall conversions for the Illinois No. 6 coal as-received or cleaned. The overall conversions were affected the most by decreasing the reaction temperature from 425 to 375°C. At the lower temperature, the Dietz seam PRB coal overall

conversion was 40%. In general, the PRB coal was more sensitive to the changing reaction variables compared to the Illinois coal, which consistently produced overall conversions in a tighter range of 84-95%.

The baseline residue products contained ash yields of about 75% in the Illinois No. 6 coal and about 50% in the PRB coal residue, and such high inorganic constituent concentrations can have negative operational and environmental impacts if used in a standard utilization process. Baseline PRB and IL#6 tests conducted with catalysts resulted in higher ash yields than their thermal liquefaction counterparts. This was very pronounced for the PRB residues, which contain approximately 19.4 and 48.8% ash in tests performed without and with catalyst, respectively. Cleaning the Illinois coal resulted in a decreased ash yield in the residue product (~30%).

Inorganic element concentrations were measured in the coals, the residue, and liquid products by use of ICP and AAS analytical techniques. The inorganic elements were concentrated in the DCL residue, but reduced levels of inorganic elements were also present in the liquid. Molybdenum, V and Zn were elements to consistently concentrate in the liquid product; while metals such as Al, Na, K, Ca, and Fe demonstrated less partitioning to the liquid products (<0.5%) in the majority of the tests. The coal derived liquids contain small mass percents of most of the feed coal's inorganic constituents. It is important to understand that even though most elements showed low *partitioning* to the liquid product, the liquid product still contained notable *concentrations* of inorganic elements (e.g., approximately 50ppm Ca, 25ppm Na, and 15ppm of Fe). Approximations of the coal derived liquids' ash yields ranged from 0.5-4.0% (2.0% average).

Sulfur recovery in the products did not exceed 75% of the initial weight of sulfur charged to the reactor which was most likely due to the formation of H_2S. In tests conducted without a catalyst, the normalized concentrations of sulfur for all three feedstocks was more evenly split between the two streams when compared to tests run with a catalyst where the sulfur was more concentrated in the solid products. This was most likely due to the FeS catalyst remaining in the solids.

In general, catalytic liquefaction residues contained higher concentrations of the inorganic elements that were charged to the reactor than the non-catalytic liquefaction residues. Coal cleaning of the Illinois No. 6 coal removed 50% of the inorganic constituents of the as received coal thereby shifting the concentrations of some elements. Lead and Ca showed decreased partitioning to the residue after coal cleaning while increasing their partitioning to the liquid product.

The partitioning of elements varied with changes in temperature and pressure; however, the variations of temperature and pressure investigated in this thesis did not produce any apparent trends or relationships in regards to the elements' partitioning. Low-temperature/low-pressure DCL compared to the baseline high-temperature/low-pressure DCL showed higher percent recoveries of its initial inorganic mass in the residue products in tests run with the PRB coal. The lowest concentrations of inorganic elements were found in the product streams of the baseline tests, and values increased during low-temperature/low-pressure and high-temperature/high-pressure tests in the IL#6 coal tests for elements of environmental concern (i.e., As and Hg). Other elements did not show

significant partitioning changes in varying reaction conditions in the IL#6 coal (i.e., Ca, Na, and K).

Inorganic constituent partitioning was not consistently related to its mode of occurrence within the feed coal. The elements that resulted in the highest partitioning to the liquid product (Zn and Mo) were present in the feed coal in a water-soluble form; however, some water-soluble elements, such as Pb, did not contain any significant concentrations in the liquid products. The PRB and IL#6 coals differed in their ion-exchangeable elements. Chemical fractionation procedures showed that the low-rank PRB coal contained more metal cations such as K^+ and Mg^{2+}, which were organically associated in the coal, as expected. In the IL#6 coal, K and Mg were more prevalently associated with the mineral matter, as expected. Regardless of their mode of occurrence, these metals concentrated in the residue products during DCL reactions of both coals and had similar partitioning to the products.

In the liquid products, the AAEM concentrations of K, Na, Mg, and Ca were higher than those in crude oil even though their partitioning to the liquids was low (typically <5%). These high concentrations (~50ppm) can result in poisoning of upgrading catalysts in transportation fuel refining processes. High concentrations of AAEMs can also corrode and foul boiler equipment if the liquid product is used as a utility fuel.

In the DCL residue, AAEM concentrations were higher than in the parent coals, which can cause fouling and corrosion of gasification or combustion equipment used to produce hydrogen or heat for the DCL process. Potassium, Na, Mg, and Ca constituents

were found to be concentrated in the DCL residues at concentrations of 6,600ppm, 4,000ppm, 720ppm, and 10,000ppm, respectively (Illinois No. 6 residue whole basis). At these concentrations, they are a cause of concern because they can corrode and foul equipment in combustion and gasification. Cleaning the Illinois No. 6 coal resulted in lower concentrations of K, Na, Mg, and Ca and were 3,200ppm, 2,900ppm, 75ppm, and 4ppm, respectively, which were reductions of 51.5%, 27.5%, 89.6%, and 100.0% respectively.

Elements that have adverse effects on human health, such as Hg, Se, and As, were also concentrated in the residue products at concentrations about 1.5, 3.0, and 6.0 times that of the feed coal, respectively. If the residue is utilized in combustion facilities without the proper emission control equipment, the high concentrations of Hg, As, and Se can produce harmful emissions which would pollute the atmosphere, water and food chain. In the liquid products, these elements were within the range of concentrations that are found in crude oils; however, compared to crude oil median concentration values, some of the liquid product values were on the high end (15ppb of Hg and 0.3ppm in Se).

Direct coal liquefaction is of interest for the production of a domestic transportation fuel and the behavior of the inorganic constituents, specifically major and minor metals, must be known. If inorganic constituents concentrate in the DCL liquid, they have the potential to remain in the refined product and could be emitted when utilized. Similarly, if the inorganic constituents concentrate in the DCL residue, they can have adverse effects on equipment and their emissions have to be controlled.

5.2 Future Work

This thesis presents data to assess the behavior of the inorganic elements in DCL processes. Although much data was generated, there is more work that should be conducted on this topic.

Initially, 31 elements were to be observed in this process but only 16 had results that were easily discussed based on available analytical techniques. Analytical equipments such as inductively coupled plasma mass spectroscopy or neutron activation analysis, which have lower detection limits than the equipment available for this thesis, should be used. It would be interesting for future work to focus on all 31 elements. In fact, an individual analysis of each element could potentially answer many current issues including: what was the source of the Si contamination, and why did the Al content decrease in the IL#6 coal and increase in the PRB coal, and why was the Hg data so variable?

Other elements besides the initial 31 elements should also be studied. Chlorine was not included because the residue sample size after TGA, AAS and ICP analyses was too small for the Cl analytical system that was available for use (i.e., ion electrode measurements, ASTM D-2361-66). The hazardous element fluorine was not included in this work; future work including the partitioning of F is important because of its known human health hazards, mainly fluorosis which is associated with coal combustion emissions (Finkelman et al. 2002). Concentrations of F could be measured by ion selective electrode (Nadkarni 1980) in addition to a recently developed pyrohydrolysis technique (Sredovic and Rajakovic 2010).

The gas produced from the DCL tests should be analyzed. This would be helpful in understanding the mass balances of the elements, specifically with elements such as S and Hg. Monitoring inorganic element partitioning on larger scale, continuously operated equipment would result in obtaining a larger and more representative data set.

Additional research would be to utilize the products. Gasification of the high-ash residues would show how they would perform in a gasifier, specifically the effect of AAEMs on slag and ash physical properties. The liquid products in this work contained presaphaltenes, asphaltenes and oils, which could be individually analyzed, and the oil products could be studied through refinery distillation simulations. Inorganic elements could then be tracked through the entire process similar as they have been with crude oil. Information obtained would include their concentrations in various boiling point fractions, their concentration in the refinery residue, and their final concentrations in the gasoline or diesel products.

REFERENCES

Anderson, L.L. 1992. "Catalysis in direct coal liquefaction." In *Clean Utilization of Coal: Coal Stucture and Reactivity, Cleaning and Environmental Aspects*, ed. Y. Yurum. Dordrecht: Kluwer.

Artok, L., H. H. Schobert, and O. Erbatur. 1994. "Temperature-staged liquiefaction of selected Turkish coals." *Fuel Processing Technology* 37 (3):211-36.

ASTM Standard D3176. 2009. "Standard Practice for Ultimate Analysis of Coal and Coke" *Annual Book of ASTM Standards*. ASTM International, West Conshohocken, PA.

ASTM Standard D6751. 2009. "Standard Specification for Biodiesel Fuel Blend Stock (B100) " *Annual Book of ASTM Standards*. ASTM International, West Conshohocken, PA.

ASTM Standard D388. 2009. "Standard Classification of Coals by Rank" *Annual Book of ASTM Standards*. ASTM International, West Conshohocken, PA.

ASTM Standard D3172. 2009. "Standard Practice for Proximate Analysis of Coal and Coke" *Annual Book of ASTM Standards*. ASTM International, West Conshohocken, PA.

Babcock & Wilcox. 2005. *Steam / Its Generation and Use*. Edited by J. B. Kitto and S. C. Stultz. Vol. Edition, 41. New York [etc.],: McDermott Company.

Bergerioux, C., J. L. Galinier, and L. Zikovsky. 1979. "Determination of trace-element pathways in a petroeum distillation unit by instumental neutron-activation analysis." *Journal of Radioanalytical Chemistry* 54 (1-2):255-65.

Borio, R.W., A.L Plumley, and W.R. Sylvester. 1977. Factors affecting metal wastage in pulverized coal-fired steam generators. International Conference on Ash Deposits and Corrosion from Impurities in Combustion Gases, at New England College.

Brown, R. S., D. W. Hausler, J. W. Hellgeth, and L. T. Taylor. 1982. "Application of Inductively Coupled Plasma Atomic Emission-Spectrometry (ICP-AES) to Metal Quantitation and Speciation in Synfuels." *Acs Symposium Series* 205:163-83.

Bunt, J. R., and F. B. Waanders. 2008. "Trace element behaviour in the Sasol-Lurgi MK IV FBDB gasifier. Part 1 - The volatile elements: Hg, As, Se, Cd and Pb." *Fuel* 87 (12):2374-87.

Burgess, C. E., and H. H. Schobert. 1996. "Effect of coal characteristics and molybdenum sulfide catalyst on conversions and yields of heavy products from liquefaction in phenanthrene." *Energy & Fuels* 10 (3):718-25.

Bustin, R. M. 1985. *Coal petrology : its principles, methods, and applications*. 2nd rev. ed. [Waterloo, Ontario]: Geological Association of Canada.

Chu, X., W. Li, and H. Chen. 2006. "Gasification property of direct coal liquefaction residue with steam." *Process Safety and Environmental Protection* 84 (B6):440-5.

Clarke, L. B. 1993. "The fate of trace-elements during coal combustion and gasification - an overview." *Fuel* 72 (6):731-6.

Cloke, M., S. Hamilton, and J. P. Wright. 1987a. "Changes in trace element concentrations and catalyst activity during the hydrocracking of a coal extract solution." *Fuel* 66 (5):678-82.

Cloke, M., S. Hamilton, and J. P. Wright. 1987b. "Evidence for mineral matter Forms in Coal-Liquefaction Extracts." *Fuel* 66 (12):1685-90.

Coleman, W. M., P. Perfetti, H. C. Dorn, and L. T. Taylor. 1978. "Trace-element distribution in various solvent refined coal fractions as a function of feed coal." *Fuel* 57 (10):612-6.

Cui, H., J. L. Yang, Z. Y. Liu, and J. C. Bi. 2003. "Characteristics of residues from thermal and catalytic coal hydroliquefaction." *Fuel* 82 (12):1549-56.

Cui, H., J. Yang, Z. Liu, and J. Bi. 2002. "Effects of remained catalysts and enriched coal minerals on devolatilization of residual chars from coal liquefaction." *Fuel* 81 (11-12):1525-31.

Dadyburjor, Dady B., and Zhenyu Liu. 2000. *Coal Conversion Processes Liquefaction*: John Wiley & Sons, Inc.

Derbyshire, F. 1989. "Role of catalysis in coal-liquefaction research and development." *Fuels* 3 (3):273-7.

Duyck, C., N. Miekeley, C. L. P. da Silveira, R. Q. Aucelio, R. C. Campos, P. Grinberg, and G. P. Brandao. 2007. "The determination of trace elements in crude oil and its heavy fractions by atomic spectrometry." *Spectrochimica Acta Part B-Atomic Spectroscopy* 62 (9):939-51.

Evironmental Protection Agency. 2010 In *Technology Transfer Network: Air Toxics Web Site*. Washington, DC.: National Center for Environmental Assessment, Office of Research and Development.

Evironmental Protection Agency. *Drinking Water Contaminants*, Wednesday, June 02, 2010. [cited. Available from http://water.epa.gov/drink/contaminants/index.cfm.]

Falcone Miller, S. , and B.G. Miller. 2005. "The effect of cofiring coal and biomass on utilization of coal combustion products: the U.S. perspective." University Park, Pennsylvania, USA: The Energy Institute, The Pennsylvania State University.

Falcone Miller, S., and B.G. Miller. 2008. "Refinery inegration for production of coal-based fuels." In *Refinery Integration of By-Products from Coal-Derived Jet Fuels* ed. C. E. Burgess, A. Boehman, B. G. Miller, G. D. Mitchel, L. Rudnick, C. Song and H. H. Schobert. University Park, PA: The Energy Institute, The Pennsylvania State University.

Falcone Miller, Sharon. 1992. A comparison study of ash formation during pilot-scale combustion of pulverized coal and coal-water slurry fuels. PhD Thesis, Fuel Science, The Pennsylvania State University, State College, PA.

Feng, X., and Y. Hong. 1999. "Modes of occurrence of mercury in coals from Guizhou, People's Republic of China." *Fuel* 78 (10):1181-8.

Fernandez-Turiel, J. L., A. Georgakopoulos, D. Gimeno, G. Papastergios, and N. Kolovos. 2004. "Ash deposition in a pulverized coal-fired power plant after high-calcium lignite combustion." *Energy & Fuels* 18 (5):1512-8.

Filby, R. H., K. R. Shah, and C. A. Sautter. 1977a. "Study of trace-element distribution in solvent refined coal (SRC) process using neutron-activation analysis." *Journal of Radioanalytical Chemistry* 37 (2):693-704.

Filby, R.H., K. R. Shah, and F Yaghane. 1977b. The nature of metals in petroleum fuels and coal-derived synfuels. International Conference on Ash Deposits and Corrosion from Impurities in Combustion Gases, at New England College.

Finkelman, R. B. 1999. "Trace elements in coal - Environmental and health significance." *Biological Trace Element Research* 67 (3):197-204.

Finkelman, R. B., W. Orem, V. Castranova, C. A. Tatu, H. E. Belkin, B. S. Zheng, H. E. Lerch, S. V. Maharaj, and A. L. Bates. 2002. "Health impacts of coal and coal use: possible solutions." *International Journal of Coal Geology* 50 (1-4):425-43.

Finkelman, R. B., C. A. Palmer, M. R. Krasnow, P. J. Aruscavage, G. A. Sellers, and F. T. Dulong. 1990. "Combustion and leaching behavior of elements in the Argonne Premium Coal Samples." *Energy & Fuels* 4 (6):755-66.

Gangstad, Audun, and Ståle Berg. 2006. "Mercury in crude oil and natural gas: A concern for the oil and gas industry." Statoil.

Ganguly, B., F. E. Huggins, Krpm Rao, and G. P. Huffman. 1993. "Determination of the particle-size distribution of iron-oxide catalysts from superparamagnetic mossbauer relaxation spectra." *Journal of Catalysis* 142 (2):552-60.

Garg, D., and E. N. Givens. 1982. "Pyrite catalysts in coal-liquefaction." *Industrial & Engineering Chemistry Process Design and Development* 21 (1):113-7.

Gentzis, T., and F. Goodarzi. 1999. "Chemical fractionation of trace elements in coal and coal ash." *Energy Sources* 21 (3):233-56.

George, G. N., M. L. Gorbaty, S. R. Kelemen, and M. Sansone. 1991. "Direct determination and quantification of sulfur forms in coals from the Argonne premium sample program." *Energy & Fuels* 5 (1):93-7.

Given, P. H., D. C. Cronauer, W. Spackman, H. L. Lovell, A. Davis, and B. Biswas. 1975. "Dependence of coal liquefaction behavior on coal characteristics 2. Role of petrographic composition." *Fuel* 54 (1):40-9.

Glick, D. C.; Mitchell, G. D.; Davis, A. 2005." Coal sample preservation in foil multilaminate bags." *International Journal of Coal Geology* 63, 178-189

Goyer, R. A. 1996. "Results of lead research: Prenatal exposure and neurological consequences." *Environmental Health Perspectives* 104 (10):1050-4.

Gozmen, B., L. Artok, G. Erbatur, and O. Erbatur. 2002. "Direct liquefaction of high-sulfur coals: Effects of the catalyst, the solvent, and the mineral matter." *Energy & Fuels* 16 (5):1040-7.

Gray, R. H. 1984. "Chemical and toxicological aspects of coal liquefaction and other complex mixtures." *Regulatory Toxicology and Pharmacology* 4 (4):380-90.

Gray, R. H., R. W. Hanf, D. D. Dauble, and J. R. Skalski. 1982. "Chronic effects of a coal liquid on a fresh-water alga, Selenastrum-Capricornutum." *Environmental Science & Technology* 16 (4):225-9.

Guin, J. A., C. W. Curtis, and K. C. Kwon. 1983. "Pyrite-catalysed coal-liquefaction using quinoline tetrahydroquinoline as an H-donor system." *Fuel* 62 (12):1412-6.

Guin, J. A., A. R. Tarrer, J. W. Prather, D. R. Johnson, and J. M. Lee. 1978. "Effects of coal minerals on hydrogenation, desulfurization, and solvent-extraction of coal." *Industrial & Engineering Chemistry Process Design and Development* 17 (2):118-26.

Hattori, H., T. Yamaguchi, K. Tanabe, S. Yokoyama, J. Umematsu, and Y. Sanada. 1984. "Catalystic activities and selectivities of complex metal-oxides for hydrocracking of bituminous coal." *Fuel Processing Technology* 8 (2):117-22.

Hausler, D. W., J. W. Hellgeth, L. T. Taylor, J. Borst, and W. B. Cooley. 1981. "Trace-metal distribution in fractions of solvent-refined coal by ICP-OES and implications regarding metal speciation." *Fuel* 60 (1):40-6.

Hellgeth, J. W., R. S. Brown, and L. T. Taylor. 1984. "Effect of coal-liquefaction conditions on the trace-element content of the soluble nonvolatile product." *Fuel* 63 (4):453-62.

Herod, A. A., A. George, C. A. Islas, I. Suelves, and R. Kandiyoti. 2003. "Trace-element partitioning between fractions of coal liquids during column chromatography and solvent separation." *Energy & Fuels* 17 (4):862-73.

Huang, L. L., and H. H. Schobert. 2005. "Comparison of temperature conditions in direct liquefaction of selected low-rank coals." *Energy & Fuels* 19 (1):200-7.

Huffman, G. P., B. Ganguly, J. Zhao, K. R. P. M. Rao, N. Shah, Z. Feng, F. E. Huggins, M. M. Taghiei, F. L. Lu, I. Wender, V. R. Pradhan, J. W. Tierney, M. S. Seehra, M. M. Ibrahim, J. Shabtai, and E. M. Eyring. 1993. "Structure and dispersion of iron-based catalysts for direct coal-liquefaction." *Energy & Fuels* 7 (2):285-96.

Huffman, G. P., S. Mitra, F. E. Huggins, N. Shah, S. Vaidya, and F. L. Lu. 1991. "Quantitative-analysis of all major forms of sulfur in coal by x-ray absorption fine-structure spectroscopy." *Energy & Fuels* 5 (4):574-81.

Huggins, F. E. 2002. "Overview of analytical methods for inorganic constituents in coal." *International Journal of Coal Geology* 50 (1-4):169-214.

Huggins, F. E., and G. P. Huffman. 1995. "Chlorine in coal - an XAFS spectroscopic investigation." *Fuel* 74 (4):556-69.

Huggins, F. E., L. B. A. Seidu, N. Shah, G. P. Huffman, R. Q. Honaker, J. R. Kyger, B. L. Higgins, J. D. Robertson, S. Pal, and M. S. Seehra. 2009. "Elemental modes of occurrence in an Illinois #6 coal and fractions prepared by physical separation techniques at a coal preparation plant." *International Journal of Coal Geology* 78 (1):65-76.

Jackson, P.J. 1977. Deposition ofiInorganic material in oil-fired boilers. International Conference on Ash Deposits and Corrosion from Impurities in Combustion Gases, at New England College.

Jones, Peter. 1975. *Trace metals and other elements in crude oil : a literature review*. Sunbury: The British Petroleum Co. Ltd.

Joseph, J. T., and T. R. Forrai. 1992. "Effect of exchangeable cations on liquefaction of low rank coals." *Fuel* 71 (1):75-80.

Kaneko, T., K. Tazawa, T. Koyama, K. Satou, K. Shimasaki, and Y. Kageyama. 1998. "Transformation of iron catalyst to the active phase in coal liquefaction." *Energy & Fuels* 12 (5):897-904.

Karner, F. R., H. H. Schobert, S. K. Falcone, and S. A. Benson. 1986. "Elemental distribution and association with inorganic and organic-components in North-Dakota lignites." *Acs Symposium Series* 301:70-89.

Keogh, Robert A, Darrell N Taulbee, James C Hower, Bribal Chawla, and Burtron H Davis. 1992. "Liquefaction characteristics of the three major maceral groups separated from a single coal." *Energy & Fuels* 6:614-8.

Klein, D.H., A.W. Andren, J.A. Carter, J.F. Emery, C. Feldman, W. Fulkerson, W.S. Lyon, J.C. Ogle, Y. Talmi, R.I. Vanhook, and N. Bolton. 1975. "Pathways of 37 trace-elements through coal-fired power-plant." *Environmental Science & Technology* 9 (10):973-9.

Kotrba, Ron. 2010. "Year of the SCR System." *Biodiesle Magazine*, February 2019, 45-9.
Kuznetsov, P. N., G. I. Sukhova, J. Bimer, P. D. Salbut, E. D. Korniyets, N. A. Belskaya, and N. M. Ivanchenko. 1991. "Coal-characterization for liquefaction in tetralin and alcohols." *Fuel* 70 (9):1031-8.
Lambert, J. M. 1982. "Alternative interpretation of coal-liquefaction catalysis by pyrite." *Fuel* 61 (8):777-8.
Lee, J. M., and C. E. Cantrell. 1991. "Effect of coal rank and quality on 2-stage liquefaction." *Fuel Processing Technology* 29 (3):171-97.
Li, X., S. X. Hu, L. J. Jin, and H. Q. Hu. 2008. "Role of iron-based catalyst and hydrogen transfer in direct coal liquefaction." *Energy & Fuels* 22 (2):1126-9.
Luttrell, G. H., J. N. Kohmuench, and R. H. Yoon. 2000. "An evaluation of coal preparation technologies for controlling trace element emissions." *Fuel Processing Technology* 65:407-22.
Miller, R. N., and P. H. Given. 1986. "The association of major, minor, and trace inorganic elements with lignites 1. experimental approach and study of a Norh-Dakota Lignite." *Geochimica Et Cosmochimica Acta* 50 (9):2033-43.
Mitchell, Gareth D. 2008. "Direct Coal Liquefaction." In *Applied Coal Petrology: The Role of Petrology in Coal Utilization*, ed. I. Suárez-Ruiz and J. C. Crelling. Amsterdam; Boston: Elsevier / Academic Press.
Mochida, I., R. Sakata, and K. Sakanishi. 1989. "Effects of deashing and low-pressure hydrogen on hydrogen trasferring liquefaction at reduced solvent coal ratio." *Fuel* 68 (3):306-10.
Montano, P. A., and B. Granoff. 1980. "Stoichiometry of iron sulfides in liquefaction residues and correlation with conversion." *Fuel* 59 (3):214-6.
Mukherjee, D. K., and P. B. Chowdhury. 1976. "Catalytic effect of mineral matter constituents in a north assam coal on hydrogenation." *Fuel* 55 (1):4-8.
Mukherjee, D. K., and J. R. Mitra. 1984. "Catalytic roles of iron and hydrogen-sulfide on hydrogenation of coal." *Fuel* 63 (5):722-3.
Murillo, M., and J. Chirinos. 1994. "Use of emulsion systems for the determination of sulfur, nickel, and vanadium in heavy crude-oil samples by inductively-coupled plasma-atomic emission-spectrometry." *Journal of Analytical Atomic Spectrometry* 9 (3):237-40.
Nadkarni, R. A. 1980. "Multi-technique multi-elemental analysis of coal and fly-ash." *Analytical Chemistry* 52 (6):929-35.
Nadkarni, R. A. 1984. "Applications of microwave-oven sample dissolution in analysis." *Analytical Chemistry* 56 (12):2233-7.
Oberg, Erik, Franklin D Jones, Holbrook L Horton, and Henry H Ryffel. 1992. *Machinery's Handbook*. Edited by R. E. Green. 24 ed. New York, New York: Industrial Press Inc.
Orchin, M., and H. H. Storch. 1948. "Solvation and hydrogenation of coal." *Industrial and Engineering Chemistry* 40 (8):1385-9.
Painter, P., N. Pulati, R. Cetiner, M. Sobkowiak, G. Mitchell, and J. Mathews. 2010. "Dissolution and dispersion of coal in ionic liquids." *Energy & Fuels* 24:1848-53.
Pennsylvania Department of Environmental Protection. 2010. "Pennsylvania's Mercury Reduction Rule" www.portal.state.pa.us/portal/server.pt/community/mercury/

Pringle, T. G., and R. E. Jervis. 1987. "The Redistribution of trace and minor elements during coal-liquefaction." *Canadian Journal of Chemical Engineering* 65 (3):494-9.

Probstein, Ronald F., and R. Edwin Hicks. 1982. *Synthetic Fuels*. New York: McGraw-Hill.

Richardson, J. T. 1972. "Thermo-magnetic studies of iron compounds in coal char." *Fuel* 51 (2):150-2.

Richaud, R., H. Lachas, M. J. Lazaro, L. J. Clarke, K. E. Jarvis, A. A. Herod, T. C. Gibb, and R. Kandiyoti. 2000. "Trace elements in coal derived liquids: analysis by ICP-MS and Mossbauer spectroscopy." *Fuel* 79 (1):57-67.

Robinson, K. K. 2009. "Reaction engineering of direct coal liquefaction." *Energies* 2 (4):976-1006.

Scaroni, Alan W., Alan Davis, David C. Glick, Patrick G. Hatcher, Gareth D. Mitchell, Daniel Carson, and Lei Hou. 1999. "*Maintenance of the Coal Sample Bank and Database*." Department of Energy. University Park, PA: The Pennsylvania State University.

Schobert, H. H. 1992. "Catalytic and chemical behavior of coal mineral matter in the coal conversion process." In *Clean utilization of coal: coal structure and reactivity, cleaning, and environmental aspects*, ed. Y. Yurum. Dordrecht: Kluwer Academic Publishers.

Schobert, Harold H. 1990. *The Chemistry of Hydrocarbon Fuels*. London; Boston: Butterworths.

Schroeder, William H., and John Munthe. 1998. "Atmospheric mercury--An overview." *Atmospheric Environment* 32 (5):809-22.

Senior, C. L., T. Zeng, J. Che, M. R. Ames, A. F. Sarofim, I. Olmez, F. E. Huggins, N. Shah, G. P. Huffman, A. Kolker, S. Mroczkowski, C. Palmer, and R. Finkelman. 2000. "Distribution of trace elements in selected pulverized coals as a function of particle size and density." *Fuel Processing Technology* 63 (2-3):215-41.

Shah, K. R., R. H. Filby, and W. A. Haller. 1970. "Determination of trace elements in petroleum by neutron activation analysis. 1. Determination of Na, S, Cl, K, Ca, V, Mn, Cu, Ga, and Br." *Journal of Radioanalytical Chemistry* 6 (1):185-&.

Shui, H. F., Z. Y. Cai, and C. B. Xu. 2010. "Recent advances in direct coal liquefaction." *Energies* 3 (2):155-70.

Sikonia, J. G. 1985. "Arsenic management in shale oil upgrading." *Environmental Geochemistry and Health* 7 (2):64-8.

Simeonova, M., V. Georgieva, and C. Alexiev. 1989. "Crytogenetic investigations of human-subjects occupationally exposed to chemicals from the petroleum-processing industry." *Environmental Research* 48 (2):145-53.

Sondreal, Everett A., G.H. Gronhovd, P.H. Tufte, and W Beckering. 1977. Ash fouling studies of low-rank western U.S. coals. International Conference on Ash Deposits and Corrosion from Impurities in Combustion Gases, at New England College.

Song, C. S., A. K. Saini, and H. H. Schobert. 1994. "Effects of drying and oxidation of Wyodak subbituminous coal in its thermal and catalytic liquefaction - Spectroscopic characterization and products distribution." *Energy & Fuels* 8 (2):301-12.

Spears, D. A., L. I. Manzanares-Papayanopoulos, and C. A. Booth. 1999. The distribution and origin of trace elements in a UK coal; the importance of pyrite.

Speight, J.G. 1983. *The Chemistry and Technology of Coal*. New York, New York: Marcel Decker.

Speight, James G. 2001. *Handbook of Petroleum Analysis*. New York: Wiley-Interscience.

Sredovic, I., and L. Rajakovic. 2010. "Pyrohydrolytic determination of fluorine in coal: A chemometric approach." *Journal of Hazardous Materials* 177 (1-3):445-51.

Suzuki, T., O. Yamada, Y. Takahashi, and Y. Watanabe. 1985. "Hydroliquefaction of low-sulfur coals using iron carbonyl-complexes sulfur as catalysts." *Fuel Processing Technology* 10 (1):33-43.

Swaine, Dalway J., and F. Goodarzi. 1995. *Environmental Aspects of Trace Elements in Coal*. Dordrecht ; Boston: Kluwer Academic Publishers.

Tanabe, K., H. Hattori, T. Yamaguchi, T. Iizuka, H. Matsuhashi, A. Kimura, and Y. Nagase. 1986. "Function of metal-oxide and complex oxide catalysts for the hydrocracking of coal." *Fuel Processing Technology* 14:247-60.

Taylor, L. T., D. W. Hausler, and A. M. Squires. 1981. "Organically bound metals in a solvent-refined coal - Metallograms for a Wyoming subbituminous coal." *Science* 213 (4508):644-6.

Thakur, D. S., and M. G. Thomas. 1985. "Catalyst deactivation in heavy petroleum and synthetic crude oil processing - A review." *Applied Catalysis* 15 (2):197-225.

Thiessen, Gilbert. 1945. "Forms of Sulfur in Coal." In *Chemistry of Coal Utilization*, ed. H. H. Lowry. Pittsburgh, Pennsylvania: John Wiley & Sons., Inc.

Toole-O'Neil, B., S. J. Tewalt, R. B. Finkelman, and D. J. Akers. 1999. "Mercury concentration in coal - unraveling the puzzle." *Fuel* 78 (1):47-54.

Trewhella, M. J., and A. Grint. 1987. "The role of sulfur in coal hydroliquefaction." *Fuel* 66 (10):1315-20.

Tye, C., H. H. Schobert, and R. Neumann. 1985. Uses of dielectric spectra and immersional calorimetry in the characterization of low rank coals, at Miami Beach, FL, USA.

U.S. Energy and Information Administration. "U.S. Primary Energy Flow by Source and Sector, 2009" Annual Energy Review. November 2010, [cited. Available from http://www.eia.doe.gov/emeu/aer/pecss_diagram.html]

Valkovi, Vlado. 1983. *Trace Elements in Coal*. Boca Raton, Fla.: CRC Press.

Van Krevelen, D. W. 1961. *Coal: Typology, Chemistry, Physics, Constitution*. Amsterdam: Elsevier.

Vejahati, Farshid, Zhenghe Xu, and Rajender Gupta. 2010. "Trace elements in coal: Associations with coal and minerals and their behavior during coal utilization - A review." *Fuel* 89 (4):904-11.

Walker, P. L., W.P. Spackman, P. H. Given, E.W. White, A. Davis, P.C Painter, and R.G. Jenkins. 1980. "Characterization of mineral matter in coals and coal liquefaction residues." In *EPRI Report*, ed. W. C. Rovesti. Universtiy Park, PA: The Pennsylvania State University.

Whitehurst, D. Duayne, Thomas O. Mitchell, and Malvina Farcasiu. 1980. *Coal Liquefaction: the Chemistry and Technology of Thermal Processes*. New York: Academic Press.

Witschi, H. P., L. H. Smith, E. L. Frome, M. E. Pequetgoad, W. H. Griest, C. H. Ho, and M. R. Guerin. 1987. "Skin tumorigentic potention of crude and refined coal liquids and analogous petroleum-roducts." *Fundamental and Applied Toxicology* 9 (2):297-303.

Yagminas, A., P. A. Devries, and D. C. Villeneuve. 1988. "Systematic toxicity of coal-liquefaction products - Results of a 14-day dermal exposure." *Bulletin of Environmental Contamination and Toxicology* 40 (3):433-8.

Yarzab, R. F., P. H. Given, W. Spackman, and A. Davis. 1980. "Dependence of coal-liquefaction behavior on coal characteristics 4. Cluster Analyses for Characteristics of 104 Coals." *Fuel* 59 (2):81-92.

Yoshimura, Y., S. Endo, S. Yoshitomi, T. Sato, H. Shimada, N. Matsubayashi, and A. Nishijima. 1991. "Deactivation of huydrotreating molybdate catalysts by metal-deposition." *Fuel* 70 (6):733-9.

Zhang, L., T. Takanohashi, S. Kutsuna, I. Saito, Q. Y. Wang, and Y. Ninomiya. 2008. "Coordination structures of organically bound paramagnetic metals in coal and their transformation upon solvent extraction." *Fuel* 87 (12):2628-40.

Zhang, S. F., B. Xu, A. A. Herod, G. M. Kimber, D. R. Dugwell, and R. Kandiyoti. 1996. "Effect of coal rank on hydrocracking reactivities of primary coal extracts prepared in a flowing-solvent reactor - The Argonne premium coal sample set." *Fuel* 75 (13):1557-67.

APPENDIX A: Coal minerals

The following chart defines coal minerals and lists potential inorganic elements that the mineral can contain.

Group	Species	Formula	Potential Elements (Not including C,H,N,O)						
Shale	Muscovite	$(K,Na,H_3O,Ca)_2(Al,Mg,Fe,Ti)_4$	Al	Ca	Fe	K	Mg	Na	Ti
	Hydromuscovite	$(Al,Si)_8O_{20}(OH,F)_4$	Al	F	Si				
	Illite	$(HO)_4K_2(Si_6{\cdot}Al_2)Al_4O_{20}$	Al	K	Si				
	Montmorillonite	$Na_2(Al\ Mg)Si_4O_{10}(OH)_2$	Al	Mg	Na	Si			
Kaolin	Kaolinite	$Al_2Si_2O_5(OH)_4$	Al	Si					
	Livesite	$Al_2Si_2O_5(OH)_4$	Al	Si					
	Metahalloysite	$Al_2Si_2O_5(OH)_4$	Al	Si					
Sulfide	Pyrite	FeS_2	Fe	S					
	Marcasite	FeS_2	Fe	S					
	Sphalerite	ZnS	Zn	S					
	Chalcopyrite	CoS_2	Co	S					
	Galena	PbS_2	Pb	S					
Carbonate	Ankerite	$CaCO_3{\cdot}(Mg,Fe,Mn)CO_3$	Ca	Fe	Mg	Mn			
	Calcite	$CaCO_3$	Ca						
	Dolomite	$CaCO_3{\cdot}MgCO_3$	Ca	Mg					
	Siderite	$FeCO_3$	Fe						
Chloride	Sylvite	KCl	Cl	K					
	Halite	NaCl	Cl	Na					

Coal Minerals Cont.

Accessory and Heavy minerals										
Heavy min	Quartz	SiO_2		Si						
	Rutile	TiO_2		Ti						
	Feldspare	$(K,Na)_2O{\cdot}Al_2O_3{\cdot}6SiO_2$		Al	K	Na	Si			
	Garnet	$3CaO{\cdot}Al_2O_3{\cdot}3SiO_2$		Al	Ca	Si				
	Hornblende	$CaO{\cdot}3FeO{\cdot}4SiO_2$		Ca	Fe	Si				
	Gypsum	$CaSO_4{\cdot}2H_2O$		Ca	S					
	Apatite	$9CaO{\cdot}3P_2O_5{\cdot}CaF_2$		Ca	F	P				
	Zircon	$ZrSiO_4$		Si	Zr					
	Epidote	$4CaO{\cdot}3Al_2O_3{\cdot}6SiO_2{\cdot}H_2O$		Al	Ca	Si				
	Biotite	$K_2O{\cdot}MgO{\cdot}Al_2O_3{\cdot}3SiO_2{\cdot}H_2O$		Al	K	Mg	Si			
	Orthoclase	$KAlSi_3O_8$		Al	K	Si				
	Augite	$CaO{\cdot}MgO{\cdot}2SiO_2$		Ca	Mg	Si				
	Prochlorite	$2FeO{\cdot}2MgO{\cdot}Al_2O_3{\cdot}2SiO_2{\cdot}H_2O$		Al	Fe	Mg	Si			
	Diaspore	$Al_2O_3{\cdot}H_2O$		Al						
	Lepidocrocite	$Fe_2O_3{\cdot}H_2O$		Fe						
	Goethite	α-FeO(OH)		Fe						
	Magnetite	Fe_3O_4		Fe						
	Kyanite	$Al_2O_3{\cdot}SiO_2$		Al	Si					
	Staurolite	$2FeO{\cdot}5Al_2O_3{\cdot}4SiO_2{\cdot}H_2O$		Al	Fe	Si				
	Topaz	$2AlFO{\cdot}SiO_2$		Al	F	Si				
	Tourmaline	$3Al_2O_3{\cdot}4BO(OH){\cdot}8SiO_2{\cdot}9H_2O$		Al	B	Si				
Oxide ore	Hematite	Fe_2O_3		Fe						
	Penninite	$5MgO{\cdot}Al_2O_3{\cdot}3SiO_2{\cdot}2H_2O$		Al	Mg	Si				
	Chlorite	$10(Mg,Fe)O{\cdot}2Al_2O_3{\cdot}6SiO_2{\cdot}8H_2O$		Al	Fe	Mg	Si			
	Barite	$BaSO_4$		Ba	S					
	Pyrphillite	$Al_2O_3{\cdot}4SiO_2{\cdot}H_2O$		Al	Si					
	Periclase	MgO		Mg						
	Alumina	Al_2O_3		Al						

APPENDIX B: Pringle and Jarvis (1987) product concentrations compared to Luchner thesis results

The following table contains DCL test results from this thesis (1B and 2B) along with results from literature (ppmw). The test conditions of each set of results can be found in the table below.

SOLIDS Element	2B No Catalyst	1B FeS Catalyst	Pringle (1987)
Al	25700	18500	19100
Ba	460	390	4870
Ca	10300	10000	11260
Fe	56500	59600	9500
Mn	200	220	38
Na	4000	3600	1260
Ti	2200	2000	1290
As	8	10	8.7
Co	320	300	5.4
Cr	270	115	164
Pb	2700	2300	36
Sb	26	5	2.5
V	120	250	109
Zn	240	630	182

LIQUIDS Element	2B No Catalyst	1B FeS Catalyst	Pringle (1987)
Al	2	4	38
Ba	0.5	1	4.3
Ca	63	49	75
Fe	12	4	<1
Mn	1	0.5	6.9
Na	9	23	105
Ti	100	100	5.6
As	0.5	0.5	0.64
Co	1	0.5	1.2
Cr	0.5	0.5	4.3
Pb	2	2	-
Sb	0.5	0.5	0.5
V	1	1	1.1
Zn	34	33	-

Test condition comparison:

Condition	2B and 1B Thesis	Pringle (1987)
Reactor	Batch micro reactor	Batch autoclave
Coal	Bituminous (5grams)	Bituminous (10grams)
Reaction Solvent	Tetralin	Tetralin
Reaction Catalyst	2B-None, 1B - FeS	Not available
Reaction Temperature	425 ˚C	440 ˚C
Reaction Gas / Pressure	H_2 / 1000psi	H_2 / 800psi
Reaction Time	1 Hour	30 Minutes
Extraction / Solvent	Soxhlet / THF	Soxhlet / THN
Analytical Technique	ICP & AAS	NAA

APPENDIX C: Details of computer-controlled scanning electron microscopy (CCSEM)

The following insert was taken from the University of North Dakota Energy and Environmental Research Center detailing their CCSEM analysis.

STANDARD OPERATING PROCEDURE FOR COAL/ASH MINERAL ANALYSIS BY COMPUTER-CONTROLLED SCANNING ELECTRON MICROSCOPY

Scope

This procedure is used for sizing, chemically classifying, and quantifying the inorganic constituents in coal and coal ash using a computer-controlled scanning electron microscopy (CCSEM) technique (Lee and Kelly, 1980; Huggins and others, 1980, 1982).

Summary of Method

Coal to be analyzed is pulverized to a standard combustion grind (˜80 % of the particles -200 mesh), mounted in carnauba wax, cross-sectioned, and polished. Coal ash is ultrasonically dispersed and mounted on filter paper or in epoxy resin. Ash epoxy mounts are cross-sectioned and polished. Samples are sputter coated with carbon to minimize electron-beam charging artifacts. An automated SEM, operating in the BSE imaging mode, is programmed to scan in a grid pattern that covers the entire sample.

A modified version of NORAN Instruments Feature Sizing and Chemical Typing program is used to locate, size, and chemically analyze individual coal/ash mineral particles. Mineral particles are automatically detected by an increase in the BSE signal above a preset video threshold and a binary image is created for the coal particles and the mineral particles. The pixel areas of the mineral particles are analyzed to determine the particle′s minimum, maximum, and average diameter. The perimeter, and shape factor (circularity) are also determined during the image analysis as well as whether the mineral particle is included in a coal particle or not. After the image analysis, an energy-dispersive x-ray (EDX) spectrum (0-10 keV) is acquired from the particle's center. Spectral regions-of-interest (ROI) are defined to measure the characteristic x-ray emission intensities of common, mineral-forming, major and minor elements (Na, Mg, Al, Si, P, S, Cl, K, Ca, Ti, Fe, and Ba). X-ray emission intensities are quantified using the ZAF correction method. X-ray quantitative data, location, size, and shape parameters for a statistically significant number of particles are collected at three magnifications (50X for 22 to 100 μm, 250X for 4.6 to 22 μm, and 800x for 1.0 to 4.6 μm diameter particles) and

transferred to a personal computer where they are tabulated and stored to disk for data reduction, report generation, and archival.

A particle characterization (PARTCLASS) program, classifies the Feature Sizing and Chemical Typing analyses based on compositional criteria into one of 33 mineral/chemical and mineral association categories. Analyses that do not conform to any of the specified criteria are termed unclassified. The program allocates the classified particles according to average diameter based on the pixel dimension of equivalent spheres into six intervals (1.0-2.2 μm, 2.2-4.6 μm, 4.6-10 μm, 10-22 μm, 22-46 μm, 46-100 μm) so that the size distribution of mineral/chemical types can be determined. The particle-diameter intervals are a geometric progression based on the cube root of ten. A geometric size distribution is used to lessen sectioning effects present in fly ash epoxy mounts that cause the measured cross-sectional diameters of the particles to be less than or equal to the maximum diameter of the particles (DeHoff and Rhines, 1968; Hurley, 1990). A report is generated that summarizes the results in a series of tables containing information on the number and proportions of minerals in their respective size intervals. Mineral weight percentages are calculated assuming that particle areas are proportional to volumes (e.g. point-counting method of Chayes, 1950) and mineral densities are constants. The CCSEM analysis generates three Feature Sizing and Chemical Typing raw data files, one for each magnification that each has a size extension. A PARTClass data output file, and a summary report output file are archived on CD via a computer network system. The format and content of these files are described in sections 11 and 13 of this SOP.

Preparation of Coal

Bulk coal sample is pulverized to a standard combustion grind (˜80 % of the particles -200 mesh).

A representative sample is obtained by splitting.

The coal sub-sample is dried in a vacuum oven at 70EC to constant weight.

Two grams of coal is mixed with three grams of molten carnauba wax in a 1" (2.54 cm) diameter mold and allowed to cool under ambient conditions.

The resulting coal-carnauba pellet is cross sectioned using a slow-speed diamond saw.

The sectioned pellet surface is polished according to ASTM Standard Practice D2797 (ASTM, 1991). The final polishing steps are performed with 6 μm, 1 μm, and 0.25 μm diamond paste.

Coal pellet is cleaned by sonication in trichloro-trifluoroethane or in some cases, toluene is used.

The coal pellet is sputter coated with carbon to minimize electron-beam charging artifacts.

Referenced Documents

American Society for Testing and Materials (ASTM). "Standard Practice for Preparing Coal Samples for Microscopical Analysis by Reflected Light (D2797)," *Annual Book of ASTM Standards*; 1991, Vol. 5.05, p. 308-311.

Casuccio, G.S.; Gruelich, F.A.; Hamburg, G.; Huggins, F.E.; Nissen, D.A.;Vleeskens, J.M. "Coal mineral analysis: a check on interlaboratory agreement," *Scanning Microscopy* 1990, Vol. 4, No. 2, p. 227-236.

Chayes, F. "On the bias of grain-size measurements made in thin section," *Journal of Geology* 1950, Vol. 58, p. 156-160.

DeHoff, R.T.; Rhines, F.N. *Quantitative Microscopy*. Materials Science and Engineering Series, McGraw-Hill Book Company, 1968, 422 pp.

Huggins, F.E.; Kosmack, D.A.; Huffman, G.P.; Lee, R.J. "Coal mineralogies by SEM automatic image analysis," *Scanning Electron Microscopy*; 1980, *I*, 531-540.

Huggins, F.E.; Huffman, G.P.; Lee, R.J. "Scanning electron microscope-based automated image analysis (SEM-AIA) and mössbauer spectroscopy: quantitative characterization of coal minerals," In *Coal and Coal Products*: *Analytical Characterization Techniques*; Fuller, E.L., Jr., Ed.; American Chemical Society Symposium Series 205; 1982, Chapter 12, p. 239-258.

Hurley, J.P. *A pilot-scale study of the formation of ash during pulverized low-rank coal combustion*, University of North Dakota, Ph.D. Dissertation, 1990, 247 pp.

Jones, M.L.; Kalmanovitch, D.P.; Steadman, E.N.; Zygarlicke, C.J.; Benson, S.A. "Application of SEM techniques to the characterization of coal and coal ash products," *Advances in Coal Spectroscopy*; Meuzelaar, M.L.C., Ed.; Plenum Publishing Corp.: New York, 1992; Chapter 1, p. 1-27.

Lee, R.J.; Kelly, J.F. "Overview of SEM-based automated image analysis," *Scanning Electron Microscopy*; 1980, *I*, p.303-310.

Vorres, K.S. *Users Handbook for the Argonne Premium Coal Sample Program*; Argonne National Laboratory, 1989, 64 p.

Zygarlicke, C.J.; Steadman, E.N. "Advanced SEM techniques to characterize coal minerals," *Scanning Microscopy*; 1990, Vol. 4, No. 3, p. 579-590.

Zygarlicke, C.J.; Steadman, E.N.; Benson, S.A. "Studies of transformations of inorganic constituents in a Texas lignite during combustion," *Prog. Energy Combust. Sci.*; 1990, Vol. 16, p. 195-204.

APPENDIX D: Experimental detection limits from ICP and AAS elemental analysis

The following experimental detection limits are the instruments' detection limits (ppm); they also take into account the dilution factors associated with the digestions for this specific research.

Element	Al	Ba	Ca	Fe	K	Mg	Mn	Na	S	Si	Sr	Ti
Exp. Detection Limit	0.1	0.1	1	1	1	0.2	0.1	1	50	10	0.05	10

Element	Ag	As	Be	Cd	Co	Cr	Cu	Hg	Mo	Ni	P	Pb
Exp. Detection Limit	0.1	0.1	0.01	0.02	0.1	0.1	0.1	0.002	0.1	0.1	5	0.1

Element	Sb	Se	Sn	Te	Tl	V	Zn
Exp. Detection Limit	0.2	0.2	0.2	0.2	0.2	0.1	1

APPENDIX E: Chemical fractionation results

The following figures are the results of the chemical fractionations that were preformed on the three feed coals.

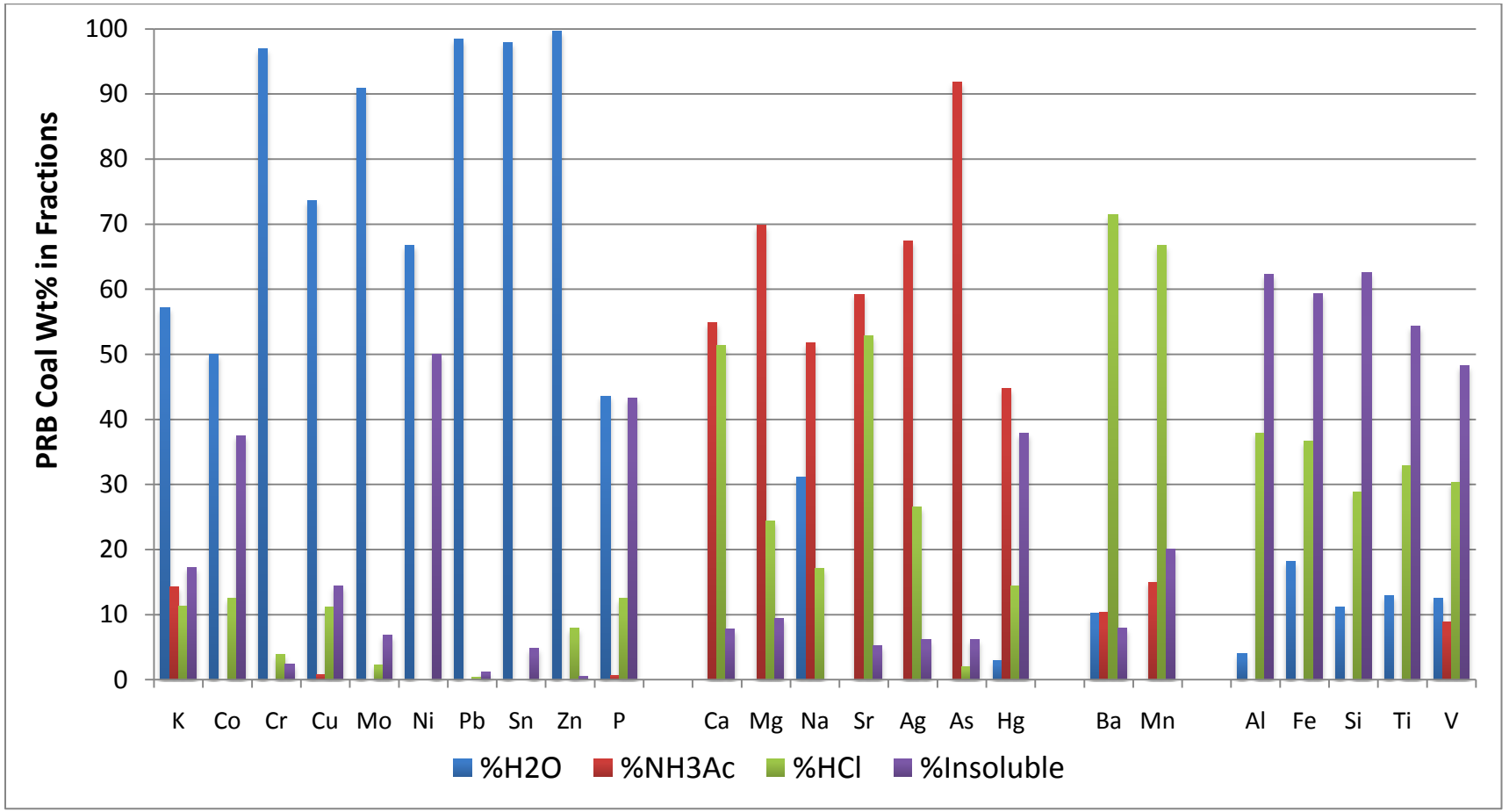

PRB coal chemical fractionation results: %H2O-mass percent water soluble, %NH3Ac-mass percent ammonium acetate soluble, %HCl- mass percent hydrochloric acid soluble

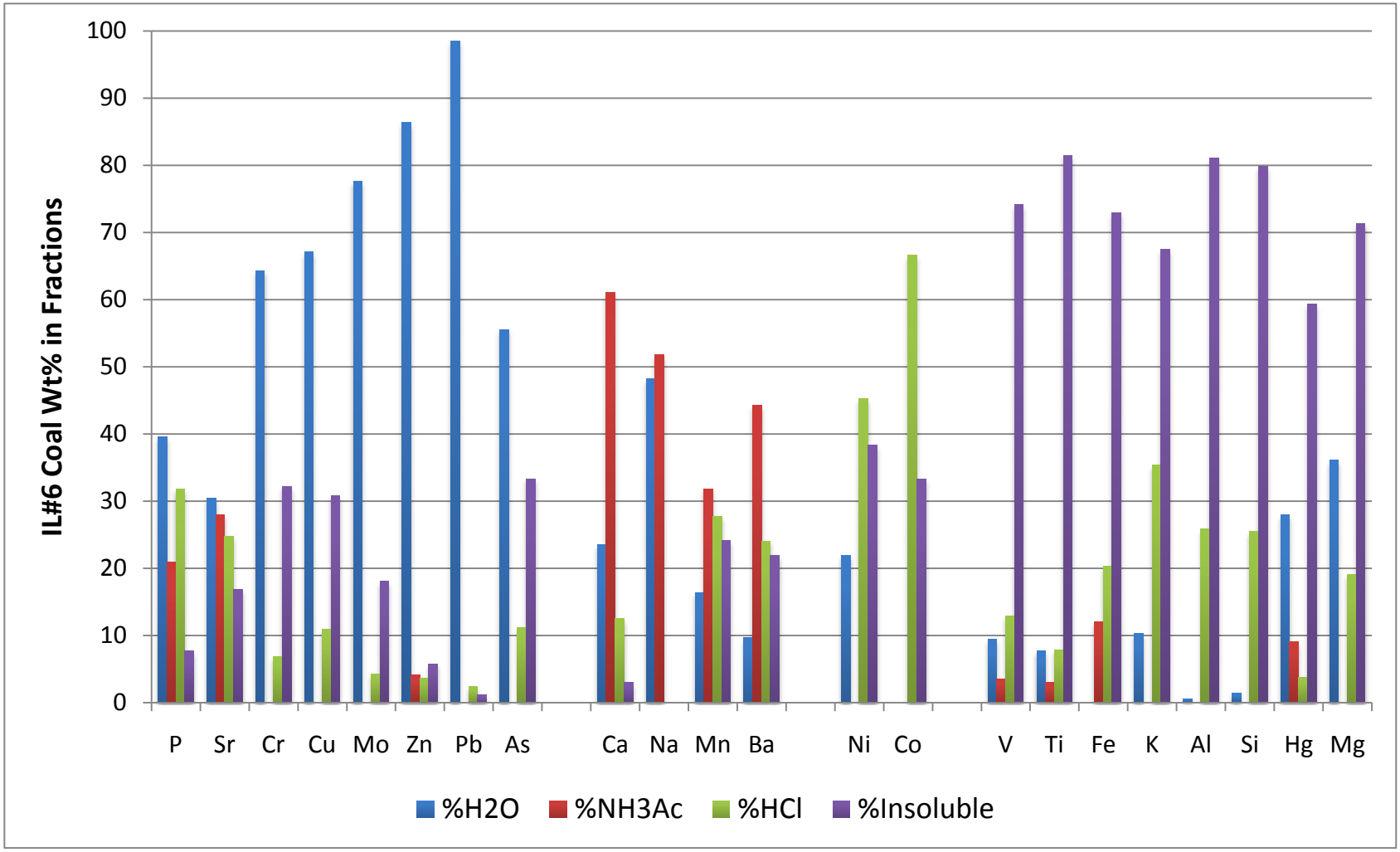

IL#6 coal chemical fractionation results: %H2O-mass percent water soluble, %NH3Ac-mass percent ammonium acetate soluble, %HCl- mass percent hydrochloric acid soluble

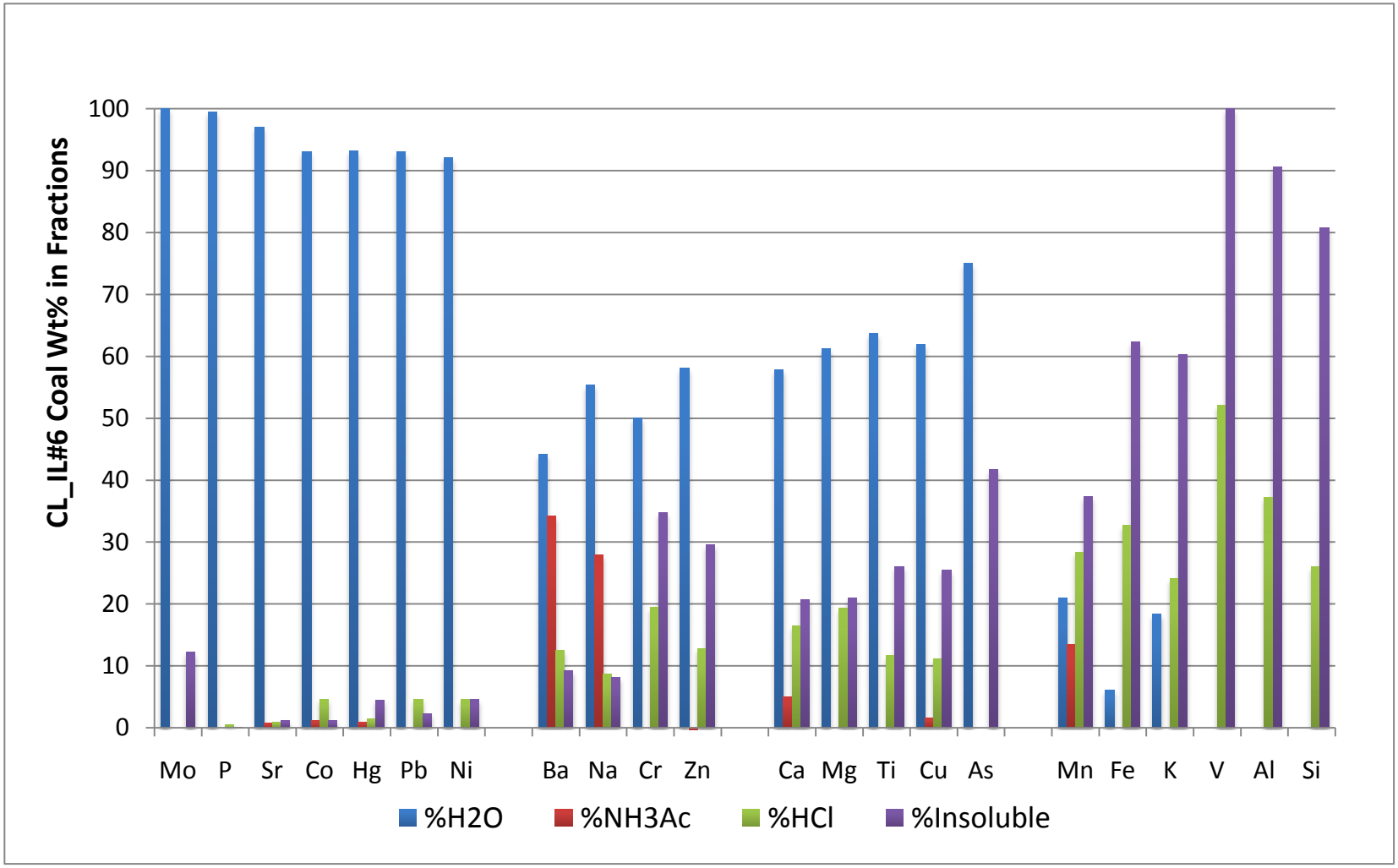

Cleaned IL#6 coal chemical fractionation results: %H2O-mass percent water soluble, %NH3Ac-mass percent ammonium acetate soluble, %HCl- mass percent hydrochloric acid soluble

APPENDIX F: Complete CCSEM results

The following documents display the complete set of results from CCSEM analysis of the three feed coals. The first three pages relate to the PRB coal results, the next three are the IL#6 coal results, and the last three are for the CL_IL#6 coal (labels are also located at the top of each page).

SAMPLE DESCRIPTION ---> DECS-38 Dietz Seam Big Horn Co MT -200 mesh

SUMMARY OF PARAMETERS

PERCENT EPOXY USED	=	60.8
TOTAL MINERAL AREA ANALYZED AT 800.0 MAG	=	1759.7
NORMALIZED AREA ANALYZED AT 800.0 MAG	=	436774.3
MINERAL AREA ANALYZED 250.0 MAG	=	24311.5
NORMALIZED AREA ANALYZED 250.0 MAG	=	613835.4
TOTAL MINERAL AREA ANALYZED AT 50.0 MAG	=	491147.2
NUMBER OF FRAMES AT 800.0 MAG	=	100
NUMBER OF FRAMES AT 250.0 MAG	=	100
NUMBER OF FRAMES AT 50.0 MAG	=	100
TOTAL MINERAL WGHT % ON A COAL BASIS	=	2.056
TOTAL NUMBER OF POINTS ANALYZED	=	1503
NUMBER OF POINTS UNDER THRESHOLD	=	171

WEIGHT PERCENT ON A MINERAL BASIS

	1.0 TO 2.2	2.2 TO 4.6	4.6 TO 10.0	10.0 TO 22.0	22.0 TO 46.0	46.0 TO 100.0	TOTALS	% EXCLUDED
QUARTZ	1.8	2.3	4.9	5.2	4.9	1.7	20.9	59.2
IRON OXIDE	.3	.2	.2	.0	.0	.0	.7	21.5
PERICLASE	.0	.0	.0	.0	.0	.0	.0	.0
RUTILE	.2	.0	.2	.4	.1	.0	1.0	67.5
ALUMINA	.0	.0	.2	.0	.5	.3	1.0	93.6
CALCITE	.0	.1	.0	.0	.0	.0	.1	.0
DOLOMITE	.0	.0	.0	.0	.0	.0	.0	.0
ANKERITE	.0	.0	.0	.0	.0	.0	.0	.0
KAOLINITE	1.9	4.5	3.7	6.6	3.6	1.2	21.7	37.8
MONTMORILLONITE	1.6	1.2	.5	.7	.3	.0	4.3	10.6
K AL-SILICATE	.3	.2	.5	1.4	.5	.0	2.9	64.7
FE AL-SILICATE	.1	.5	.3	.1	.4	.0	1.5	61.9
CA AL-SILICATE	.7	.1	.1	.0	.0	.0	.9	.0
NA AL-SILICATE	.0	.0	.0	.0	.0	.0	.0	.0
ALUMINOSILICATE	.0	.3	.1	.0	.1	.1	.6	50.9
MIXED AL-SILICA	.1	.2	.3	.0	.1	.0	.7	12.0
FE SILICATE	.0	.0	.0	.0	.0	.0	.0	.0
CA SILICATE	.1	.0	.0	.0	.0	.0	.1	86.8
CA ALUMINATE	.0	.0	.0	.0	.0	.0	.0	.0
PYRITE	.0	.0	.1	.0	.0	.0	.1	100.0
PYRRHOTITE	2.1	2.7	2.6	2.4	7.1	6.3	23.2	77.0
OXIDIZED PYRRHO	.4	.4	.3	.0	.2	.8	2.1	61.4
GYPSUM	.2	.1	.2	.3	.0	.0	.8	63.0
BARITE	.1	.4	.1	.0	.5	.3	1.4	54.1
APATITE	.0	.0	.0	.0	.0	.0	.0	100.0
CA AL-P	.6	.7	.1	.0	.0	.0	1.4	8.4
KCL	.0	.0	.0	.0	.0	.0	.0	100.0
GYPSUM/BARITE	.0	.0	.0	.0	.0	.0	.0	.0
GYPSUM/AL-SILIC	.3	.2	.0	.0	.0	.1	.6	3.9
SI-RICH	.2	.1	.4	.5	.4	.0	1.5	48.0
CA-RICH	.0	.0	.0	.0	.0	.0	.0	.0
CA-SI RICH	.0	.0	.0	.0	.0	.0	.0	.0
UNCLASSIFIED	1.6	1.0	1.0	3.8	3.5	1.4	12.4	66.5
TOTALS	12.4	15.3	16.1	21.5	22.4	12.3	100.0	

SAMPLE DESCRIPTION ---> DECS-38 Dietz Seam Big Horn Co MT -200 mesh

SUBMITTER ---> Eylands

ICC # AND FUND # ---> 24981410

RUN DATE AND TIME ---> 12 18 2008 9:36

Percent excluded as a function of particle size and phase.

	1.0 TO 2.2	2.2 TO 4.6	4.6 TO 10.0	10.0 TO 22.0	22.0 TO 46.0	46.0 TO 100.0
QUARTZ	.7	5.4	52.3	79.1	78.7	94.6
IRON OXIDE	12.0	.0	60.2	.0	.0	.0
PERICLASE	.0	.0	.0	.0	.0	.0
RUTILE	.0	.0	64.5	100.0	100.0	.0
ALUMINA	.0	.0	67.6	.0	100.0	100.0
CALCITE	.0	.0	.0	.0	.0	.0
DOLOMITE	.0	.0	.0	.0	.0	.0
ANKERITE	.0	.0	.0	.0	.0	.0
KAOLINITE	1.2	3.7	33.3	54.4	64.8	64.2
MONTMORILLONITE	2.1	.0	34.3	19.4	40.0	.0
K AL-SILICATE	.0	.0	56.6	91.4	63.2	.0
FE AL-SILICATE	.0	45.8	91.6	.0	89.8	.0
CA AL-SILICATE	.0	.0	.0	.0	.0	.0
NA AL-SILICATE	.0	.0	.0	.0	.0	.0
ALUMINOSILICATE	.0	46.4	.0	.0	48.6	100.0
MIXED AL-SILICA	.0	.0	18.7	.0	22.8	.0
FE SILICATE	.0	.0	.0	.0	.0	.0
CA SILICATE	77.6	.0	100.0	.0	.0	.0
CA ALUMINATE	.0	.0	.0	.0	.0	.0
PYRITE	.0	.0	100.0	.0	.0	.0
PYRRHOTITE	8.4	39.3	71.6	71.9	94.7	100.0
OXIDIZED PYRRHO	5.9	.0	78.3	.0	100.0	100.0
GYPSUM	24.7	.0	80.6	100.0	100.0	.0
BARITE	.0	.0	.0	.0	100.0	100.0
APATITE	100.0	.0	.0	.0	.0	.0
CA AL-P	7.4	.0	52.9	.0	.0	.0
KCL	.0	.0	100.0	.0	.0	.0
GYPSUM/BARITE	.0	.0	.0	.0	.0	.0
GYPSUM/AL-SILIC	.0	.0	.0	.0	51.0	.0
SI-RICH	.0	.0	29.6	61.0	86.3	.0
CA-RICH	.0	.0	.0	.0	.0	.0
CA-SI RICH	.0	.0	.0	.0	.0	.0
UNCLASSIFIED	5.3	6.6	48.2	74.4	93.3	100.0

SAMPLE DESCRIPTION ---> DECS-38 Dietz Seam Big Horn Co MT -200 mesh

SUBMITTER ---> Eylands
ICC # AND FUND # ---> 24981410
RUN DATE AND TIME ---> 12 18 2008 9:36

Average phase composition.

(Percent Relative X-ray Intensity)

	SI	AL	FE	TI	P	CA	MG	NA	K	S	BA	CL
QUARTZ	96.1	.4	.7	.3	.3	.6	.2	.1	.3	.3	.4	.2
IRON OXIDE	.9	.7	95.2	.4	.1	1.1	.4	.2	.2	.8	.0	.2
PERICLASE	.0	.0	.0	.0	.0	.0	.0	.0	.0	.0	.0	.0
RUTILE	3.7	1.1	.7	72.7	.1	1.4	.3	.2	.1	.9	18.9	.0
ALUMINA	2.3	95.7	.5	.1	.1	.5	.0	.1	.2	.2	.2	.2
CALCITE	.2	.1	2.2	.0	1.4	95.2	.0	.4	.2	.0	.0	.3
DOLOMITE	.4	.5	5.5	.9	.0	70.4	21.9	.0	.4	.0	.0	.0
ANKERITE	.0	.0	.0	.0	.0	.0	.0	.0	.0	.0	.0	.0
KAOLINITE	56.3	39.7	.8	.2	.2	.8	.1	.1	.4	.6	.6	.3
MONTMORILLONITE	57.2	35.5	1.1	.5	.4	1.5	.3	.3	1.0	1.4	.5	.4
K AL-SILICATE	52.7	26.3	2.9	.9	.2	1.5	.9	.3	11.3	1.8	.7	.2
FE AL-SILICATE	46.8	30.2	14.1	1.3	.3	1.3	2.7	.7	1.5	.6	.3	.2
CA AL-SILICATE	49.1	34.0	1.3	.7	.4	7.9	.7	.6	.9	2.2	1.1	1.1
NA AL-SILICATE	70.9	17.9	.0	.0	.2	1.1	.0	8.7	.9	.0	.0	.3
ALUMINOSILICATE	61.9	30.3	.9	.6	.1	.7	.4	.2	1.7	1.8	.5	.9
MIXED AL-SILICA	50.6	27.1	6.0	1.0	.4	3.1	1.0	.5	5.4	2.2	2.4	.4
FE SILICATE	.0	.0	.0	.0	.0	.0	.0	.0	.0	.0	.0	.0
CA SILICATE	76.0	1.9	1.5	1.3	.5	10.5	1.4	.9	1.1	.3	3.0	1.6
CA ALUMINATE	.0	.0	.0	.0	.0	.0	.0	.0	.0	.0	.0	.0
PYRITE	1.7	4.5	28.7	1.6	.0	6.0	.1	.0	1.3	56.2	.0	.0
PYRRHOTITE	.5	.4	52.1	.1	.0	.5	.1	.2	.1	45.4	.2	.1
OXIDIZED PYRRHO	1.0	1.0	62.8	.1	.0	1.6	.2	.4	.2	32.4	.2	.2
GYPSUM	1.0	1.0	.9	.2	.0	58.4	.1	.2	.2	37.1	.3	.4
BARITE	.6	.9	.3	.5	.0	.7	.2	.3	.3	21.8	74.1	.2
APATITE	.1	.2	.0	.0	24.6	72.7	.0	.0	.3	.0	2.0	.0
CA AL-P	.3	33.3	1.6	.4	21.9	30.8	.9	.6	.5	1.6	7.6	.5
KCL	.8	.0	.6	.2	.0	.7	.1	.0	53.2	.0	.5	43.9
GYPSUM/BARITE	.0	.0	.0	.0	.0	.0	.0	.0	.0	.0	.0	.0
GYPSUM/AL-SILIC	35.4	23.7	3.0	1.7	.3	12.2	1.3	.5	1.1	18.6	.6	1.6
SI-RICH	71.7	8.9	3.2	.9	.4	2.9	3.3	.7	5.0	1.9	.8	.4
CA-RICH	.0	.0	.0	.0	.0	.0	.0	.0	.0	.0	.0	.0
CA-SI RICH	.0	.0	.0	.0	.0	.0	.0	.0	.0	.0	.0	.0
UNCLASSIFIED	22.2	9.3	6.0	2.0	1.3	5.3	1.4	.9	3.2	13.8	33.7	1.1

SAMPLE DESCRIPTION ---> DECS-24 Ill#6 -200 mesh

SUMMARY OF PARAMETERS

PERCENT EPOXY USED	=	59.3
TOTAL MINERAL AREA ANALYZED AT 800.0 MAG	=	3843.4
NORMALIZED AREA ANALYZED AT 800.0 MAG	=	808462.6
MINERAL AREA ANALYZED 250.0 MAG	=	74404.8
NORMALIZED AREA ANALYZED 250.0 MAG	=	1204251.0
TOTAL MINERAL AREA ANALYZED AT 50.0 MAG	=	1237713.0
NUMBER OF FRAMES AT 800.0 MAG	=	59
NUMBER OF FRAMES AT 250.0 MAG	=	78
NUMBER OF FRAMES AT 50.0 MAG	=	50
TOTAL MINERAL WGHT % ON A COAL BASIS	=	9.694
TOTAL NUMBER OF POINTS ANALYZED	=	3579
NUMBER OF POINTS UNDER THRESHOLD	=	59

WEIGHT PERCENT ON A MINERAL BASIS

	1.0 TO 2.2	2.2 TO 4.6	4.6 TO 10.0	10.0 TO 22.0	22.0 TO 46.0	46.0 TO 100.0	TOTALS	% EXCLUDED
QUARTZ	1.6	3.1	1.8	.7	.0	.0	7.2	7.7
IRON OXIDE	.0	.2	.0	.0	.2	.0	.4	75.3
PERICLASE	.0	.0	.0	.0	.0	.0	.0	.0
RUTILE	.0	.1	.1	.0	.0	.0	.2	31.2
ALUMINA	.0	.0	.0	.0	.0	.0	.0	.0
CALCITE	.1	.3	.9	1.5	3.2	3.8	9.9	51.6
DOLOMITE	.0	.1	.0	.0	.0	.0	.1	.0
ANKERITE	.0	.0	.0	.0	.0	.0	.0	.0
KAOLINITE	.6	1.2	.5	.5	.2	.0	3.0	5.9
MONTMORILLONITE	.5	.5	.3	.1	.2	.2	1.8	9.0
K AL-SILICATE	.5	.9	.7	.8	.4	.0	3.3	8.0
FE AL-SILICATE	.1	.2	.1	.1	.1	.0	.5	8.3
CA AL-SILICATE	.0	.0	.0	.0	.0	.0	.0	.0
NA AL-SILICATE	.0	.0	.0	.0	.0	.0	.1	17.2
ALUMINOSILICATE	.0	.0	.0	.0	.1	.0	.1	8.9
MIXED AL-SILICA	.1	.1	.2	.1	.1	.0	.6	16.7
FE SILICATE	.0	.0	.0	.0	.0	.0	.0	.0
CA SILICATE	.0	.0	.0	.1	.0	.0	.1	100.0
CA ALUMINATE	.0	.0	.0	.0	.0	.0	.0	.0
PYRITE	.0	.0	.1	.2	.5	.2	1.1	59.0
PYRRHOTITE	2.6	3.6	9.3	15.9	20.3	9.1	60.8	58.7
OXIDIZED PYRRHO	.2	.4	.3	.2	1.1	.3	2.6	62.9
GYPSUM	.0	.0	.0	.0	.0	.0	.0	.0
BARITE	.0	.0	.0	.0	.0	.0	.0	.0
APATITE	.0	.0	.2	.1	.1	.0	.5	67.1
CA AL-P	.0	.0	.0	.0	.0	.0	.0	.0
KCL	.0	.0	.0	.0	.0	.0	.0	.0
GYPSUM/BARITE	.0	.0	.0	.0	.0	.0	.0	.0
GYPSUM/AL-SILIC	.0	.0	.0	.0	.0	.0	.0	100.0
SI-RICH	.2	.4	.3	.2	.1	.1	1.3	18.6
CA-RICH	.0	.0	.0	.0	.0	.0	.1	11.6
CA-SI RICH	.0	.0	.0	.0	.0	.0	.0	.0
UNCLASSIFIED	1.4	1.7	1.2	1.2	.5	.3	6.3	13.8
TOTALS	8.2	12.7	16.1	21.8	27.1	14.1	100.0	

SAMPLE DESCRIPTION ---> DECS-24 Ill#6 -200 mesh

SUBMITTER ---> Eylands

ICC # AND FUND # ---> 24981409

RUN DATE AND TIME ---> 12 17 2008 8:49

Percent excluded as a function of particle size and phase.

	1.0 TO 2.2	2.2 TO 4.6	4.6 TO 10.0	10.0 TO 22.0	22.0 TO 46.0	46.0 TO 100.0
QUARTZ	.6	.0	17.0	32.5	19.8	.0
IRON OXIDE	.0	50.0	100.0	.0	100.0	.0
PERICLASE	.0	.0	.0	.0	.0	.0
RUTILE	37.0	.0	58.5	.0	.0	.0
ALUMINA	.0	.0	.0	.0	.0	.0
CALCITE	21.0	10.3	46.7	41.8	42.8	68.5
DOLOMITE	.0	.0	.0	.0	.0	.0
ANKERITE	.0	.0	.0	.0	.0	.0
KAOLINITE	1.3	.0	19.8	.0	36.3	.0
MONTMORILLONITE	2.3	.0	2.3	50.0	43.2	.0
K AL-SILICATE	1.2	2.9	10.2	.0	32.6	100.0
FE AL-SILICATE	.0	.0	13.8	.0	22.3	.0
CA AL-SILICATE	.0	.0	.0	.0	.0	.0
NA AL-SILICATE	.0	.0	100.0	.0	.0	.0
ALUMINOSILICATE	.0	.0	.0	.0	16.9	.0
MIXED AL-SILICA	.0	.0	21.7	51.3	26.3	.0
FE SILICATE	.0	.0	.0	.0	.0	.0
CA SILICATE	.0	.0	.0	100.0	.0	.0
CA ALUMINATE	.0	.0	.0	.0	.0	.0
PYRITE	.0	.0	40.7	100.0	60.0	32.5
PYRRHOTITE	34.4	33.2	55.0	70.2	58.1	61.0
OXIDIZED PYRRHO	48.2	45.0	40.6	72.6	64.2	100.0
GYPSUM	.0	.0	.0	.0	.0	.0
BARITE	.0	.0	.0	.0	.0	.0
APATITE	.0	.0	48.2	100.0	84.1	.0
CA AL-P	.0	.0	.0	.0	.0	.0
KCL	.0	.0	.0	.0	.0	.0
GYPSUM/BARITE	.0	.0	.0	.0	.0	.0
GYPSUM/AL-SILIC	.0	.0	100.0	.0	.0	.0
SI-RICH	6.1	10.3	19.5	56.4	.0	.0
CA-RICH	.0	.0	16.8	.0	.0	.0
CA-SI RICH	.0	.0	.0	.0	.0	.0
UNCLASSIFIED	1.3	5.8	17.8	23.9	21.3	48.1

SAMPLE DESCRIPTION ---> DECS-24 Ill#6 -200 mesh

SUBMITTER ---> Eylands
ICC # AND FUND # ---> 24981409
RUN DATE AND TIME ---> 12 17 2008 8:49

Average phase composition.
(Percent Relative X-ray Intensity)

	SI	AL	FE	TI	P	CA	MG	NA	K	S	BA	CL
QUARTZ	94.0	1.3	1.2	.2	.2	.3	.2	.1	.7	1.1	.4	.2
IRON OXIDE	.7	.4	97.4	.1	.0	.2	.2	.2	.1	.4	.1	.1
PERICLASE	.0	.0	.0	.0	.0	.0	.0	.0	.0	.0	.0	.0
RUTILE	3.0	1.6	1.8	90.8	.0	.2	.2	.2	.2	.9	.9	.1
ALUMINA	3.6	85.6	.7	.3	.0	1.5	.0	.2	.5	5.4	1.4	.8
CALCITE	.4	.3	1.7	.1	.1	96.0	.3	.1	.2	.4	.3	.1
DOLOMITE	1.5	.9	4.9	.0	.3	67.9	23.0	.0	.9	.5	.0	.2
ANKERITE	.0	.0	.0	.0	.0	.0	.0	.0	.0	.0	.0	.0
KAOLINITE	56.0	39.2	1.5	.2	.2	.3	.1	.2	.7	.9	.5	.2
MONTMORILLONITE	57.0	34.5	2.1	.4	.2	.4	.2	.3	2.1	1.8	.6	.2
K AL-SILICATE	52.8	27.6	3.1	.8	.2	.5	.7	.5	10.8	2.0	.8	.2
FE AL-SILICATE	49.1	28.7	13.6	.6	.1	.4	2.4	.3	2.3	1.5	.5	.2
CA AL-SILICATE	41.8	29.0	.0	.2	7.5	14.6	.4	.0	2.1	2.1	2.4	.0
NA AL-SILICATE	68.6	18.0	1.6	.1	.5	.6	.0	8.0	1.1	1.2	.3	.0
ALUMINOSILICATE	67.1	22.7	2.7	.7	.1	.7	.4	.2	2.8	1.3	.7	.6
MIXED AL-SILICA	52.4	27.9	6.3	1.4	.2	.6	.7	.4	7.3	1.9	.6	.3
FE SILICATE	.0	.0	.0	.0	.0	.0	.0	.0	.0	.0	.0	.0
CA SILICATE	46.1	.3	1.8	.0	14.8	36.2	.1	.0	.0	.4	.0	.2
CA ALUMINATE	.0	.0	.0	.0	.0	.0	.0	.0	.0	.0	.0	.0
PYRITE	1.9	.9	33.9	.6	.1	.5	.2	.4	.5	59.7	.7	.7
PYRRHOTITE	.6	.3	51.4	.1	.0	.1	.1	.1	.1	47.0	.1	.1
OXIDIZED PYRRHO	.4	.2	66.6	.1	.0	.2	.0	.1	.1	32.0	.1	.1
GYPSUM	.0	.0	.0	.0	.0	.0	.0	.0	.0	.0	.0	.0
BARITE	1.6	.6	.0	.0	.0	.0	1.3	1.9	2.0	26.0	66.1	.5
APATITE	1.0	.4	1.1	.1	23.3	72.4	.1	.2	.2	.7	.4	.2
CA AL-P	.0	.0	.0	.0	.0	.0	.0	.0	.0	.0	.0	.0
KCL	.0	.0	.0	.0	.0	.0	.0	.0	.0	.0	.0	.0
GYPSUM/BARITE	.0	.0	.0	.0	.0	.0	.0	.0	.0	.0	.0	.0
GYPSUM/AL-SILIC	23.2	19.8	.0	.3	.0	5.3	.9	.0	4.9	41.6	.0	4.1
SI-RICH	74.3	10.8	3.7	.9	.3	.5	.6	.3	4.8	2.5	.9	.3
CA-RICH	4.8	3.6	4.6	.1	3.4	76.2	.5	.1	.8	4.3	1.2	.1
CA-SI RICH	.0	.0	.0	.0	.0	.0	.0	.0	.0	.0	.0	.0
UNCLASSIFIED	46.7	17.6	10.1	1.1	.5	3.1	1.1	.5	9.6	8.2	1.0	.7

SAMPLE DESCRIPTION ---> Ill#6 Cleaned Coal -200 mesh

SUMMARY OF PARAMETERS

PERCENT EPOXY USED	=	61.6
TOTAL MINERAL AREA ANALYZED AT 800.0 MAG	=	3138.5
NORMALIZED AREA ANALYZED AT 800.0 MAG	=	2434453.0
MINERAL AREA ANALYZED 250.0 MAG	=	57682.4
NORMALIZED AREA ANALYZED 250.0 MAG	=	2173748.0
TOTAL MINERAL AREA ANALYZED AT 50.0 MAG	=	476560.8
NUMBER OF FRAMES AT 800.0 MAG	=	32
NUMBER OF FRAMES AT 250.0 MAG	=	67
NUMBER OF FRAMES AT 50.0 MAG	=	100
TOTAL MINERAL WGHT % ON A COAL BASIS	=	7.003
TOTAL NUMBER OF POINTS ANALYZED	=	2855
NUMBER OF POINTS UNDER THRESHOLD	=	250

WEIGHT PERCENT ON A MINERAL BASIS

	1.0 TO 2.2	2.2 TO 4.6	4.6 TO 10.0	10.0 TO 22.0	22.0 TO 46.0	46.0 TO 100.0	TOTALS	% EXCLUDED
QUARTZ	2.2	6.2	6.0	2.7	.2	.0	17.2	39.4
IRON OXIDE	.0	.0	.0	.0	.0	.0	.0	.0
PERICLASE	.0	.0	.0	.0	.0	.0	.0	.0
RUTILE	.0	.0	.0	.0	.0	.0	.0	.0
ALUMINA	.0	.0	.0	.0	.0	.0	.0	.0
CALCITE	.0	.0	.1	.2	.1	.0	.4	82.1
DOLOMITE	.0	.0	.0	.1	.0	.1	.2	89.9
ANKERITE	.0	.0	.0	.0	.0	.0	.0	.0
KAOLINITE	.9	1.7	.7	.9	.1	.0	4.3	34.9
MONTMORILLONITE	.8	1.2	.9	.3	.0	.0	3.2	22.5
K AL-SILICATE	.8	1.8	2.3	.8	.3	.0	6.0	28.7
FE AL-SILICATE	.0	.1	.0	.0	.0	.0	.2	30.3
CA AL-SILICATE	.0	.0	.0	.0	.0	.0	.0	.0
NA AL-SILICATE	.0	.1	.2	.0	.0	.0	.3	39.2
ALUMINOSILICATE	.0	.0	.0	.0	.1	.0	.1	10.9
MIXED AL-SILICA	.0	.0	.0	.1	.0	.0	.1	23.4
FE SILICATE	.0	.0	.0	.0	.0	.0	.0	.0
CA SILICATE	.0	.0	.0	.0	.0	.0	.0	.0
CA ALUMINATE	.0	.0	.0	.0	.0	.0	.0	.0
PYRITE	.1	.0	.3	.5	.2	.1	1.2	60.1
PYRRHOTITE	2.7	2.6	8.4	10.4	8.7	2.5	35.4	76.3
OXIDIZED PYRRHO	.0	.0	.0	.4	.1	.0	.6	89.8
GYPSUM	.0	.0	.0	.0	.0	.0	.0	.0
BARITE	.0	.0	.0	.0	.0	.0	.0	.0
APATITE	.0	.0	.0	.0	.0	.0	.0	.0
CA AL-P	.0	.0	.0	.0	.0	.0	.0	.0
KCL	.0	.0	.0	.0	.0	.0	.0	.0
GYPSUM/BARITE	.0	.0	.0	.0	.0	.0	.0	.0
GYPSUM/AL-SILIC	.0	.0	.0	.0	.0	.0	.0	.0
SI-RICH	.8	.5	1.0	.7	.0	.0	2.9	25.1
CA-RICH	.0	.0	.1	.0	.0	.0	.1	12.4
CA-SI RICH	.0	.0	.0	.0	.0	.0	.0	.0
UNCLASSIFIED	11.7	8.3	4.7	3.0	.4	.0	28.0	14.1
TOTALS	20.2	22.5	24.6	19.9	10.2	2.6	100.0	

SAMPLE DESCRIPTION ---> Ill#6 Cleaned Coal -200 mesh
SUBMITTER ---> Eylands
ICC # AND FUND # ---> 091344

RUN DATE AND TIME ---> 11 10 2009 11:37

Percent excluded as a function of particle size and phase.

	1.0 TO 2.2	2.2 TO 4.6	4.6 TO 10.0	10.0 TO 22.0	22.0 TO 46.0	46.0 TO 100.0
QUARTZ	19.0	27.3	42.6	73.5	81.4	.0
IRON OXIDE	.0	.0	.0	.0	.0	.0
PERICLASE	.0	.0	.0	.0	.0	.0
RUTILE	.0	.0	.0	.0	.0	.0
ALUMINA	.0	.0	.0	.0	.0	.0
CALCITE	.0	.0	80.1	100.0	63.8	.0
DOLOMITE	.0	.0	.0	100.0	.0	100.0
ANKERITE	.0	.0	.0	.0	.0	.0
KAOLINITE	6.7	17.7	51.6	85.7	52.9	.0
MONTMORILLONITE	20.3	.0	31.7	100.0	.0	.0
K AL-SILICATE	9.1	28.4	32.3	21.4	83.0	.0
FE AL-SILICATE	68.0	.0	69.5	.0	100.0	.0
CA AL-SILICATE	.0	.0	.0	.0	.0	.0
NA AL-SILICATE	.0	.0	59.2	.0	.0	.0
ALUMINOSILICATE	.0	.0	.0	.0	18.2	.0
MIXED AL-SILICA	.0	.0	52.5	.0	100.0	.0
FE SILICATE	.0	.0	.0	.0	.0	.0
CA SILICATE	.0	.0	.0	.0	.0	.0
CA ALUMINATE	.0	.0	.0	.0	.0	.0
PYRITE	80.3	.0	38.0	44.8	100.0	100.0
PYRRHOTITE	38.1	61.8	57.0	86.6	92.9	97.8
OXIDIZED PYRRHO	.0	.0	.0	100.0	100.0	.0
GYPSUM	.0	.0	.0	.0	.0	.0
BARITE	.0	.0	.0	.0	.0	.0
APATITE	.0	.0	.0	.0	.0	.0
CA AL-P	.0	.0	.0	.0	.0	.0
KCL	.0	.0	.0	.0	.0	.0
GYPSUM/BARITE	.0	.0	.0	.0	.0	.0
GYPSUM/AL-SILIC	.0	.0	.0	.0	.0	.0
SI-RICH	7.9	23.4	21.0	49.8	53.6	.0
CA-RICH	.0	.0	20.8	.0	.0	.0
CA-SI RICH	.0	.0	.0	.0	.0	.0
UNCLASSIFIED	2.0	13.6	22.8	44.4	55.3	.0

SAMPLE DESCRIPTION ---> Ill#6 Cleaned Coal -200 mesh

SUBMITTER ---> Eylands
ICC # AND FUND # ---> 091344
RUN DATE AND TIME ---> 11 10 2009 11:37

Average phase composition.
(Percent Relative X-ray Intensity)

	SI	AL	FE	TI	P	CA	MG	NA	K	S	BA	CL
QUARTZ	94.3	.8	.7	.2	.2	.2	.2	.1	.6	1.7	.4	.5
IRON OXIDE	.0	.0	.0	.0	.0	.0	.0	.0	.0	.0	.0	.0
PERICLASE	.0	.0	.0	.0	.0	.0	.0	.0	.0	.0	.0	.0
RUTILE	.0	.0	.0	.0	.0	.0	.0	.0	.0	.0	.0	.0
ALUMINA	.0	.0	.0	.0	.0	.0	.0	.0	.0	.0	.0	.0
CALCITE	.6	.5	2.2	.3	.1	92.0	.6	.2	.1	1.9	.9	.6
DOLOMITE	3.6	.7	2.3	.2	.1	76.3	12.2	.2	.7	1.5	.2	2.0
ANKERITE	.0	.0	.0	.0	.0	.0	.0	.0	.0	.0	.0	.0
KAOLINITE	54.8	38.1	1.3	.3	.2	.3	.1	.1	1.0	2.5	.4	.8
MONTMORILLONITE	56.6	34.8	1.2	.2	.2	.4	.2	.2	2.0	2.8	.4	.9
K AL-SILICATE	49.9	27.8	2.7	.3	.2	.5	.6	.4	12.1	3.9	.6	1.0
FE AL-SILICATE	38.0	27.0	22.8	.0	.1	.3	5.9	.4	1.6	2.2	1.2	.5
CA AL-SILICATE	.0	.0	.0	.0	.0	.0	.0	.0	.0	.0	.0	.0
NA AL-SILICATE	71.4	17.7	.8	.1	.1	.3	.0	8.2	.4	.8	.1	.2
ALUMINOSILICATE	68.6	22.1	2.0	.2	.1	.2	.1	.2	1.3	4.3	.0	.9
MIXED AL-SILICA	49.4	27.0	7.4	.0	.2	.4	1.3	.6	8.4	3.0	1.6	.7
FE SILICATE	.0	.0	.0	.0	.0	.0	.0	.0	.0	.0	.0	.0
CA SILICATE	.0	.0	.0	.0	.0	.0	.0	.0	.0	.0	.0	.0
CA ALUMINATE	.0	.0	.0	.0	.0	.0	.0	.0	.0	.0	.0	.0
PYRITE	1.5	1.1	31.4	.2	.0	.4	.2	.3	.4	60.0	.5	3.9
PYRRHOTITE	.3	.2	50.3	.1	.0	.1	.1	.1	.1	48.3	.1	.3
OXIDIZED PYRRHO	.2	.2	62.9	.3	.0	.2	.0	.1	.1	35.4	.5	.2
GYPSUM	.0	.0	.0	.0	.0	.0	.0	.0	.0	.0	.0	.0
BARITE	1.3	2.1	.0	.0	.0	1.1	1.0	.3	.0	25.0	63.3	6.1
APATITE	.0	.0	.0	.0	.0	.0	.0	.0	.0	.0	.0	.0
CA AL-P	.0	.0	.0	.0	.0	.0	.0	.0	.0	.0	.0	.0
KCL	.0	.0	.0	.0	.0	.0	.0	.0	.0	.0	.0	.0
GYPSUM/BARITE	.0	.0	.0	.0	.0	.0	.0	.0	.0	.0	.0	.0
GYPSUM/AL-SILIC	.0	.0	.0	.0	.0	.0	.0	.0	.0	.0	.0	.0
SI-RICH	73.9	7.2	2.3	.3	.3	.8	.4	.3	3.5	8.3	.5	2.1
CA-RICH	5.1	1.9	4.7	.5	.3	73.6	1.1	.3	.8	9.1	.9	1.8
CA-SI RICH	.0	.0	.0	.0	.0	.0	.0	.0	.0	.0	.0	.0
UNCLASSIFIED	32.6	15.8	5.4	.7	.4	.9	1.0	.6	7.2	25.6	1.2	8.7

APPENDIX G: Experimental details of all DCL batch tests.

The following table details the experimental procedures and results of the ten microreactor tests conducted in the thesis.

Test ID:	1A	1B	2A	2B	3A	3B	4A	4B	5B	6B
Coal (g)	5.0053	5.0083	4.9731	4.9742	5.007	5.0044	5.0026	5.0018	5.0116	5.0036
Catalyst (g)	0.1519	0.1519	0	0	0.1499	0.1502	0.1508	0.151	0.1519	0
Solvent (ml)	15	15.1	14.9	14.9	15	15	15	15	15	15
Temperature	425	425	425	425	370	370	425	425	425	425
Initial P (MPa)	6.9	6.9	6.9	6.9	6.9	6.9	7.9	7.9	6.9	6.9
Final P (MPa)	14.5	18.3	21.0	19.3	19.0	16.5	22.8	20.0	18.6	18.6
Change P (MPa)	7.6	11.4	14.1	12.4	12.1	9.6	14.9	12.1	11.7	11.7
End Solids (g)	0.873	1.0791	0.9242	0.8039	2.6134	1.5368	1.3137	1.1238	1.4461	1.313
End Liquids (g)	16.2564	17.3577	17.75	17.16	17.63	21.32	23.48	26.33	16.64	17.33
Conversion (%)	87.97	93.39	79.83	94.12	40.16	83.67	74.74	92.61	72.95	75.72

APPENDIX H: Raw data of DCL inorganic element partitioning

The following tables list the measured DCL partitioning data for the 31 elements analyzed: total elemental mass into the reactor and the % of initial mass measured in each product. Data listed in red text represent maximum value.

	IL 200	3Run A	3 Run A		IL 200	3 Run B	3 Run B		IL 200	3 Run C	3 Run C	
	Coal	Solids	Liquids		Coal	Solids	Liquids		Coal	Solids	Liquids	
	grams	%of initial	%of initial		grams	%of initial	%of initial		grams	%of initial	%of initial	
	3Run A	ill6 triplet	ill6 triplet	TOTAL	3 Run B	ill6 triplet	ill6 triplet	TOTAL	3 Run C	ill6 triplet	ill6 triplet	TOTAL
Al	0.0401	41.36	0.04	41.40	0.0402	45.03	0.06	45.09	0.0403	42.20	0.12	42.32
Ba	0.000291	82.47	6.19	88.66	0.000291	78.92	4.46	83.38	0.000292	78.76	8.22	86.98
Ca	0.0231	33.36	5.13	38.49	0.0231	34.61	18.91	53.52	0.0232	31.95	8.10	40.05
Fe	0.2093	26.13	0.02	26.15	0.3894	15.10	0.01	15.11	0.2109	26.36	0.35	26.71
K	0.00692	79.43	0.52	79.95	0.00693	86.53	2.78	89.31	0.00695	83.47	1.38	84.85
Mg	0.00120	50.66	2.99	53.65	0.00121	50.58	35.16	85.74	0.00121	52.96	7.94	60.90
Mn	0.000291	58.42	3.09	61.51	0.000291	61.76	2.20	63.96	0.000292	65.06	8.22	73.28
Na	0.00452	73.08	3.59	76.67	0.00452	79.61	8.82	88.43	0.00453	72.82	4.79	77.61
S	0.313599	35.40	24.04	59.44	0.636777	18.20	11.31	29.51	0.315116	34.90	35.89	70.79
Si	0.1580	60.10	112.50	172.60	0.1583	65.71	89.37	155.08	0.1586	63.05	159.26	222.31
Sr	0.000146	51.55	12.37	63.92	0.000146	54.90	8.92	63.82	0.000146	52.05	16.44	68.49
Ti	0.00406	34.45	44.29	78.74	0.00407	36.85	31.60	68.45	0.00408	31.87	58.84	90.71
Ag	0.0000040	100.00	225.00	325.00	0.0000040	100.00	160.00	260.00	0.0000040	124.13	297.91	422.04
As	0.0000080	100.00	112.50	212.50	0.0000080	112.50	80.00	192.50	0.0000081	99.30	148.96	248.26
Be	0.00000010	830.00	360.00	1190.00	0.00000010	860.00	260.00	1120.00	0.00000010	776.00	480.00	1256.00
Cd	0.00000020	800.00	900.00	1700.00	0.00000020	850.00	650.00	1500.00	0.00000020	995.02	1194.03	2189.05
Co	0.000055	543.48	32.61	576.09	0.000055	524.67	23.52	548.19	0.000055	487.48	21.67	509.15
Cr	0.000050	213.15	35.86	249.01	0.000050	268.00	12800.00	13068.00	0.000050	232.36	47.66	280.02
Cu	0.000141	1224.20	25.62	1249.82	0.000141	1378.88	18.48	1397.36	0.000141	1290.91	68.09	1359.00
Hg	0.000000502	35.86	35.86	71.72	0.000000502	31.87	27.89	59.76	0.000000504	33.73	51.59	85.32
Mo	0.000141	64.06	64.06	128.12	0.000141	66.81	45.49	112.30	0.000141	61.71	68.09	129.80
Ni	0.000251	199.28	7.17	206.45	0.000251	159.21	5.17	164.38	0.000252	170.80	9.53	180.33
P	0.00090	89.69	199.31	289.00	0.00090	95.56	144.44	240.00	0.00091	95.99	264.80	360.79
Pb	0.00181	110.70	8.97	119.67	0.00181	110.56	3.54	114.10	0.00181	100.40	10.59	110.99
Sb	0.0000020	250.00	450.00	700.00	0.0000020	248.76	318.41	567.17	0.0000020	198.61	595.83	794.44
Se	0.0000090	77.78	100.00	177.78	0.0000090	77.39	70.76	148.15	0.0000091	77.24	132.41	209.65
Sn	0.0000015	866.67	2400.00	3266.67	0.0000015	1061.71	1725.28	2786.99	0.0000015	1125.08	3176.70	4301.78
Te	0.0000010	100.00	900.00	1000.00	0.0000010	50.00	640.00	690.00	0.0000010	99.30	1191.66	1290.96
Tl	0.0000015	666.67	600.00	1266.67	0.0000015	265.43	424.68	690.11	0.0000015	311.05	794.18	1105.23
V	0.000131	137.93	27.59	165.52	0.000131	153.09	19.90	172.99	0.000131	137.49	36.67	174.16
Zn	0.000502	39.86	103.85	143.71	0.000502	43.78	97.32	141.10	0.050352	36.15	234.15	270.30

	MT 200	1A	1A	1A	IL 200	1B	1B	1B	MT 200	2A	2A	2A	IL 200	2B	2B	2B
	Coal	Solids	Liquids		Coal	Solids	Liquids		Coal	Solids	Liquids		Coal	Solids	Liquids	
	grams	%of initial	%of initial		grams	%of initial	%of initial		grams	%of initial	%of initial		grams	%of initial	%of initial	
	1A	prb cata	prb cata	TOTAL	1B	ill6 cata	ill6 cata	TOTAL	2A	prb no cata	prb no cata	TOTAL	2B	ill6 no cata	ill6 no cata	TOTAL
Al	0.0030	430.00	2.17	432.17	0.0401	49.92	0.17	50.09	0.0030	134.05	2.38	136.43	0.0398	52.02	0.09	52.11
Ba	0.001101	52.68	3.00	55.68	0.000290	144.59	5.85	150.44	0.001094	118.82	0.81	119.63	0.000289	128.25	2.98	131.23
Ca	0.0125	115.20	7.42	122.62	0.0230	43.41	3.69	47.10	0.0124	77.22	54.29	131.51	0.0229	36.27	4.72	40.99
Fe	0.1010	70.40	0.24	70.64	0.2092	30.74	0.03	30.77	0.0045	71.11	11.04	82.15	0.1119	40.57	0.18	40.75
K	0.00070	97.14	4.71	101.85	0.00691	96.94	1.50	98.44	0.00070	84.74	40.79	125.53	0.00686	77.21	1.50	78.71
Mg	0.00195	297.44	7.49	304.93	0.00120	66.56	5.74	72.30	0.00194	82.50	45.89	128.39	0.00119	48.58	8.63	57.21
Mn	0.000060	183.33	26.67	210.00	0.000290	82.62	3.00	85.62	0.000060	72.05	14.91	86.96	0.000289	69.32	5.89	75.21
Na	0.00470	65.96	10.02	75.98	0.00451	86.52	8.85	95.37	0.00467	62.04	15.96	78.00	0.00448	67.01	3.44	70.45
S	0.074630	63.92	8.71	72.63	0.313132	43.80	19.42	63.22	0.019107	34.54	36.22	70.76	0.255977	28.17	24.81	52.98
Si	0.0976	35.14	124.90	160.04	0.1578	72.89	104.52	177.41	0.0970	37.12	177.57	214.69	0.1567	63.82	104.03	167.85
Sr	0.000701	142.65	2.28	144.93	0.000145	82.62	11.70	94.32	0.000696	97.67	2.59	100.26	0.000144	58.23	11.78	70.01
Ti	0.00175	80.00	91.43	171.43	0.00406	49.30	41.91	91.21	0.00174	68.94	103.41	172.35	0.00403	44.67	42.19	86.86
		0.00	0.00	0.00		0.00	0.00	0.00		0.00	0.00	0.00		0.00	0.00	0.00
Ag	0.0000070	571.43	228.57	800.00	0.0000040	49.91	217.12	267.03	0.0000070	387.82	127.84	515.66	0.0000040	226.19	216.13	442.32
As	0.0000060	100.00	135.00	235.00	0.0000080	124.80	108.57	233.37	0.0000060	67.02	149.13	216.15	0.0000080	75.39	108.05	183.44
Be	0.00000010	30.00	330.00	360.00	0.00000010	1900.00	350.00	2250.00	0.00000010	20.20	363.64	383.84	0.00000010	1111.11	343.43	1454.54
Cd	0.00000010	400.00	1600.00	2000.00	0.00000020	1000.00	850.00	1850.00	0.00000010	404.04	1818.18	2222.22	0.00000020	1155.78	854.27	2010.05
Co	0.000005	740.00	660.00	1400.00	0.000055	544.55	30.86	575.41	0.000005	603.26	361.95	965.21	0.000055	475.18	31.07	506.25
Cr	0.000001	13000.00	0.00	13000.00	0.000050	247.59	33.94	281.53	0.000001	4723.62	894.47	5618.09	0.000050	442.28	17.29	459.57
Cu	0.000050	2540.00	162.00	2702.00	0.000140	513.43	24.96	538.39	0.000050	402.16	36.19	438.35	0.000139	660.55	12.21	672.76
Hg	0.00000025	12.00	8.00	20.00	0.000000501	45.91	23.95	69.86	0.000000249	7.63	7.23	14.86	0.000000497	40.24	24.14	64.38
Mo	0.000110	10.91	73.64	84.55	0.000140	71.31	49.20	120.51	0.000109	4.57	48.44	53.01	0.000139	64.62	49.54	114.16
Ni	0.000015	726.67	326.67	1053.34	0.000250	123.79	27.55	151.34	0.000015	482.61	241.30	723.91	0.000249	148.77	6.84	155.61
P	0.00005	800.00	320000.00	320800.00	0.00090	104.27	188.58	292.85	0.00005	522.81	3619.47	4142.28	0.00090	93.82	189.87	283.69
Pb	0.00360	108.33	0.92	109.25	0.00180	138.66	1.94	140.60	0.00358	89.37	0.50	89.87	0.00179	122.86	1.90	124.76
Sb	0.0000020	200.00	40500.00	40700.00	0.0000020	249.63	434.35	683.98	0.0000020	201.11	447.46	648.57	0.0000020	1055.28	432.16	1487.44
Se	0.0000020	50.00	40500.00	40550.00	0.0000090	88.74	96.51	185.25	0.0000020	50.28	447.46	497.74	0.0000090	67.01	96.05	163.06
Sn	0.0000010	1200.00	81000.00	82200.00	0.0000015	599.20	579.23	1178.43	0.0000010	804.02	3618.09	4422.11	0.0000015	737.27	5764.08	6501.35
Te	0.0000010	4000.00	81000.00	85000.00	0.0000010	99.80	868.26	968.06	0.0000010	5025.13	894.47	5919.60	0.0000010	40.20	864.32	904.52
Tl	0.0000010	4000.00	81000.00	85000.00	0.0000015	332.89	579.23	912.12	0.0000010	5025.13	894.47	5919.60	0.0000015	268.10	576.41	844.51
V	0.000055	60.00	29.09	89.09	0.000130	207.35	13.06	220.41	0.000055	58.50	32.90	91.40	0.000129	77.32	13.14	90.46
Zn	0.000300	36.67	163.33	200.00	0.000501	135.77	114.41	250.18	0.000298	33.51	231.91	265.42	0.000497	38.20	117.20	155.40

	MT 200	3A	3A	3A	IL 200	3B	3B	3B	MT 200	4A	4A	4A	IL 200	4B	4B	4B
	Coal	Solids	Liquid		Coal	Solids	Liquid		Coal	Solids	Liquid		Coal	Solids	Liquid	
	grams	grams	grams		grams	%of initial	%of initial		grams	grams	grams		grams	%of initial	%of initial	
	3A	prb T low	prb T low	TOTAL	3B	ill6 T low	ill6 T low	TOTAL	4A	prb P high	prb P high	TOTAL	4B	ill6 P high	ill6 P high	TOTAL
Al	0.0030	189.73	2.93	192.66	0.0400	16.24	1.17	17.41	0.0030	156.59	2.03	158.62	0.0400	12.00	0.99	12.99
Ba	0.001102	107.12	0.64	107.76	0.000290	79.24	2.20	81.44	0.001101	50.88	0.64	51.52	0.000290	99.96	0.90	100.86
Ca	0.0125	210.90	4.08	214.98	0.0230	43.87	3.80	47.67	0.0125	173.51	3.38	176.89	0.0230	43.46	2.52	45.98
Fe	0.0997	76.83	0.18	77.01	0.2080	41.54	0.23	41.77	0.1003	84.65	0.12	84.77	0.2084	31.70	0.11	31.81
K	0.00070	104.14	4.99	109.13	0.00691	99.91	0.62	100.53	0.00070	102.80	23.42	126.22	0.00690	94.17	1.52	95.69
Mg	0.00195	189.48	2.71	192.19	0.00120	57.45	28.39	85.84	0.00195	276.78	4.82	281.60	0.00120	67.48	6.58	74.06
Mn	0.000060	204.71	26.46	231.17	0.000290	75.80	2.20	78.00	0.000060	203.23	7.83	211.06	0.000290	89.62	2.72	92.34
Na	0.00471	82.86	1.87	84.73	0.00450	111.01	2.38	113.39	0.00470	99.95	3.49	103.44	0.00450	95.52	2.33	97.85
S	0.073937	67.90	90.62	158.52	0.312331	57.60	2.46	60.06	0.074220	73.43	9.18	82.61	0.312498	46.10	19.39	65.49
Si	0.0976	51.21	1.99	53.20	0.1576	81.20	18.90	100.10	0.0976	41.11	74.63	115.74	0.1576	67.53	53.50	121.03
Sr	0.000701	104.14	0.13	104.27	0.000145	675.27	1.32	676.59	0.000700	114.23	0.07	114.30	0.000145	689.41	1.45	690.86
Ti	0.00175	67.33	44.28	111.61	0.00405	29.85	0.52	30.37	0.00175	65.11	1.31	66.42	0.00405	46.90	0.64	47.54
Ag	0.0000070	299.57	12.55	312.12	0.0000040	124.88	52.45	177.33	0.0000070	142.78	16.70	159.48	0.0000040	50.00	33.00	83.00
As	0.0000060	216.38	29.96	246.34	0.0000080	174.85	26.23	201.08	0.0000060	133.27	38.31	171.58	0.0000080	149.94	32.49	182.43
Be	0.00000010	130.00	180.00	310.00	0.00000010	120.00	210.00	330.00	0.00000010	70.00	230.00	300.00	0.00000010	440.00	260.00	700.00
Cd	0.00000010	1300.00	350.00	1650.00	0.00000020	2400.00	105.00	2505.00	0.00000010	500.00	230.00	730.00	0.00000020	2100.00	130.00	2230.00
Co	0.000005	679.05	1092.47	1771.52	0.000055	726.64	15.44	742.08	0.000005	1099.34	139.92	1239.26	0.000055	672.48	14.36	686.84
Cr	0.000001	8391.61	1228.77	9620.38	0.000050	201.82	4.20	206.02	0.000001	9890.11	469.53	10359.64	0.000050	193.93	5.20	199.13
Cu	0.000050	265.63	11.96	277.59	0.000140	57.81	30.69	88.50	0.000050	279.85	253.47	533.32	0.000140	85.68	20.71	106.39
Hg	0.000000250	47.20	35.20	82.40	0.000000500	82.00	68.20	150.20	0.000000250	40.00	131.60	171.60	0.000000500	66.00	110.60	176.60
Mo	0.000110	9.08	4.81	13.89	0.000140	12.85	1.50	14.35	0.000110	10.90	2.09	12.99	0.000140	10.71	1.86	12.57
Ni	0.000015	4527.00	129.15	4656.15	0.000250	119.89	3.40	123.29	0.000015	326.49	15.33	341.82	0.000250	103.96	1.04	105.00
P	0.00005	778.91	3.59	782.50	0.00090	123.22	0.23	123.45	0.00005	439.77	4.60	444.37	0.00090	88.86	0.29	89.15
Pb	0.00361	105.13	1.17	106.30	0.00180	127.67	0.47	128.14	0.00360	161.03	0.26	161.29	0.00180	133.29	0.73	134.02
Sb	0.0000020	389.42	89.87	479.29	0.0000020	399.60	104.90	504.50	0.0000020	349.83	234.88	584.71	0.0000020	400.00	130.00	530.00
Se	0.0000020	798.80	89.87	888.67	0.0000090	55.51	23.31	78.82	0.0000020	49.98	114.94	164.92	0.0000090	22.21	28.88	51.09
Sn	0.0000010	999.00	349.65	1348.65	0.0000015	199.87	139.91	339.78	0.0000010	399.60	229.77	629.37	0.0000015	599.60	173.22	772.82
Te	0.0000010	499.50	529.47	1028.97	0.0000010	599.40	429.57	1028.97	0.0000010	299.70	469.53	769.23	0.0000010	600.00	260.00	860.00
Tl	0.0000010	299.70	1408.59	1708.29	0.0000015	9327.12	286.48	9613.60	0.0000010	99.90	229.77	329.67	0.0000015	66.62	173.22	239.84
V	0.000055	170.67	108.76	279.43	0.000130	2.31	19.68	21.99	0.000055	105.40	51.25	156.65	0.000130	83.82	26.30	110.12
Zn	0.000300	48.60	99.86	148.46	0.000500	39.96	80.93	120.89	0.000300	33.32	172.24	205.56	0.000500	47.98	105.96	153.94

CL -IL#6	5B	5B	5B	CL -ILL #6	6B	6B	6B
Coal	Solids	Liquids		Coal	Solids	Liquids	

	grams	%of initial	%of initial		grams	%of initial	%of initial	
	5B	CL ill6 cata	CL ill6 cata	TOTAL	6B	CL ill6 no cata	CL ill6 no cata	TOTAL
Al	0.01503	43.25	0.27	43.52	0.01501	4530.00%	17.00%	4547.00%
Ba	0.00012529	25.54	2.63	28.17	0.00012509	15.99	1.36	17.35
Ca	0.0001002	5.99	64.77	70.76	0.0001001	3.00	935.06	938.06
Fe	0.130579	35.76	16.54	52.30	0.034024	182.52	61.13	243.65
K	0.005513	83.44	0.45	83.89	0.005504	90.84	1.35	92.19
Mg	0.00024056	44.90	7.07	51.97	0.00024017	66.62	10.12	76.74
Mn	0.00007016	1696.12	1067.56	2763.68	0.00007005	1142.04	1039.26	2181.30
Na	0.0048111	87.30	2.97	90.27	0.0048035	83.30	2.67	85.97
S	0.337368	27.98	13.31	41.29	0.280000	20.00	14.17	34.17
Si	0.038589	155.23	0.44	155.67	0.038528	169.75	0.44	170.19
Sr	0.00005513	48.98	3.08	52.06	0.00005504	13.63	3.09	16.72
Ti	0.0022051	104.30	7.71	112.01	0.0022016	113.55	7.72	121.27
		0.00	0.00	0.00		0.00	0.00	0.00
Ag	0.000004009	24.94	82.31	107.25	0.000004003	19.99	87.43	107.42
As	0.000006515	144.28	76.75	221.03	0.000006505	118.37	79.94	198.31
Be	0.000002005	29.93	8.48	38.41	0.000002001	69.97	8.50	78.47
Cd	0.000002005	34.91	8.48	43.39	0.000002001	24.99	8.50	33.49
Co	0.000029067	756.87	103.21	860.08	0.000029021	1274.94	12.06	1287.00
Cr	0.00009021	2217.05	18.84	2235.89	0.00009006	3664.22	23.10	3687.32
Cu	0.0001503	319.36	17.70	337.06	0.0001501	386.41	6.93	393.34
Hg	0.00000019044	210.04	525.10	735.14	0.00000019014	178.82	362.89	541.71
Mo	0.00002506	75.82	6.78	82.60	0.00002502	95.92	6.79	102.71
Ni	0.000042599	11502.62	70.42	11573.04	0.000042531	38795.23	85.58	38880.81
P	0.000501	19.96	339.32	359.28	0.000500	20.00	340.00	360.00
Pb	0.00022552	13.30	25.10	38.40	0.00022516	7.99	24.65	32.64
Sb	0.000003508	108.32	190.99	299.31	0.000003503	99.91	48.53	148.44
Se	0.00000501	59.88	33.93	93.81	0.00000500	64.00	34.00	98.00
Sn	0.00000501	11.98	33.93	45.91	0.00000500	60.00	34.00	94.00
Te	0.000014032	28.51	35.63	64.14	0.000014010	3.57	62.10	65.67
Tl	0.000007016	14.25	47.04	61.29	0.000007005	242.68	24.27	266.95
V	0.0001002	159.68	1.70	161.38	0.0001001	199.80	1.70	201.50
Zn	0.00031072	34.11	117.79	151.90	0.00031022	36.10	201.15	237.25

APPENDIX I: Thermogravimetric weight reduction

The following graph depicts the results from the TGA of the DCL residues. The weight loss per temperature increase is the greatest for the PRB and cleaned coal. 5B and 6B were run twice to confirm data.

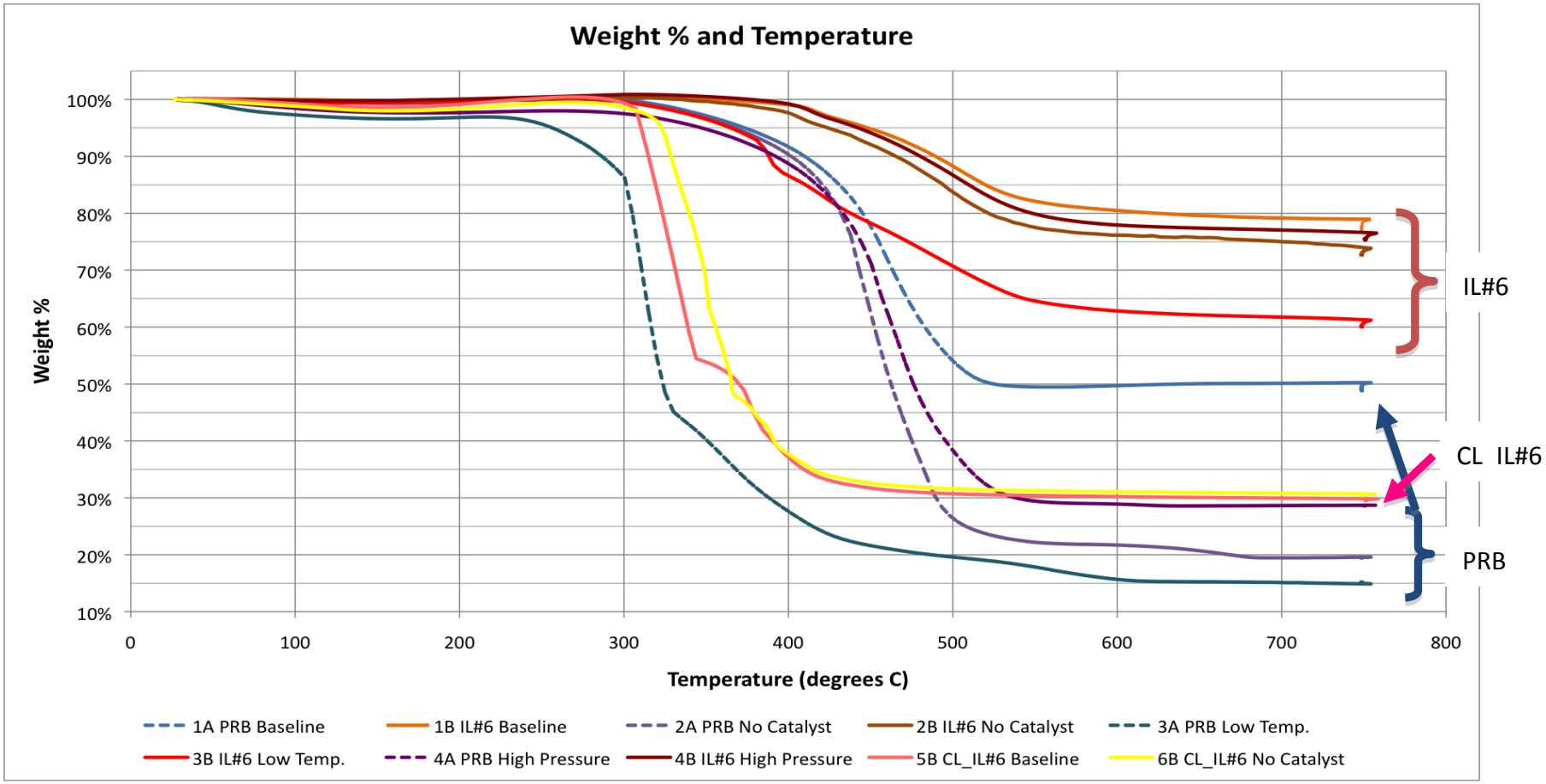

APPENDIX J: Partitioning results of varying temperatures and pressures

The following figure is of the PRB coal's elements of environmental interest during DCL tests of varied temperature and pressure.

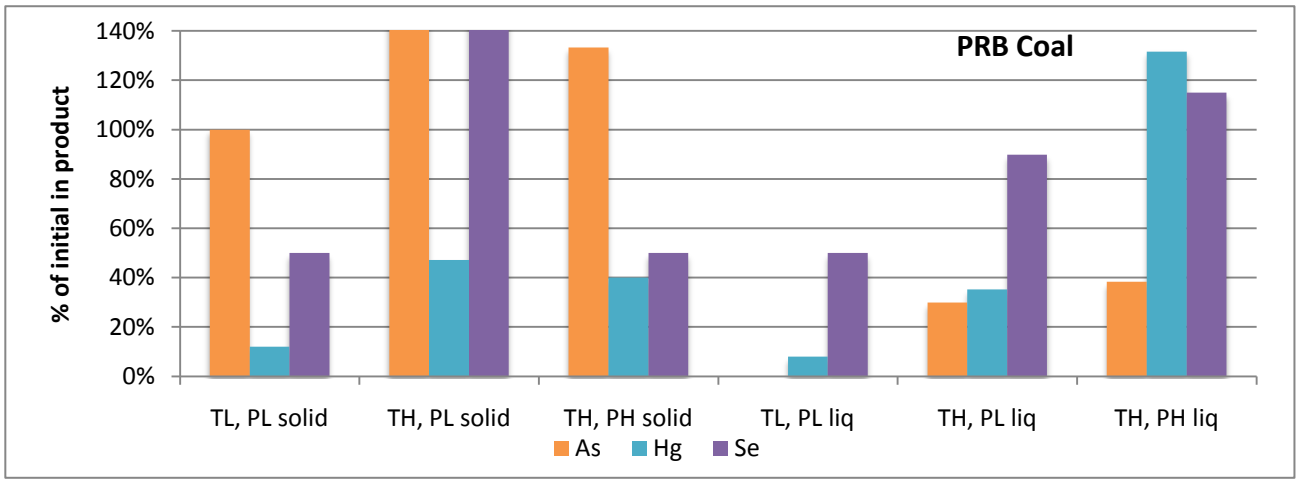

Partitioning of arsenic, mercury and selenium in PRB coal DCL products from reactions of varying temperature and pressure

The following figure is similar to the above, but contains elements of that have operational concerns.

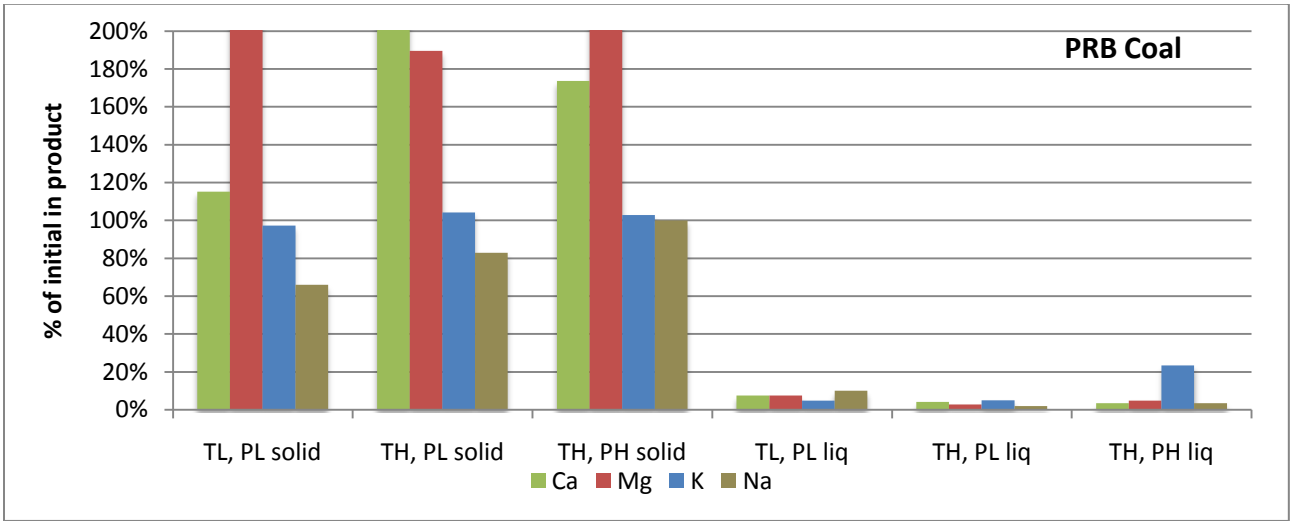

Partitioning of calcium, magnesium, potassium, and sodium in PRB coal DCL products from reactions of varying temperature and pressure

The next two figures illustrate the effect of temperature and pressures on inorganic element partitioning for the other elements of interest.

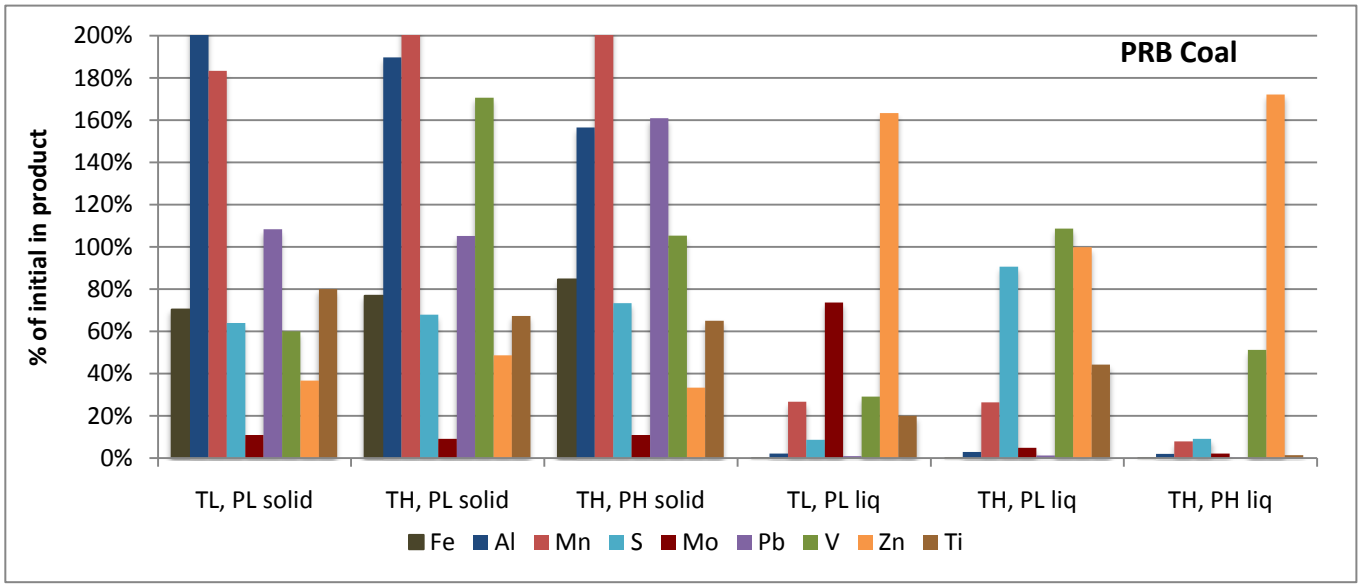

Partitioning of remaining inorganic elements in PRB coal DCL products from reactions of varying temperature and pressure

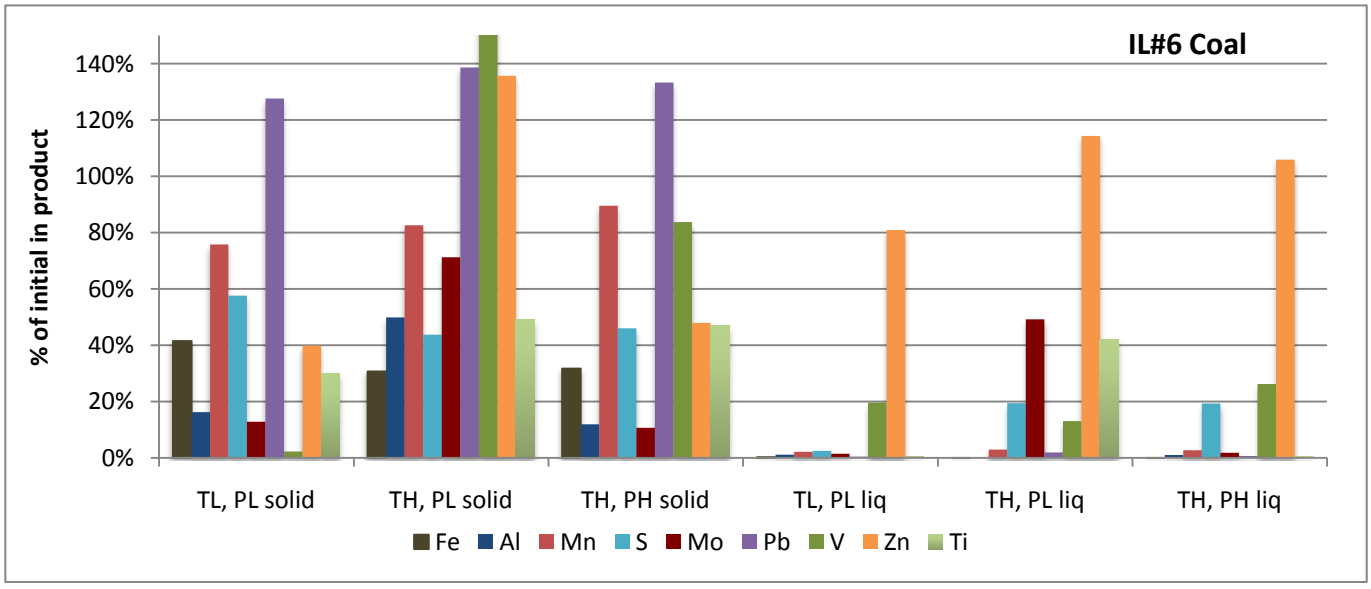

Partitioning of remaining inorganic elements in IL#6 coal DCL products from reactions of varying temperature and pressure

APPENDIX K: Concentration of major, minor, and trace elements on a per barrel basis

The following table was prepared by combining data from Appendixes G and H to determine the mass of each element in a volume equivalent to a barrel of oil, approximately 159 liters.

Calculated concentration of elements in a barrel of THF-soluble product for the ten test runs conducted in this thesis

PRB Coal	1A Baseline	2A No Catalyst	3A Low Temperature	4A High Pressure	**IL#6 Coal**	1B Baseline	2B No Catalyst	3B Low Temperature	4B High Pressure	5B Clean Baseline	6B Clean No Catalyst
g/barrel					**g/barrel**						
S	63.57	61.99	604.22	46.13	S	556.99	588.74	57.30	365.88	429.03	363.99
Fe	2.39	4.45	1.63	0.79	Fe	0.63	1.91	3.50	1.43	206.36	190.81
Ca	9.07	60.46	4.61	2.86	Ca	7.79	10.01	6.52	3.50	0.62	8.59
Na	4.61	6.68	0.79	1.11	Na	3.65	1.43	0.80	0.63	1.37	1.18
Mg	1.43	7.97	0.48	0.64	Mg	0.63	0.95	2.54	0.48	0.16	0.22
Mn	0.16	0.08	0.14	0.03	Mn	0.08	0.16	0.05	0.05	7.16	6.68
Al	0.64	0.64	0.79	0.41	Al	0.62	0.33	3.49	2.39	0.39	0.23
K	0.32	2.54	0.32	1.11	K	0.95	0.95	0.32	0.63	0.24	0.68
Pb	0.32	0.16	0.38	0.06	Pb	0.32	0.32	0.06	0.08	0.54	0.51
Mo	0.79	0.47	0.05	0.02	Mo	0.63	0.64	0.02	0.02	0.02	0.02
V	0.16	0.16	0.54	0.19	V	0.16	0.16	0.19	0.21	0.02	0.00
mg/barrel					**mg/barrel**						
Se	0.00	8.96	16.23	15.57	Se	9.16	79.73	15.66	15.70	16.24	15.60
As	0.00	17.91	16.23	15.57	As	0.00	0.00	15.66	15.70	47.77	47.71
Hg	0.00	0.00	0.90	2.03	Hg	0.92	0.93	2.24	3.62	9.55	6.42